Chapter 8
Mars Science Laboratory

Andre Makovsky, Peter Ilott, and Jim Taylor

8.1 Mars Science Laboratory Mission and Spacecraft Summary

The Mars Science Laboratory (MSL) mission has the primary objective of placing and operating a mobile science laboratory on the surface of Mars to assess the biological potential of the landing site, characterize the geology of the landing region, investigate planetary processes that influence habitability, and characterize the broad spectrum of surface radiation. MSL is conducting fundamentally new observations of Mars geology using advanced micro-imagery and spectrometry, while assessing the radiation environment and studying the surface environments.

This chapter is written from the perspective that the MSL spacecraft was launched in 2011; it cruised to Mars; it went through entry, descent, and landing (EDL) in 2012; and its rover has since operated on the surface of Mars.

Launched on November 26, 2011 with rover touchdown on Mars on August 6, 2012, the MSL mission aims to achieve its objectives on the surface of Mars in a manner that will offer the excitement and wonder of space exploration to the public. Fig. 8-1 is an artist's conception of the Curiosity rover on the surface with its instrument arm deployed.

The span of planned launch dates was between mid-October and early December 2011 with possible arrival dates at Mars in August 2012. Geometries

that enable communications during the EDL phase were a mission design driver.

The MSL candidate cruise trajectories [1,2] were limited to type I trajectories for the 2011 launch[1]. A type I Earth–Mars interplanetary trajectory carries the spacecraft less than 180 degrees (deg) around the Sun, and type II is greater than 180 deg [3].

Table 8-1 lists the opening and closing of the 2011 trajectory launch periods and the trajectory types that were considered. The designators Ia, Ib, and Ic were arbitrarily assigned for launch/arrival date pairs. The actual November 26 launch and August 6 arrival were on a Type Ib trajectory.

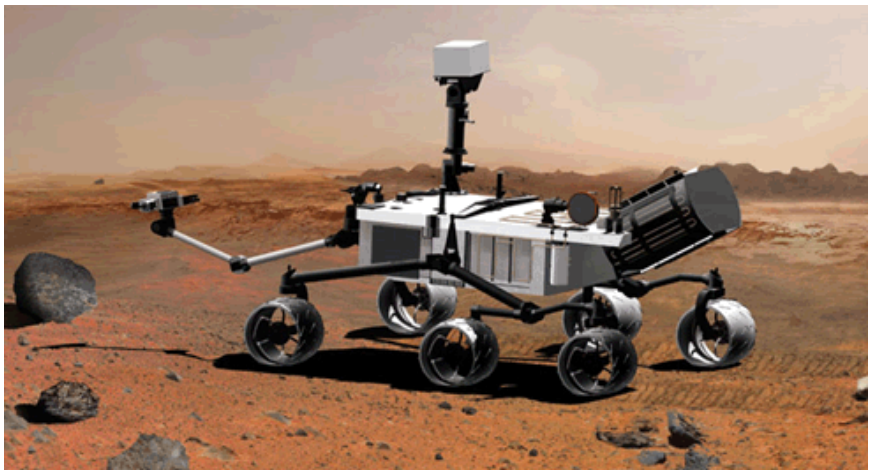

Fig. 8-1. Artist's conception of Mars Science Laboratory on Mars.

Table 8-1. 2011 launch and 2012 arrival dates for type I trajectories.

Cruise Trajectory	Launch date	Arrival date
Type Ia open	11/25/11	8/06/12
Type Ia close	12/18/11	8/20/12
Type Ib open	11/25/11	8/06/12
Type Ib close	12/18/11	8/06/12
Type Ic open	11/29/11	8/08/12
Type Ic close	12/18/11	8/13/12

[1] The MSL mission originally was intended for a 2009 launch and 2010 arrival at Mars. The telecommunications system design, in particular the antenna characteristics, accommodated both type I and type II candidate cruise trajectories for 2009. This chapter mentions some of the antenna drivers of the 2009 trajectory candidates.

MSL's initial telecom capability after launch employed a non-directive low-gain antenna (LGA) and depended on the spacecraft orientation and the limited distance between Earth and the spacecraft. Starting three months after launch, a medium-gain antenna (MGA) was used. As shown in Fig. 8-2, the cruise stage had a solar array on a surface surrounding the horn of the MGA. The array is the flat blue surface at the top-left of the drawing. This array powered the cruise loads and charged the batteries. Therefore, the cruise-stage orientation to the Sun was driven by power and thermal subsystem constraints. The solar array normal had to be pointed near the Sun line, at a Sun-view angle that optimized the solar cell power output, without being heated too much. Conversely, the telecom link would be optimized if the antenna boresight (and, hence, the spacecraft –Z axis) were pointed towards Earth.

Figure 8-3 shows the array and the MGA edge-on in the cruise stage at the top. The –Z axis is toward the top of the figure. The competing power and telecom needs were major factors in the design trades in cruise stage orientation. The telecom and power/thermal constraints are linked by the Sun–Probe–Earth (SPE) angle [4].

Figure 8-4 shows the profiles of two angles during cruise: (a) the Sun–Craft–Earth angle, and (b) the off-Earth pointing angle of the PLGA and MGA. The broad beam of an LGA would have a poor pattern at angles greater than about 80 degrees (deg) off boresight[2] due to spacecraft obstructions. The type I trajectories result in a maximum off-Earth angle of about 63 deg.

8.1.1 Mission Description

The MSL mission has completed three major phases, and is in the fourth.

1) Launch.
2) Cruise/Approach.
3) Entry, Descent, and Landing (EDL).
4) Surface Operations.

Table 8-2 provides more detail regarding these phases. Prior to surface operations, time references are in terms of the familiar Earth hours and days.

---

[2] Boresight refers to a direction in which an antenna's gain is the maximum. A fixed antenna (one not on a gimbal), such as the MSL MGA or any of the LGAs, is defined in terms of the spacecraft axis (or axes) direction along which that antenna is mounted. That direction, for example the –Z axis for both the parachute LGA (PLGA) and the MGA used during cruise, is loosely referred to as the boresight.

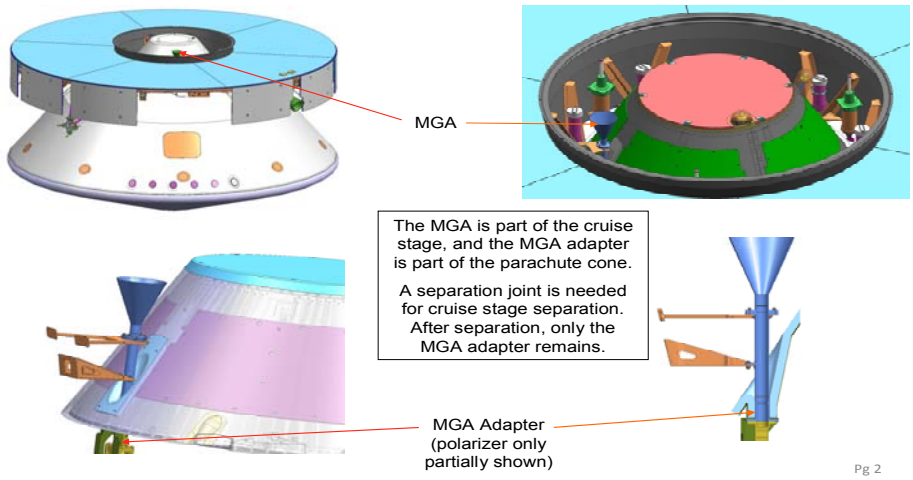

Fig. 8-2. MSL solar array and MGA locations on the cruise stage.

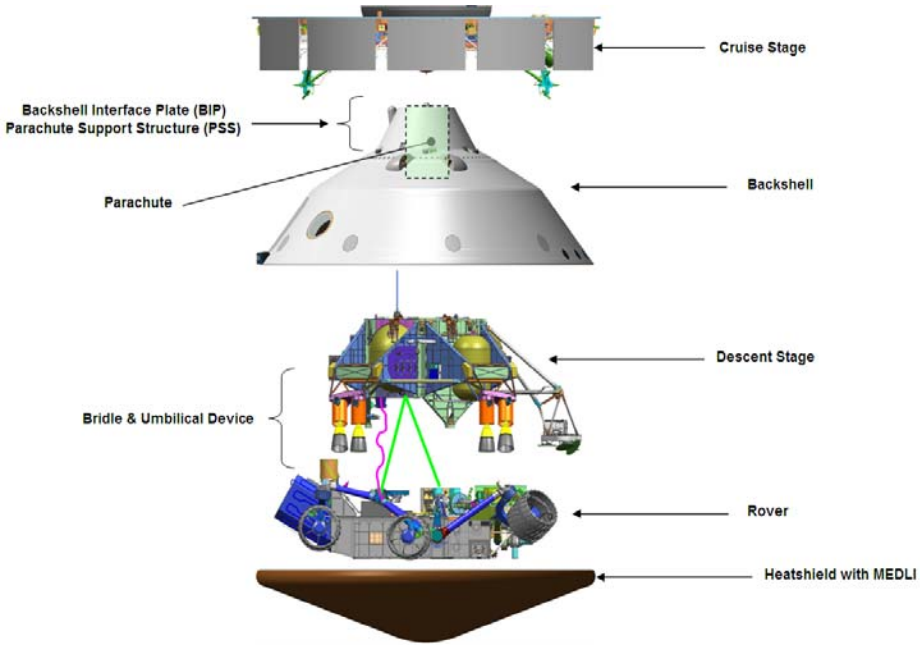

Fig. 8-3. Exploded view of the five major stages of the MSL spacecraft (flight system). (MEDLI = MSL EDL instrumentation)

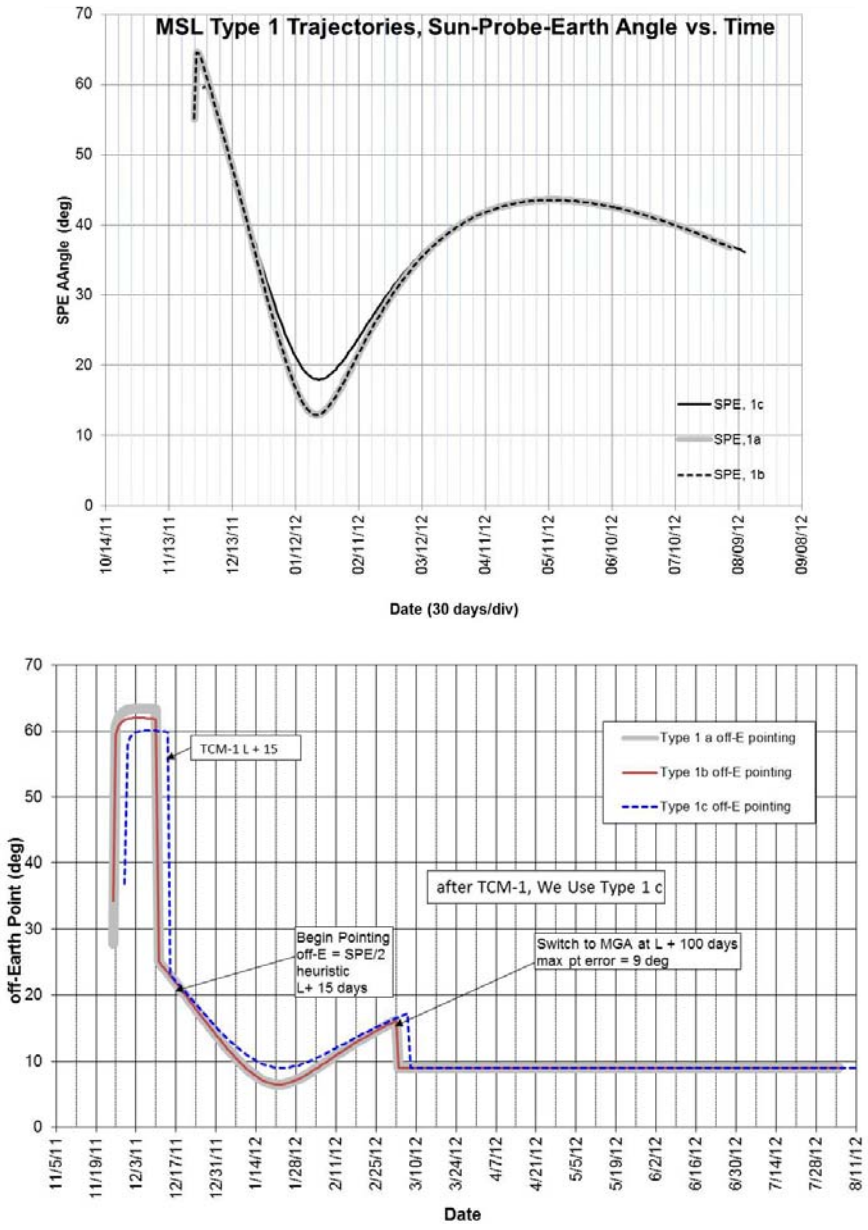

Fig. 8-4. Antenna geometry for MSL cruise trajectories: (a) Sun–Probe–Earth (SPE) angles versus time, and (b) Planned maximum off-Earth angles for PLGA and MGA (TCM is trajectory correction maneuver).

Table 8-2. MSL major mission phases.

Mission Phase	Description	Approximate Duration
Launch	The launch phase was defined to begin at the point where the spacecraft transferred to internal power prior to launch. It was complete (after spacecraft separation from the launch vehicle's upper stage) when the spacecraft reached a thermally stable, positive energy balance, commandable configuration	1 hour
Cruise	The cruise phase began when the launch phase ended, and it ended 45 days prior to atmospheric entry (E–40 days).	208 days
Approach	The approach phase was defined to begin at 45 days prior to atmospheric entry (E–45 days) and ended when the spacecraft reached the Mars atmospheric entry interface point. That point is defined at a Mars radius of 3522.2 km.	45 days
EDL	Entry, descent, and landing (EDL) began when the spacecraft reached the entry interface point (Mars radius of 3522.2 km) and ended when the rover reached a thermally stable, positive energy balance, commandable configuration on the surface.	7 minutes
Surface	The surface mission began when EDL ended, and it will end when the mission is declared complete. The design of the rover must provide for a surface mission duration of at least one Mars year (669 sols, equivalent to 687 Earth days).	Prime mission: 669 sols (with possible additional extensions)

On the surface of Mars, all planning and rover activity is in terms of sols (Martian days). One sol, in terms of Earth time, is approximately 24 hours, 39 minutes, and 35 seconds long. A sol is equivalent to about 1.027 Earth days. A sol is divided into 24 (Martian) hours, each of which is 60 (Martian) minutes, and so forth, analogous to the time units on Earth.

8.1.2 Launch/Arrival Period Selection

A year before launch, candidate landing sites on Mars were narrowed to four (Mawrth Vallis (Valley), Gale Crater, Eberswalde Crater, and Holden Crater), spanning latitudes between 27 deg S and 25 deg N. The final selection, near Mount Sharp in Gale Crater, was made in July 2011 (4 months before launch).

With these sites, the parameter limits that drove the launch and arrival periods can be summarized as a set of constraints [5].

- Spacecraft injected mass = 4050 kilograms (kg)
- Launch-specific energy (C3) capability < 20.1 kilometers squared per second squared (km^2/s^2) (Atlas V 541, instantaneous launch window)
- Atmospheric entry velocity < 5.9 kilometers per second (km/s) (not a hard constraint due to EDL heating performance study results)

- Declination of launch asymptote < 40 deg
- Arrival no later than 30 days before the start of solar conjunction
- Launch eclipse duration ≤ 65 minutes
    - Early cruise SPE angle constraints:
        - Launch vehicle separation (SEP) attitude (SEP to SEP + 18 days):
            - Angle between –Z axis and Sun ≤ 64.0 deg and ≥ 20.0 deg
            - Angle between –Z axis and Earth ≤ 68.8 deg
    - EDL communications strategy constraints:
        - Relay:
            - Mars Reconnaissance Orbiter (MRO) Local Mean Solar Time (LMST) node as close to nominal value (3:00 p.m.) as possible
            - Odyssey LMST node at 3:00 p.m. because of propellant issues related to orbiter lifetime
            - View angle to orbiters (MRO/Odyssey) ≤135 deg
            - MRO/Odyssey elevation at landing + 1 min ≥ 10 deg
        - Direct to Earth (DTE):
            - View angle to Earth ≤ 75 deg
            - Earth elevation at landing + 1 min ≥ 10 deg
    - 20-day launch period.
    - Declination of launch asymptote < 28.5 deg
    - Atmospheric entry velocity < 5.6 km/s.
    - EDL communications strategy constraints:
        - Full ultra-high frequency (UHF) EDL coverage via MRO and Odyssey from Entry[3] to Landing + 1 minute. (Relay coverage is not possible for all of EDL due to geometric constraints from cruise stage separation (CSS until entry).
        - Full DTE EDL coverage (For type I only possible for Mawrth Vallis).

[3] Entry defined as the point where the entry vehicle is at a radius of 3522.2 km from nominal Mars center. Entry is also considered at a time beginning 600 seconds after nominal cruise state separation.

8.1.2.1 Cruise Mission Phase Telecom Trades

An example of the significant decisions involving telecom is the one involving cruise trajectory type (I vs. II), launch window, power subsystem constraints, and LGA pattern.

- Type I vs. type II trajectory: The type II trajectory (candidate only for the originally planned 2009 launch) had very large initial SPE angles (as shown in Fig. 8-4), greater than 120 deg at the start of the launch period. At the other end of cruise, the EDL geometry of the type II offered better UHF coverage opportunities. (One year before the 2011 MSL launch, only type I trajectories with launch dates between November 25 and December 18, 2011 were still in contention.)
- Launch period: With a 2011 launch, Juno's launch period, driven by the complex trajectory to get the Juno spacecraft into orbit around Jupiter, overlapped MSL's launch period. When MSL's launch was changed from 2009 to 2011, the MSL trajectory design (which included launch period) had to accommodate the Juno launch period of August 5–27 that was required to get that spacecraft to Jupiter. Both Juno and MSL launched on Atlas V launch vehicles, and both used the same launch pad at Kennedy Space Center (KSC). The time required to refurbish the launch pad after Juno launched and to complete MSL pre-launch activities established an earliest launch date of November 25 for the MSL Type Ib trajectory.
- Solar array[4] and antenna pointing: Power output and thermal considerations required the solar array to be pointed within an optimum range of angles from the Sun: too far from the Sun, not enough power; too close to the Sun, too much heating. This range of angles tended to force the PLGA angle to Earth to be too far off boresight in the first weeks after launch.
- Solar array pointing (thermal constraint): Until Sun–spacecraft distance increased sufficiently, the solar array was to be pointed not too close to the Sun, to avoid overheating the solar panels and losing efficiency.

Based on gain pattern measurements with a spacecraft mock-up, telecom imposed a mission design constraint of 80-deg offpoint from PLGA boresight. The measured PLGA patterns described in Section 8.2 (Figs. 8-36 and 8-37) can be compared with this 80-deg constraint.

---

[4] The solar array was on the cruise stage (Figs. 8-3 and 8-4) and augmented the radioisotope-thermoelectric generator (RTG) during cruise. Without the need for a solar array, the RTG alone, with a battery for peak loads, is sufficient for surface operations.

These trades resulted in the following telecom configurations and operating modes for launch and cruise [6].

- We launched using the PLGA. This antenna has a very broad beam, and near Earth we can cover as much as 90 deg off—afterward as much as 80 deg off.
- From a telecom downlink margin point of view, we could have launched using either the traveling-wave tube amplifier (TWTA) on the descent stage or the solid state power amplifier (SSPA) on the rover. The plan was to launch on the TWTA (to avoid having to switch to it from the SSPA early in cruise and being exposed to a switch failure).
- Operationally, being on the TWTA meant having a 210-s outage after launch vehicle (LV) separation, while the TWTA warmed up.
- For the 2011 launch, the plan was to transition from the PLGA to the MGA no later than March 2012. The driver for this is ranging, which requires a ranging power-to-noise spectral-density ratio (P_r/N_0) of at least –20 decibel-hertz [dB-Hz]. Ranging is weaker than either the command link or the telemetry link. Ranging incurs two-way space loss as well as thermal noise in the small deep space transponder (SDST) receiver's ranging channel bandwidth of ~1.5 megahertz (MHz).

8.1.2.2 EDL and Surface Mission Phase Telecom Trades

The telecom constraints during surface operations are defined in Makovsky and Danos [6], and they can be summarized as follows:

- The Mars–Earth range at arrival was greater than it was for the Mars Exploration Rover (MER) (MER was ~1.53 astronomical units [AU] [2.29×10^8 km] compared to 1.66 AU [2.48×10^8 km] for MSL). The X-band performance was correspondingly weaker than MER's, and this was reflected in lower downlink rates.
- UHF (Relay via MRO or Odyssey) is intended as primary for communications; HGA has been a low-data volume back-up and the RLGA has been used for emergency commanding)

Telemetry during EDL was transmitted via the MSL UHF subsystem and the spacecraft (sometimes called relay assets) orbiting Mars and by DTE at X-band to the Deep Space Network (DSN). The UHF relay transmitted real-time EDL data in a continuous stream at a rate of 8 kilobits per second (kbps) in bit stream mode.[5] The UHF bit stream broadcast by MSL during EDL was received by

[5] Bit steam mode is a non-acknowledged transmission mode that includes no Proximity-1 protocol formatting and no data retransmission mechanisms. After

multiple orbiters that had their UHF relay radios set to operate in a compatible listen-only bit stream mode. The data for DTE was in the form of semaphores, the so-called multiple frequency shift keying (MFSK) tones. As with the MER landers in 2004 and the Phoenix Lander in 2008, the possibility existed to monitor the UHF carrier signal from a large Earth-located ground station that had Mars in view at the right time.

The relay assets available to MSL for EDL were the MRO and the Odyssey orbiter. Each orbiter played a unique role in capturing the UHF signal from the rover during this phase.[6] Odyssey performed realtime demodulation of the EDL relay data so UHF telemetry data returned first from Odyssey. MRO performed open loop recording for later demodulation and thus acted in a secondary role. However, if Odyssey's closed loop data capture had failed for any reason, MSL would have depended on the MRO open loop record data.

Due the limitations of geometry during EDL for the chosen Type Ib trajectory, simultaneous coverage by both an orbiter for UHF and an Earth station for DTE was not possible for the entire EDL phase. The mission strategy ensured DTE coverage during the period from CSS until at least atmospheric entry. During this period, relay coverage began after CSS. There was substantial overlap of X-band and UHF coverage during entry, after the relay link began to be viable. During hypersonic entry, we included in our plans the expected loss of as much as 100 s of UHF coverage due to plasma blackout. The actual blackout was about 40 s. DTE coverage during the UHF blackout period was planned. The descent stage in fact continued to transmit X-band DTE MFSK tones all the way to landing.

For the 2011 launch opportunity, and to simplify the preliminary verification of EDL communications coverage, the following actions were performed in the trajectory selection process by Mission Design.

- For MRO relay coverage:

---

landing, Curiosity had multiple opportunities to transmit a superset of the real-time data that had been stored on-board during the event. The post-landing transmission used the Proximity-1 mode.

[6] It would also have been possible for MSL to plan to use the European Mars Express (MEX) orbiter in a limited capacity if either MRO or Odyssey (or both) became unavailable. However, this use would have had to be planned in advance to enable MEX to phase for the MSL EDL. MEX has subsequently performed UHF relay operations with Curiosity during surface operations.

  - Check that there would be a line of sight between MSL and MRO at the time of Entry interface and at landing + 1 minute.
  - Assume that MRO could be phased anywhere in its orbit for optimal coverage of MSL EDL.
  - Check that the orbiter elevation was greater than 10 deg at landing and landing + 1 minute.
  - Check that the angle from the MSL anti-velocity vector to the orbiter at entry was less than 135 deg.
- Similarly for DTE coverage (directly to Earth):
  - Check that there was a line of sight between MSL and Earth at the entry interface and landing times.
  - Check that Earth elevation was greater than 10 deg at landing.
  - Check that the angle from the MSL anti-velocity vector to Earth at entry was less than 75 deg.

Orbiter coverage was strongly desired since it provided return link telemetry at a single planned rate of 8 kbps versus the X-band MFSK tones at a maximum rate of a new tone every 10 seconds. Each MFSK tone could carry one of 256 messages represented as a "subcarrier frequency" (the frequency spacing between carrier and subcarrier). Each tone therefore notified the flight team of one event (for example, "parachute deploy"). In addition, use of signal processing recovered frequency characteristics of the X-band signal (such as Doppler-shift due to deceleration) could help reconstruct events during EDL. UHF, by contrast, provided a large amount of real-time engineering telemetry. The maximum planned data latency was 1 second for the UHF transmitted telemetry during EDL. Minimizing the data latency ensured that the ground received as complete a history of events as possible. Happily, a detailed forensic reconstruction was not needed.

Figure 8-5 illustrates the quality of the coverage during the post-entry phase of EDL for UHF via MRO and Odyssey and for X-band DTE, for the four candidate landing sites and the two types of trajectories. All four sites were considered viable in terms of safety and engineering considerations (including communications during EDL), allowing the final choice of Gale Crater to be on the basis of science.

The figure shows there were some differences however. Green shading indicates good coverage for the full duration of EDL for the indicated link type, yellow indicates coverage for only part of the EDL, and red indicates little or no coverage. DTE coverage for the type I trajectory would be complete (that is, all the way until landing) only for the northern site, Mawrth Vallis. This is due to the Earth setting below the horizon for the southern sites (red shading).

Conversely, UHF coverage for the type II trajectory was only partial from Odyssey for the southern sites (yellow shading), though MRO coverage was still available. Orbital phasing and survivability considerations limited Odyssey coverage. For either trajectory, only the Mawrth site offered complete EDL telecom coverage after atmospheric entry for DTE and both orbiters.

Section 8.2 of this chapter contains more detailed information regarding the EDL communications geometry and the rationale behind the 135-deg orbiter and the 75-deg Earth angles from the anti-velocity vector for relay and DTE coverage.

8.1.3 Launch Phase and Initial Acquisition

The Launch phase began when the spacecraft transferred to internal power on the launch pad. It ended when the spacecraft was declared stable, healthy, and ready to accept commands, and when the launch telemetry had been played back. The major activities in the Launch phase included the Liftoff and Boost phase of the launch vehicle; insertion into a circular parking orbit, a coast period (followed by additional launch vehicle upper stage burns necessary to inject the spacecraft onto the beginning of the planned trajectory to Mars), separation of the spacecraft from the launch vehicle, initial acquisition by the DSN, verification of the initial spacecraft health and operating conditions, and the verified execution of a minimal set of post-launch commands. Table 8-3 shows the launch window times for different phases of the launch periods (time is in Universal Time Coordinated [UTC]) [2].

EDL Coverage Summary

Launch Period	Asset	Mawrth (24.0N)	Gale (4.5S)	Eberswalde (23.9S)	Holden (26.4S)
Type 2	MRO				
	ODY				
	DTE*				
Type 1	MRO				
	ODY				
	DTE*				

*Drop outs are possible between landing – 60 s and landing – 20 s due to parachute and powered descent dynamics.

Fig. 8-5. EDL coverage after entry for Mars Reconnaissance Orbiter and Odyssey.

Table 8-3. Launch period / window durations.

Launch Period	Launch Date	Launch Day	Launch Window (UTC)
Type Ia	11/25/2001	Open	15:15 to 17:15
	12/06/2011	Middle	14:16 to 16:13
	12/18/2011	Close	11:48 to 13:48
Type Ib	11/25/2001	Open	15:15 to 17:15
	12/06/2011	Middle	12:35 to 14:35
	12/18/2011	Close	11:06 to 13:06
Type Ic	11/29/2011	Open	15:22 to 17:22
	12/08/2011	Middle	12:50 to 14:50
	12/18/2011	Close	11:11 to 13:11

In June 2006, the Atlas V 541 was selected as the launch vehicle for MSL. The Atlas 541, shown in Fig. 8-6, provides a 5-meter (m) fairing, the addition of four solid-rocket motors to the central booster, and a single-engine Centaur upper-stage. The Lockheed Martin website [7] provides more details about the launch vehicle. Figure 8-7 illustrates the launch events.

Table 8-4 provides a legend for the acronyms used in these two figures.

Table 8-4. Legend for LV and launch phase figures.

ATS	aft transition structure	MAD	Madrid Deep Space Center
BECO	booster engine cutoff	MECO	main engine cutoff
BODA	burnout detection algorithm	MES	main engine start
CAN	Canberra Deep Space Center	NPO	NPO Energomash is a Russian manufacturer
CCAM	collision and contamination avoidance maneuver	PLF	payload fairing
CCB	common core booster	RP	rocket propellant or refined petroleum (kerosene)
C-ISA	Centaur interstage adapter	SEC	Single-Engine Centaur
DEC	Dual-Engine Centaur	SEP	Separation
EOM	end of mission	SRB	solid rocket boosters
GDS	Goldstone Deep Space Center	SRBJ	solid rocket booster jettison
ISA	interstage adapter	TIP	target interface point
LH_2	liquid hydrogen	T/W	ratio of thrust and weight on pad
LO_2	liquid oxygen		

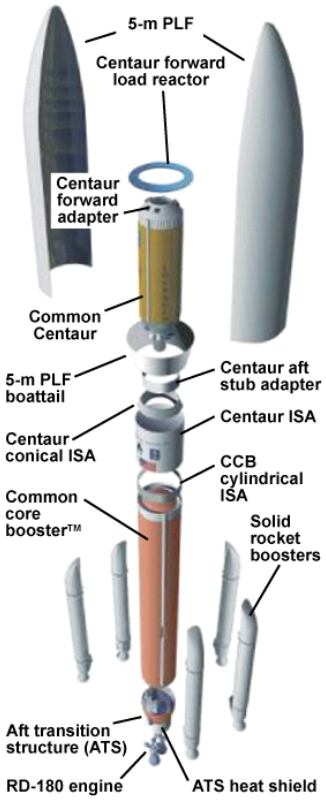

PAYLOAD FAIRING (PLF)

Features	5-m Short	5-m Medium	5-m Long
Diameter:	5.4 m	5.4 m	5.4 m
Length:	20.7 m	23.4 m	26.5 m
Mass:	3,540 kg	4,019 kg	4,394 kg

Subsystems

Fairing: Bisector: sandwich construction with graphite epoxy face sheets & an aluminum honeycomb core

Boattail: Fixed, composite sandwich construction

Separation: Vertical separation by a linear piston & cylinder activated by a pyrotechnic cord; horizontal separation by an expanding tube shearing a notched frame, activated by a pyrotechnic cord

COMMON CENTAUR

Features — **Common with Atlas 400 series**

Size: 3.05-m dia x 12.68-m length with extended nozzle

Inert mass: 2,138 kg

Propellant: 20,830-kg LH_2 & LO_2

Guidance: Inertial

Subsystem

Structure: Pressure stabilized stainless steel tanks separated by common ellipsoidal bulkhead

Propulsion: One or two Pratt & Whitney restartable engine(s)

—Model: RL 10A-4-2

—Thrust: 99.2 kN (SEC) 198.4 kN (DEC)

—I_{SP}: 450.5 s

(SEC) One electromechanically actuated 51-cm columbium fixed nozzle
Four 27-N hydrazine thrusters
Eight 40-N lateral hydrazine thrusters

(DEC) Two hydraulically actuated 51-cm columbium extendible nozzles
Eight 40-N lateral hydrazine thrusters
Four 27-N hydrazine thrusters

Pneumatics: Helium & hydrogen autogenous tank pressurization

Avionics: Guidance, navigation & control vehicle sequencing, computer-controlled vent & pressurization, telemetry, tracking, range safety command, electrical power

Insulation: Polyvinyl chloride foam (1.6-cm thick), modified adhesive bonding with optional radiation shields

SOLID ROCKET BOOSTERS (SRB)

Zero-to-Five: Ground-lit

Size: 155-cm dia x 19.5-m length

Mass: 46,559 kg (each fueled)

Thrust: 1,361 kN (each)

I_{SP}: 275 s

Nozzle cant: 3 deg

CENTAUR INTERSTAGE ADAPTER (C-ISA LARGE)

Features

Size: 3.81-m dia x 4.46-m length

Mass: 2,292 kg (includes ISA, aft stub adapter & boattail)

Subsystems

Structure: Composite sandwich (aluminum core graphite epoxy face sheets)

CCB CONICAL INTERSTAGE ADAPTER

Features

Size: 3.81-m dia x 0.32-m length

Mass: 282 kg

Subsystems

Structure: Aluminum machined rolled-ring forging

COMMON CORE BOOSTER™ (CCB)

Features — **Common with Atlas V 400 series**

Size: 3.81-m dia x 32.46-m length

Propellant: 284,089-kg LO_2 & RP-1

Inert Mass: 21,336 kg for 55Z configuration

Guidance: From upper stage

Subsystems

Structure: Structurally stable aluminum Isogrid tanks; Integrally machined aft transition structure; composite heat shield

Separation: Eight retro rockets

Propulsion: Pratt & Whitney/NPO Energomash RD-180 booster engine (2 chambers)
SL 100% thrust =3,827 kN, I_{SP}=311.3 s
Vac 100% thrust = 4,152 kN, I_{SP}=338.4 s

Pneumatics: Helium for tank pressurization, computer-controlled pressurization system

Hydraulics: Integral with engine provides gimbal control

Avionics: Flight control, flight termination, telemetry, redundant rate gyros, electrical power

Fig. 8-6. Atlas V 541 launch vehicle.

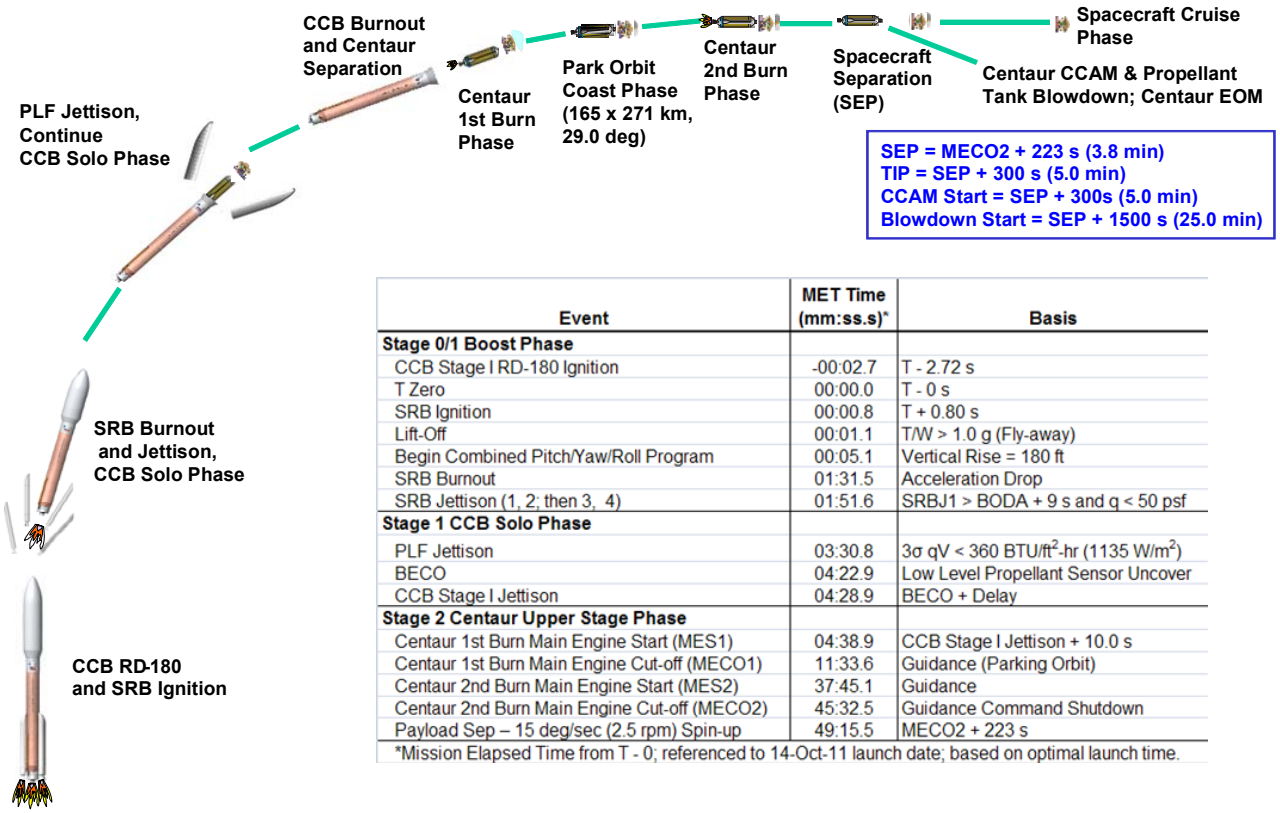

Event	MET Time (mm:ss.s)*	Basis
Stage 0/1 Boost Phase		
CCB Stage I RD-180 Ignition	-00:02.7	T - 2.72 s
T Zero	00:00.0	T - 0 s
SRB Ignition	00:00.8	T + 0.80 s
Lift-Off	00:01.1	T/W > 1.0 g (Fly-away)
Begin Combined Pitch/Yaw/Roll Program	00:05.1	Vertical Rise = 180 ft
SRB Burnout	01:31.5	Acceleration Drop
SRB Jettison (1, 2; then 3, 4)	01:51.6	SRBJ1 > BODA + 9 s and q < 50 psf
Stage 1 CCB Solo Phase		
PLF Jettison	03:30.8	3σ qV < 360 BTU/ft^2-hr (1135 W/m^2)
BECO	04:22.9	Low Level Propellant Sensor Uncover
CCB Stage I Jettison	04:28.9	BECO + Delay
Stage 2 Centaur Upper Stage Phase		
Centaur 1st Burn Main Engine Start (MES1)	04:38.9	CCB Stage I Jettison + 10.0 s
Centaur 1st Burn Main Engine Cut-off (MECO1)	11:33.6	Guidance (Parking Orbit)
Centaur 2nd Burn Main Engine Start (MES2)	37:45.1	Guidance
Centaur 2nd Burn Main Engine Cut-off (MECO2)	45:32.5	Guidance Command Shutdown
Payload Sep – 15 deg/sec (2.5 rpm) Spin-up	49:15.5	MECO2 + 223 s

*Mission Elapsed Time from T - 0; referenced to 14-Oct-11 launch date; based on optimal launch time.

Fig. 8-7. Launch Phase Illustration.

Depending on the specific launch date, planning had to account for an eclipse of the Sun by the Earth after launch vehicle separation. The traveling wave tube amplifier (TWTA) was scheduled to be powered on at eclipse exit[7]. The TWTA started the X-band downlink after a 4-minute warm-up period.

The plots in Fig. 8-8 (for a type Ia first possible launch date) and Fig. 8-9 (for a type Ic last possible launch date) show the ground tracks for the first 24 hours after launch based on the optimum launch windows. Each ground track begins south and east of the launch site in Florida, goes through TIP and then SEP. Enter and exit Earth occultation times are indicated. For both trajectory types, the first DSN site to view the spacecraft after launch, called the "initial acquisition" site, was Canberra, Australia. An important mission consideration was whether the spacecraft would be in view of the initial acquisition site when it separated from the launch vehicle. Because separation data is very important for launch-phase performance assessment, the MSL mission contracted with a non-DSN network, the Universal Space Network (USN), which would have a station with line-of-sight at separation time for any of the type I trajectories.

As was shown in Table 8-3, all launch dates (for the type Ia, type Ib, or type Ic trajectories under consideration) had windows with 2-hour durations on any launch date. The center of the 2-hour period is optimal. Figure 8-12 shows the ground track during the first ten minutes after TWTA power-on for these trajectories for launches at window open, optimal, and window close.

Figures 8-10 and 8-11 show the station elevation angles for the first 48 hours after injection for trajectories of type Ia and type Ic assuming a launch on the first possible launch date for Type Ia and the last possible launch date for type Ic. Because the initial trajectory was slightly south of the Equator for type Ia, the Canberra site, which has higher elevation angles, was favored. The opposite is true for the type Ic last possible launch date trajectory, for which Goldstone, California, and Madrid, Spain (both northern sites) would have been favored.

---

[7] There is nothing in terms of spacecraft power subsystem capability about associating MSL TWTA power-on with eclipse exit. However, defining it at this time allowed for a reasonable interval after the initial ascent for the microwave circuitry to vent residual gases to vacuum before subjecting it to high power radio frequency (RF) energy, thus adhering to the TWTA maker's recommendation for a period of hard vacuum before generating RF power for the first time after launch. The added time also reduced the possibility of RF breakdown or arcing in the waveguides or the TWTA itself.

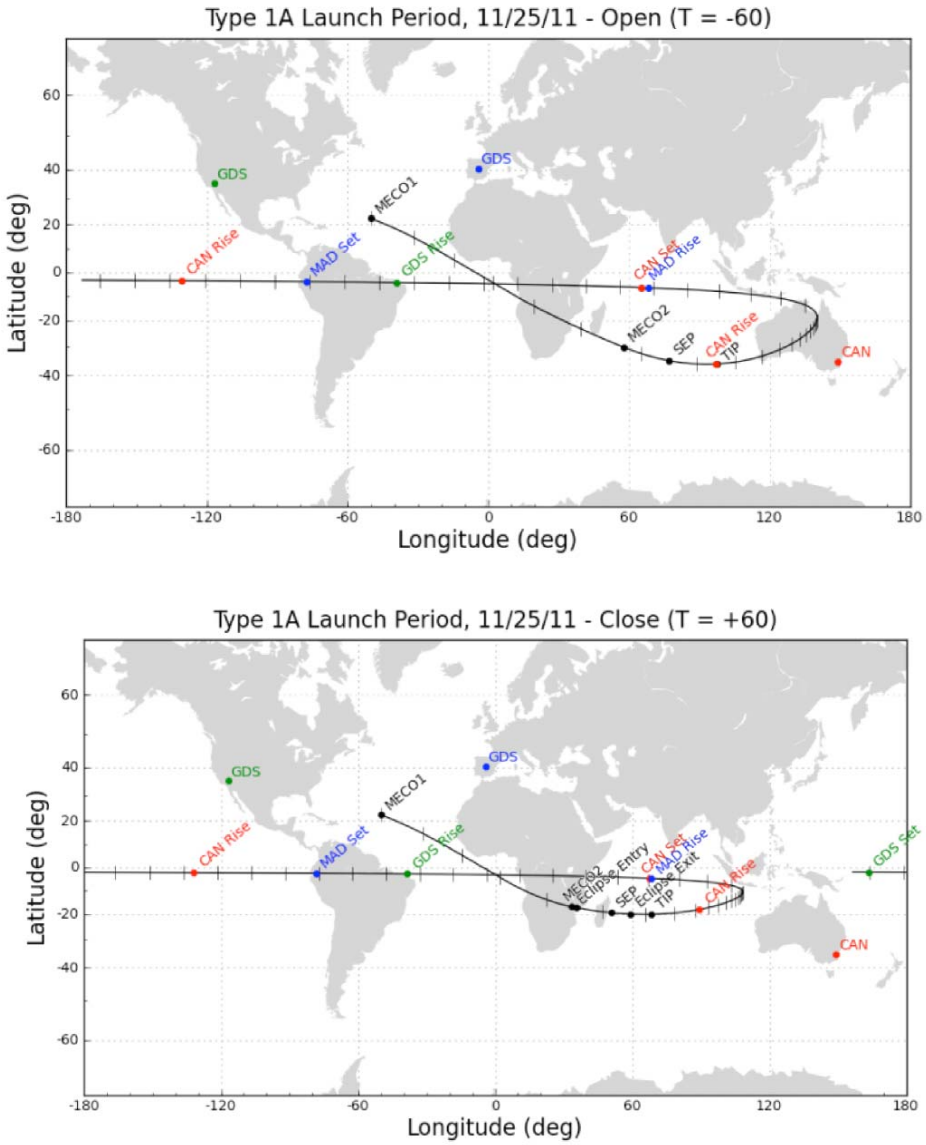

Fig. 8-8. Launch trajectory ground tracks for optimal launch windows (first possible launch day for type Ia trajectory).

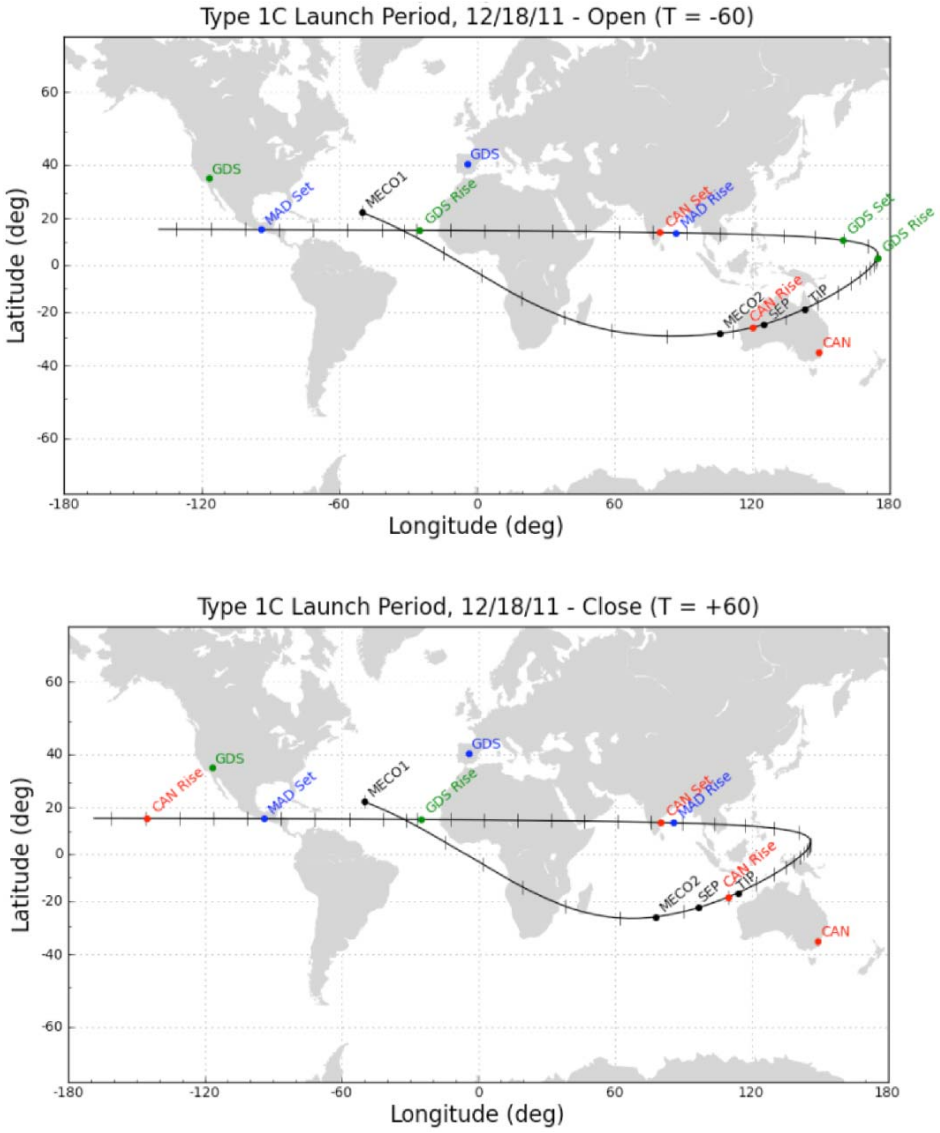

Fig. 8-9. Launch trajectory ground tracks for optimal launch windows (type Ic last possible launch day).

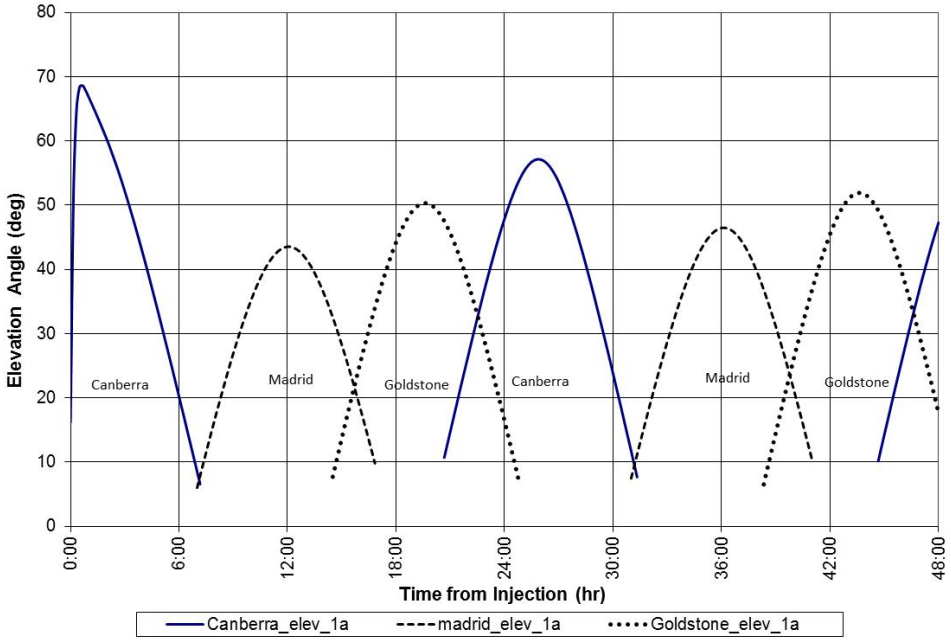

Fig. 8-10: Station elevation angle (type Ia trajectory for the first possible launch day).

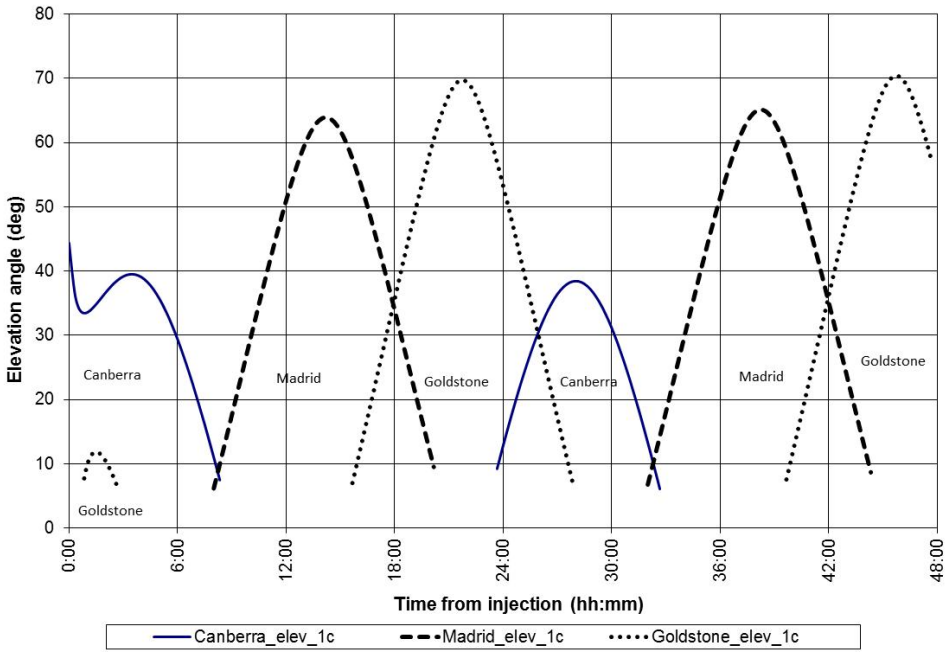

Fig. 8-11. Station elevation angle (type Ic trajectory for the last possible launch day).

A station has two minimum-elevation coverage ‘masks’, the higher (10 deg) for transmitting and the lower (about 6 deg) for receiving. Stations are not allowed to transmit below 10 deg (in order to limit the radio frequency (RF) power flux density that hits the Earth). Depending on the terrain in the vicinity of the station, a station does not have line-of-sight to receive below approximately 6 deg elevation; this elevation is, therefore, taken as the mask. For navigation, with both receiving and transmitting required, the minimum mask is 10 deg.

In addition to the DSN sites, the Universal Space Network (USN) and European Space Agency (ESA) have tracking stations at Mauritius and in Western Australia. These sites (Fig. 8-13) offered views to the spacecraft sooner after separation than the DSN sites. Figure 8-14 presents the minimum–maximum envelope of spacecraft–Earth ranges for the first 48 hours for type Ia and type Ic trajectories. The three curves are early type Ia and Ic and late type Ic trajectories (late type Ia is nearly identical to late type Ic). The purpose of this figure is to show how fast the spacecraft moves away from Earth after launch. By the third deep space station (DSS) pass (about 20 hours past injection), the spacecraft was already at Moon-distance (about 380,000 km).

With antenna pointing angles constant, the communications capability falls off with the square of the distance between transmitter and receiver. This decrease in capability is called space loss, and it is an important factor in the link budget or design control table (DCT) that defines performance at a given point in time. As a number, the space loss changes as 1/(range squared) and in decibels (dB) as $-20 \times \log$ (range). Figure 8-15 shows how the space loss increases, as a function of time (in hours), almost 30 dB in the first 24 hours, then about another 5 dB in the next 24 hours.

After 48 hours (Fig. 8-14), depending on date within the launch window, the range would be between 660,000 and 840,000 km for a type I trajectory. Because of the logarithmic character in space loss, the span of the signal strength due to range differences for these four cases at 48 hours is approximately 2 dB, as shown in Fig. 8-15.

Like other deep-space missions, MSL began its flight under tracking station strong-signal constraints that are unique to the initial acquisition portion of the mission. To accommodate the 40-dB decrease in signal level that occurred during initial acquisition day. MSL used the following common uplink and downlink DSN configurations. (Section 8.3 includes a block diagram for a 34-m tracking station, showing the elements involved in these configurations.)

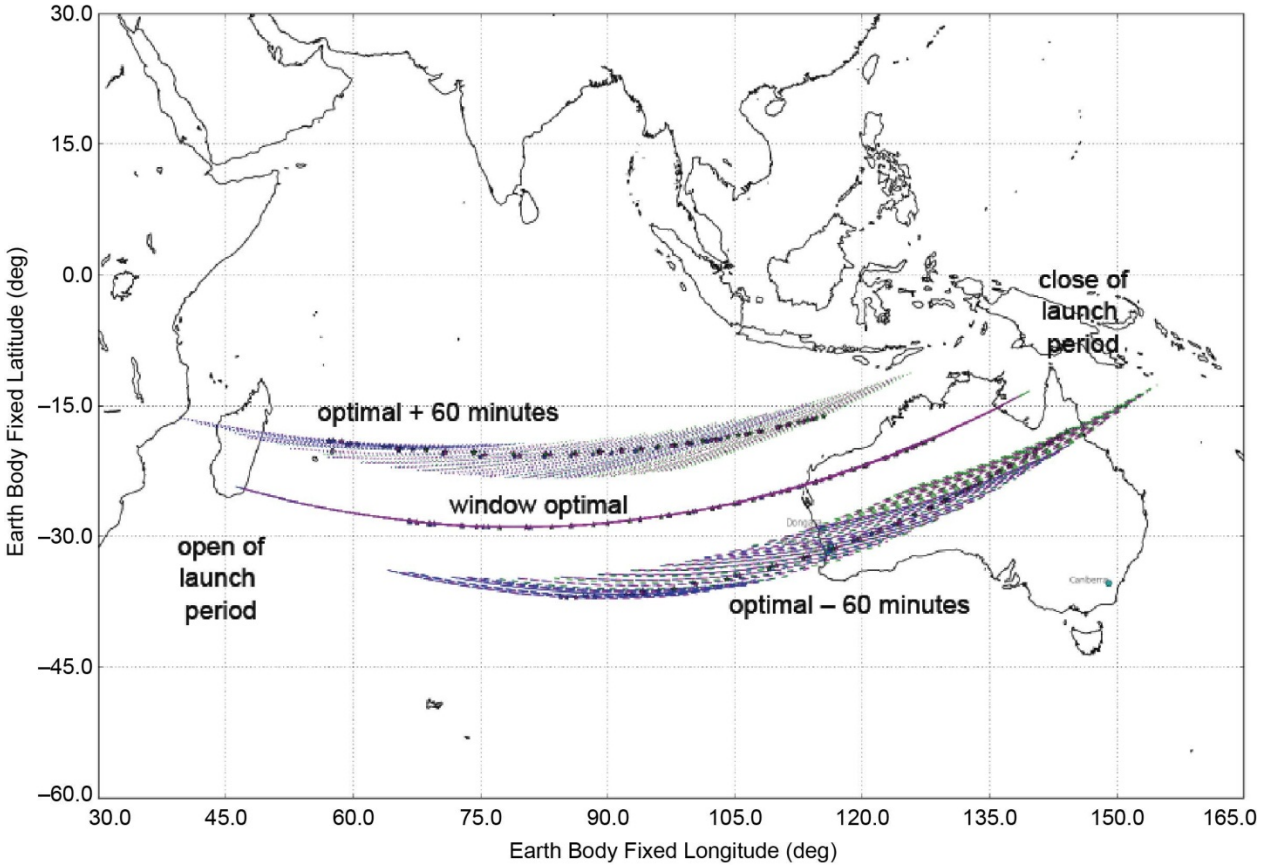

Fig. 8-12. Initial (first 10 min) ground track for type I trajectories (Earth body fixed longitude in degrees).

Fig. 8-13. USN and ESA tracking sites for MSL after separation.

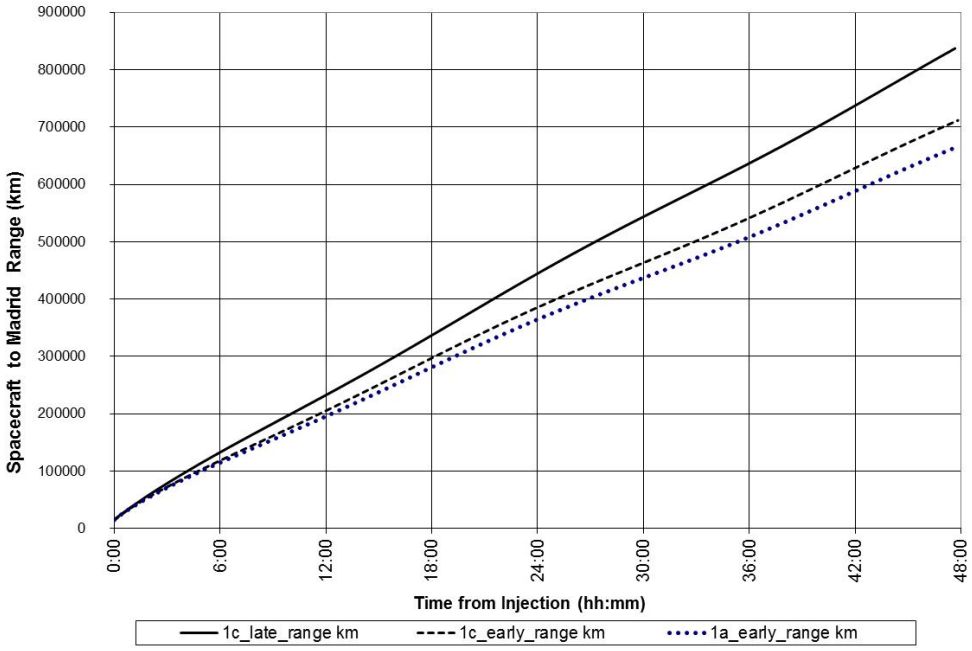

Fig. 8-14. Madrid DSS range to MSL for 48 hours after injection.

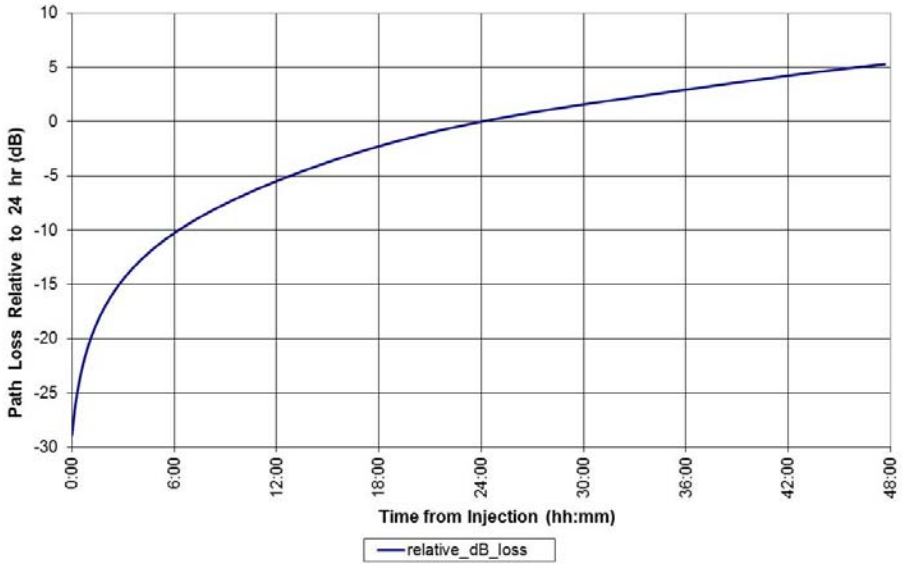

Fig. 8-15. Madrid space loss to MSL, type Ia nominal trajectory.

- Uplink: The station transmitter operated at 200 watts (W, normal is 18 kilowatts [kW]) for the first three passes (spanning about 24 hours total), then operated at the normal power level.
- Downlink: For the first pass only, the station microwave system was configured to receive the opposite polarization from that transmitted. For MSL, this meant the initial acquisition 34-m station received the RCP downlink while configured for left circular polarization (LCP). Since the distance was so close and the signal so strong, polarization leakage still provided a strong enough signal to close the link.

From the project's press releases and status reports [8], the following are highlights of the launch and early cruise phases.

November 26, 2011. Liftoff of Curiosity from the Cape Canaveral Air Force Station aboard an Atlas V rocket occurred at 15:02 UTC (10:02 a.m. EST). The Atlas V initially lofted the spacecraft into Earth orbit and then, with a second burst from the vehicle's upper stage, pushed it out of Earth orbit into a 352-million-mile (567-million-kilometer) journey to Mars. Based on subsequent radio navigation data and trajectory determination, this launch produced one of the most accurate interplanetary injections ever.

December 1. The project postponed the early trajectory correction maneuver (TCM-1), to early January. That first of six planned course adjustments during

the 254-day journey from Earth to Mars had originally been scheduled for 15 days after the Nov. 26 launch.

Prior to TCM-1, the spacecraft's initial trajectory had been deliberately planned and executed to miss Mars by about 35,000 miles (mi) (56,400 km). This precaution protected Mars from Earth's microbes, because the Centaur upper stage of the launch vehicle, which was not thoroughly cleaned the way the spacecraft was, left Earth on nearly the same trajectory as the spacecraft. This trajectory would miss Mars by about 38,000 mi (61,200 km).

January 11, 2012. Starting with TCM-1, trajectory correction maneuvers were planned to put the spacecraft on course and on timing to land at Mars' Gale Crater on Aug. 6, 2012, Universal Time.

Following TCM-1, if not subsequently refined by TCM-2, the trajectory would have put Curiosity about 3,000 mi (5,000 km) and 20 minutes away from entering Mars' atmosphere at the right place and time.

8.1.4 Cruise Phase

Similar to the Mars Exploration Rover (MER) mission [9],[8] the interplanetary trajectory attitude control plan for MSL had the cruise stage spinning at 2 revolutions per minute (rpm) until shortly before entry into the Martian atmosphere. The cruise antennas (a medium gain antenna and a low gain antenna) were mounted with their boresights co-aligned with the spacecraft –Z axis. The –Z axis was closely aligned with the spin axis of the spacecraft. In Fig. 8-3, the –Z axis is a line from bottom to top and in the plane of the drawing. Due to mass imbalances, the center of mass was slightly offset from the –Z axis, resulting in a small wobble as the spacecraft spun. Because of the spinning, the worst-case antenna gain around the axis of revolution faced Earth at least once every revolution (thus every 30 s); therefore that worst-case value was modeled for link prediction.

The major activities in the Cruise phase included checkout and maintenance of the spacecraft in its flight configuration, routine monitoring of spacecraft health and subsystem performance, characterization and calibration of the spacecraft and payload subsystems (and associated parameter updates), attitude

[8] The MER program included two rovers that launched in 2003. Spirit landed on Mars on January 4 and Opportunity on January 24, 2004. Spirit's end of mission was declared May 25, 2011 when the rover did not communicate with Earth after a Martian winter. Opportunity has continued to operate, going into 10 years of operation on the surface.

maintenance turns; navigation activities for determining and correcting the vehicle's flight path (for example, trajectory correction maneuvers [TCMs]), and preparation for EDL and surface operations. The three forms of navigation data that involved the telecom links were:

1. Two-way Doppler, provided whenever the spacecraft receiver was in coherent mode and in lock with an uplink carrier, and the downlink carrier was in lock in the station receiver.

2. Turnaround ranging, provided with the uplink and downlink carriers in the two-way Doppler mode and when the spacecraft ranging channel was on and the uplink carrier modulated with the ranging signal.

3. Delta differential one-way ranging (DOR) provided when the spacecraft transmitted a one-way downlink and the spacecraft DOR tones were sequenced on. Two tracking stations would, in coordination, each alternately track the spacecraft and a quasar so as to fix the angular location of the spacecraft relative to the quasar.

The MSL mission planned for as many as six TCMs, with the expectation the last few would be cancelled if the trajectory remained good for entry without them (see Table 8-5 for more detailed TCM information).

The propulsion system was designed to execute axial and lateral propulsive velocity corrections in the spacecraft reference frame. A vector mode maneuver is one that combines the axial and lateral segments so that the vector sum produces the desired inertial change in velocity (the "delta V") in magnitude and direction. This is a powerful maneuver-implementation mode that spinning spacecraft such as MSL could accomplish without executing a turn. A no-turn vector mode maneuver reduces operational risk by eliminating the estimation and control of a new attitude with potentially unknown characteristics. Additionally, the existing attitude was part of the nominal plan and well characterized; it provided adequate spacecraft power, and supported ground communication. The downside to vector mode maneuvers, though not a problem for MSL, is mainly higher propellant costs, especially for large "delta V" corrections [10].

8.1.5 Approach Phase

The Approach phase was defined to begin 60 days prior to entry into the Martian atmosphere and to end when the spacecraft reached the atmospheric entry interface point, defined as a radius of 3522.2 km from the center of Mars. The principal activities during the Approach phase included the acquisition and processing of navigation data needed to make decisions on the need for the

final three TCMs (and to support their development if any of them had been required) and the spacecraft activities leading up to the separation from the cruise stage and start of EDL.

From a Telecom point of view, Approach was considered just late cruise in terms of range, antennas, link performance, etc. Cruise stage configurations and station configurations continued in use.

Table 8-5. Trajectory correction maneuvers planned during Cruise.

TCM	Time	OD Data Cutoff*	Description
TCM-1	L + 15 days	L + 10 days	Corrected injection errors; removed part of injection bias for planetary protection; partial retargeting to entry aimpoint for desired landing site; aimpoint biased for planetary protection. This TCM was postponed to Jan. 11, 2012 [8] TCM-1 took 3 hours. It first made a 19-minute velocity change in the direction of the axis of rotation, then more than 200 five-second timed bursts to achieve a velocity change perpendicular to that axis.
TCM-2	L + 120 days	L + 115 days	Corrected TCM-1 errors; remove part of injection bias for planetary protection; partial retargeting to entry aimpoint for desired landing site; aimpoint biased for planetary protection; vector-mode maneuver. Executed March 26, 2012. TCM-7 was 1/7 as large as TCM-1, with 3-minutes of thrust in the direction of the axis of rotation, followed by more than 60 five-second timed bursts for a velocity change perpendicular to that axis.
TCM-3	E– 60 days	E – 65 days	Corrected TCM-2 errors; target to entry aimpoint for desired landing site; vector-mode maneuver executed June 26, 2012. Four thruster firings totaling 40 seconds, to move the atmospheric entry point by 125 mi (201 km) and to advance the time of entry by about 70 seconds.
TCM-4	E– 8 days	E – 8.5 days	Corrected TCM-3 errors; vector-mode maneuver, planned prior to launch and executed on July 29, 2012. Two thruster firings totaling 6 seconds, to move the atmospheric entry point by 13 mi (21 km).
TCM-5	E– 2 days	E – 2.5 days	To correct TCM-4 errors; final entry targeting maneuver required to achieve EFPA delivery accuracy requirement, vector-mode maneuver. Cancelled, not required [8].
TCM-5X	E– 1 days	E – 1.5 days	Contingency maneuver for failure to execute TCM-5; vector mode maneuver. Because TCM-5 was cancelled, TCM-5X was (also) cancelled.
TCM-6	E – 9 hours	E – 14 hours	Contingency maneuver; final opportunity to target entry aimpoint; vector-mode maneuver. Cancelled, not required.

* Time measured from launch (L) or entry (E); OD = orbit determination; EFPA = entry flight path angle.

From the project's press releases and status reports [8], the following were highlights of the cruise and approach phases of the mission.

March 26, 2012. Halfway to Mars, the spacecraft adjusted its flight path for delivery of Curiosity to the surface of Mars in August. The spacecraft ignited thrusters for TCM-2 for nearly nine minutes, nudging the spacecraft one-seventh as much as TCM-1. Spacecraft data and Doppler-effect changes in radio signal from the craft indicate the TCM-2 maneuver succeeded.

June 26. TCM-3 executed, with four thruster firings totaling just 40 seconds. The maneuver served both to correct errors in the flight path that remained after earlier correction maneuvers and to carry out a decision that month to shift the landing target about 4 mi (7 km) closer to the mountain, informally named Mount Sharp. Shifting the landing target shaved months off the time needed for driving from the touchdown location to selected destinations.

TCM-3 altered the spacecraft's velocity by about one-tenth of a mile per hour (mph) (50 millimeters per second [mm/s]). The flight's first and second trajectory correction maneuvers produced velocity changes about 150 times larger on Jan. 11 and about 20 times larger on March 26, respectively.

July 11. The spacecraft completed an attitude control turn (not a TCM), adjusting its orientation for keeping its medium-gain antenna pointed toward Earth for communications. This was the third-to-last attitude control turn planned before landing day.

July 28. TCM-4 altered the flight path less than any of the spacecraft's three previous trajectory correction maneuvers on the way from Earth to Mars. Without this maneuver, the spacecraft would have hit a point at the top of the Martian atmosphere about 13 mi (21 km) east of the target entry point. The thruster firings altered the spacecraft's velocity by about one-fortieth of 1 mph (1 centimeter per second [cm/s]).

8.1.6 EDL Phase

Following a 5-day final approach, Entry Descent and Landing (EDL) was divided into three stages, lasting a total of 21 minutes. Figures 8-16 through 8-20 are pictorials of the various stages of EDL.

- First stage, Fig. 8-16 (15 minutes ending at entry), included:
    - EDL start, ending with cruise stage separation.

  - Exo-atmospheric, ending with switch to the tilted low-gain antenna (TLGA), bypassing the descent stage diplexer[9], and reaching the reference entry interface.
- Second stage, Fig. 8-17 (5 minutes beginning at entry), included:
  - Entry, including a period of potential UHF blackout due to plasma generation.
  - Parachute descent, including heat shield separation and using the landing radar, formally called the terminal descent sensor (TDS) and described in Section 8.2.
- Third stage, Fig. 8-18 (less than 1 minute starting at entry plus 309 s and ending at touchdown), included:
  - Powered descent phase, including backshell separation with switch to X-band descent low gain antenna (DLGA) and the descent UHF (DUHF) antennas.
  - Sky crane phase (during which the descent stage acted as a sky crane to lower the rover shortly before it landed), including touchdown and electrical bridle cut.
  - Flyaway of the sky crane.

Figures 8-16 and 8-17 show, respectively, the spacecraft events connected with the first two stages. Figure 8-19 shows the final stage, and Fig. 8-20 provides an overview of the entire process.

The pre-EDL (PEDL in Fig. 8-16) spacecraft maneuvers for EDL started approximately 10 minutes before Entry, with cruise stage separation (CSS). Unlike MER, the spacecraft remained pointed toward Earth during CSS.

After CSS, the spacecraft reduced its spin rate from the 2 rpm that existed throughout cruise. After approximately 1 minute, the spacecraft performed the turn to entry (TTE) maneuver. At this point, the attitude of the entry body was no longer optimal for Earth communications.

Prior to the spacecraft reaching the entry interface point, the EDL sequence separated the cruise balance masses (CBM), as shown in the second from last sketch in Fig. 8-16, moving the center of mass of the entry body to induce the proper angle of attack to enable aerodynamic lift.

---

[9] The EDL sequence bypassed the descent stage diplexer to prevent coronal discharge within the diplexer during the repressurization during entry. Since receive capability was no longer required during entry, diplexer bypass had no effect on meeting telecommunications requirements.

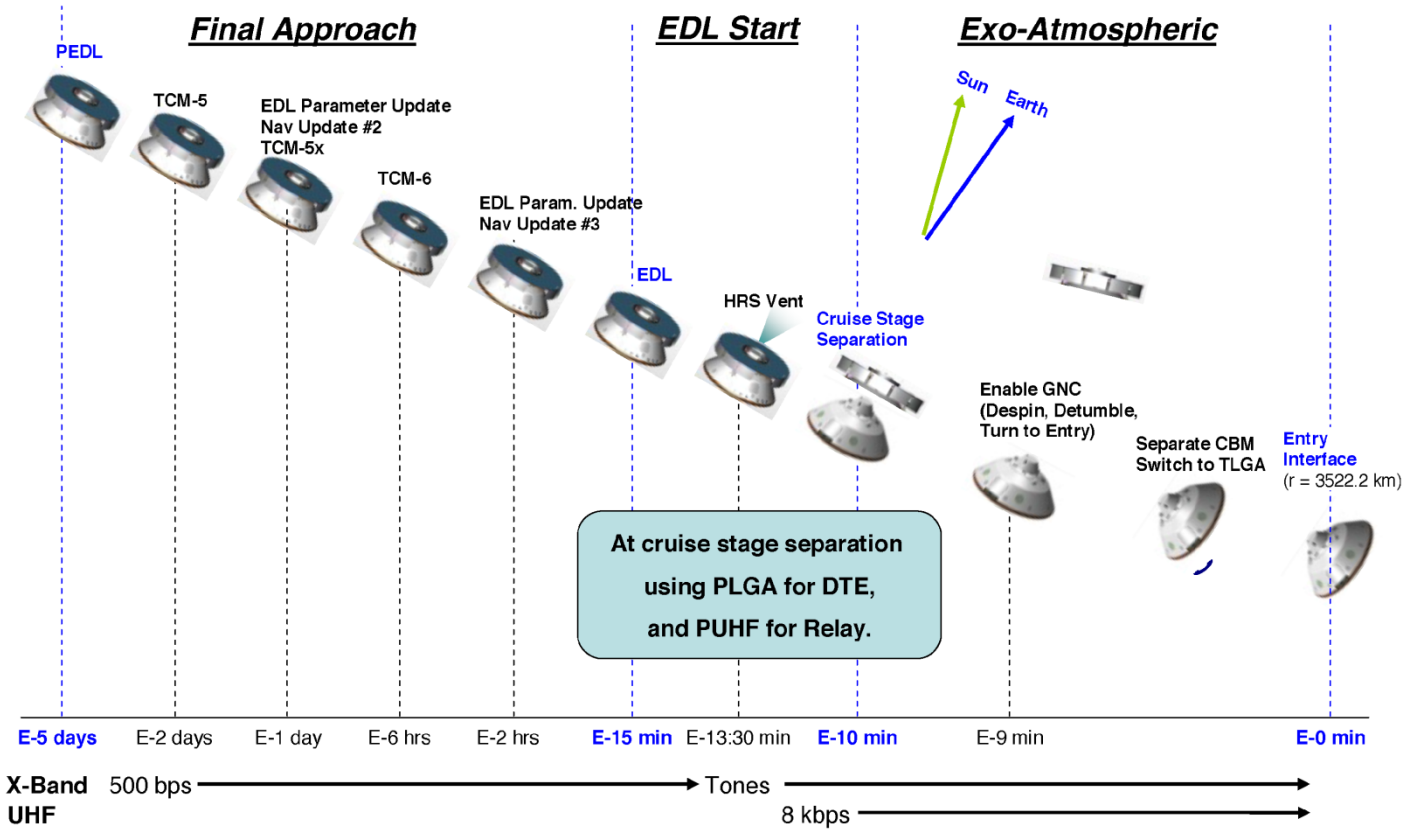

Fig. 8-16. Timeline: Cruise Stage separation to entry interface (CBM = cruise balance mass; GNC = guidance, navigation, and control; HRS = heat rejection system).

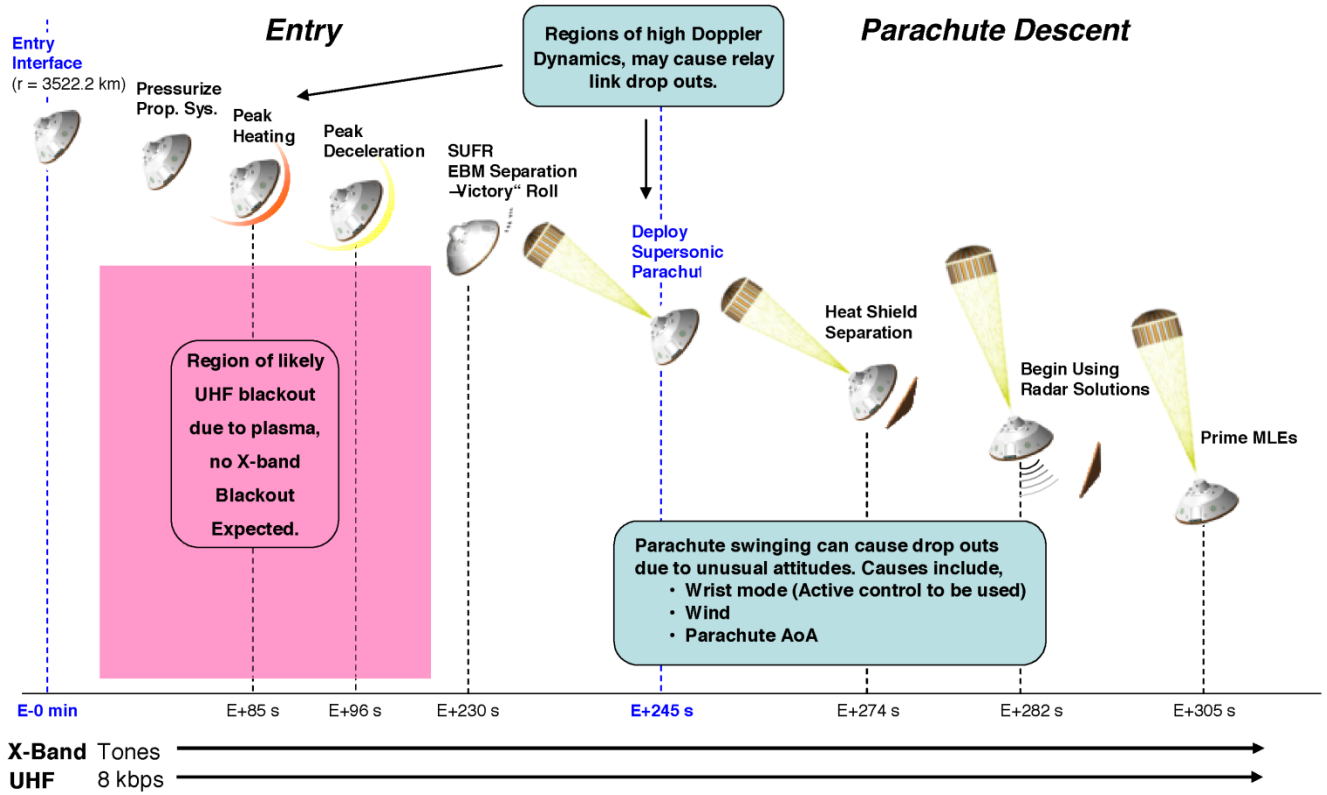

Fig. 8-17. EDL timeline: entry interface to backshell separation (EBM = entry balance mass, SUFR = straighten up and fly right).

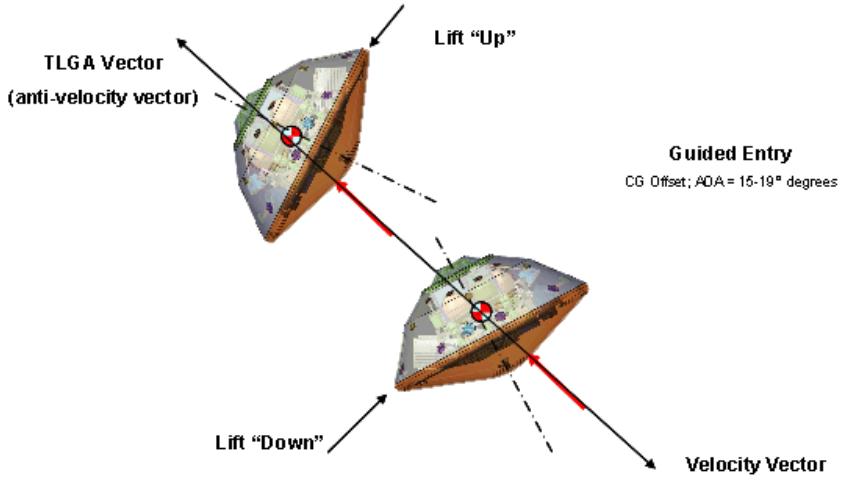

Fig. 8-18. Banking maneuver along anti-velocity vector (AOA = angle of attack, CG = center of gravity).

The nominal planned angle of attack was between 15 and 19 deg. The angle of attack varied as much as ± 2.5 deg from the design value until shortly before parachute deploy. The TLGA's beamwidth and mounting direction accommodated this range of angle. The TLGA was mounted with its boresight at 17.5 deg from the –Z axis of the spacecraft.

After entry, the vehicle performed banking maneuvers to achieve a smaller landing ellipse (guided entry). These banking maneuvers used repeated short (about 20 millisecond) firings of the reaction control system (RCS) thrusters. As shown in Fig. 8-18, where Mars is at the bottom, a "lift up" maneuver was included to tilt the heat shield slightly above the velocity vector and a "lift down" maneuver to tilt it slightly below. During this time, the angle of attack (AoA) remained in the range of 15 to 19 deg. The MSL TLGA was nominally aligned with the anti-velocity vector to minimize variations of off-boresight angles during banking. This alignment resulted in variations in off-boresight angle to be roughly equal on either side of the antenna's boresight, rather than skewed to one side of boresight.

During the period of peak heating (Fig. 8-17, centered at ~ E +85 s), it was also expected that the UHF signal could experience a dropout due to plasma shielding (see Section 8.4). The actual blackout went from about entry plus 40 s until entry plus 80 s, which was similar to MER. Next came the period of peak deceleration that caused the mission's most challenging Doppler dynamics for signal acquisition and tracking. From final approach and EDL status reports [8]:

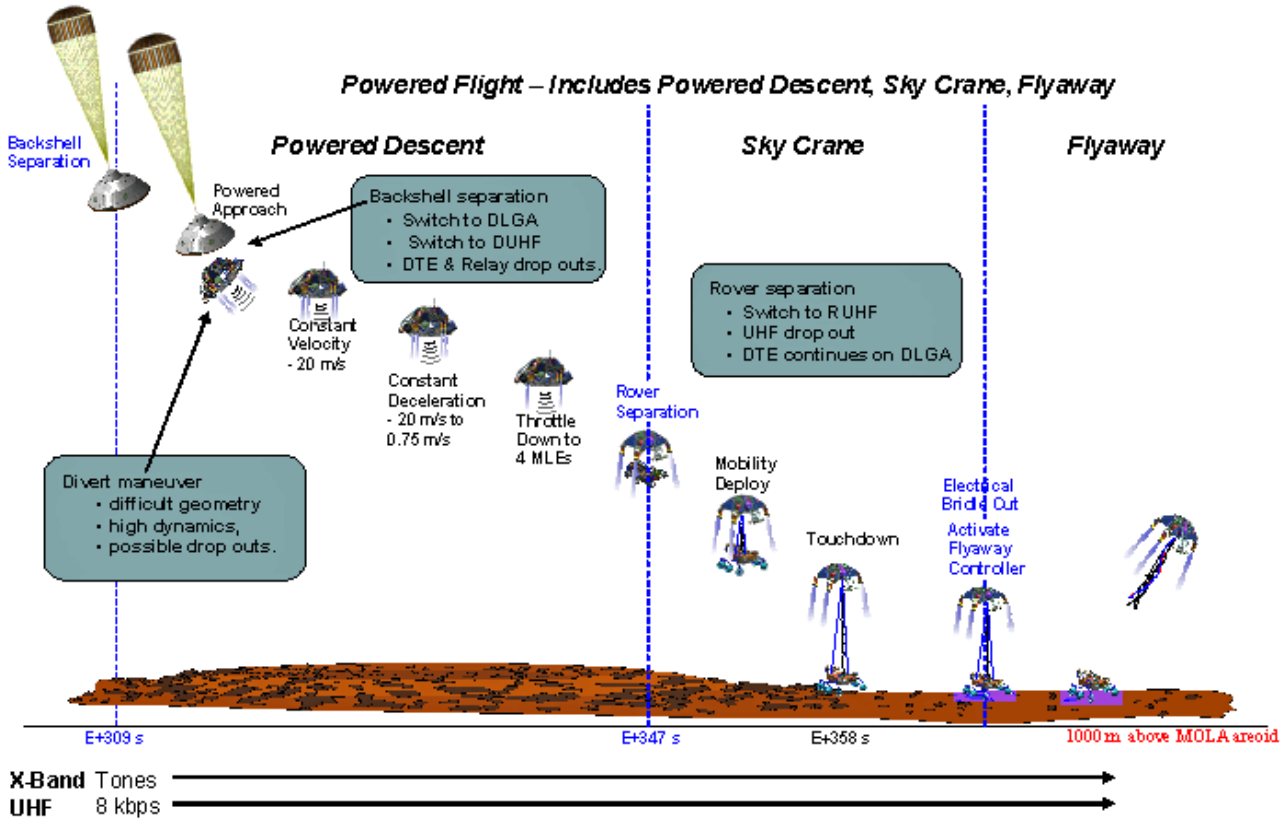

Fig. 8-19. EDL timeline: backshell separation to fly-away (MOLA = Mars Observer Laser Altimeter).

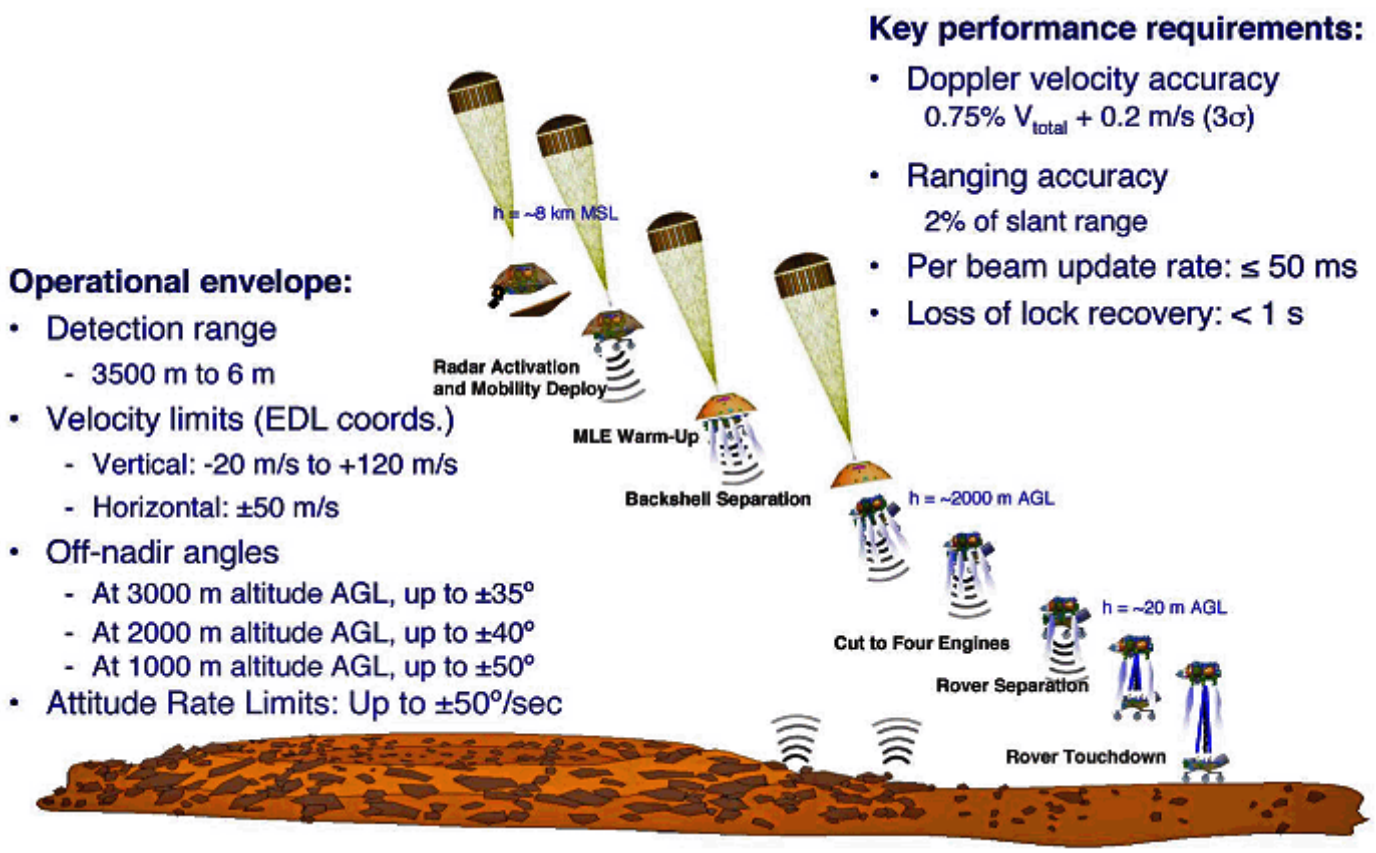

Fig. 8-20. Overview of TDS requirements during EDL (AGL = above ground level).

August 1, 2012. Curiosity began flying under the control of the autonomous EDL timeline. “Those seven minutes are the most challenging part of this entire mission,” said Pete Theisinger, the mission’s project manager at JPL. “For the landing to succeed, hundreds of events will need to go right, many with split-second timing and all controlled autonomously by the spacecraft. We’ve done all we can think of to succeed. We expect to get Curiosity safely onto the ground, but there is no guarantee. The risks are real.”

The flight team cancelled the build and test of the contingency version of Trajectory Correction Maneuver 5. This contingency maneuver, had it been needed, would have been used in the event an emergency prevented the team from executing the nominal scheduled TCM-5 maneuver, which was planned for Aug. 3, if needed. The project also canceled a corresponding update to parameters for the autonomous software controlling events during entry, descent and landing.

August 3. The project decided that the planned Trajectory Correction Maneuver 5 (TCM-5) and its corresponding update to parameters for the autonomous software controlling events during EDL would not be necessary. As of 19:35 UTC, the spacecraft was approximately 468,000 mi (753,200 km) from Mars, or a little less than twice the distance from Earth to the Moon. It was traveling at about 8,000 mph (3,576 meters per second (m/s). It would gradually increase in speed to about 13,200 mph (5900 m/s) by the time it reached the top of the Martian atmosphere.

August 4. The flight team uplinked and confirmed commands to make minor corrections to the spacecraft’s navigation reference point parameters. As part of the onboard sequence of autonomous activities leading to the landing, catalyst bed heaters were turned on to prepare the eight Mars Lander Engines (MLEs) that were part of MSL’s descent propulsion system. Also, parameters on a motion tracker were adjusted for fine-tuning determination of the spacecraft’s orientation during its descent.

August 5. Flight controllers decided to forgo the sixth and final opportunity on the mission calendar for a course-correction maneuver. The spacecraft was headed for its target entry point at the top of Mars’ atmosphere precisely enough that the maneuver was deemed unnecessary. Mission controllers also determined that no further updates would be necessary to the onboard information the spacecraft would use during EDL.

August 6. Touchdown in Mars’ Gale Crater was confirmed to be 05:32 UTC (August 5 at 10:32 p.m. at the mission control center at JPL.) The time of day at the landing site was mid-afternoon—about 3 p.m. local Mars time at Gale

Crater. Initial information received via the UHF relay links with Odyssey and MRO was that Curiosity landed facing east-southeast within Gale Crater, with a heading of 112.7 deg (±5 deg), and a few degrees of tilt. A first look at some color images taken just before landing by MSL's Mars Descent Imager provided this information on the rover's precise location. A Sol 1 overpass a few hours after EDL by Mars Odyssey provided additional information on Curiosity's position and additional imagery.

Figure 8-19 shows the last portion of EDL, starting with parachute deployment and followed by heat shield separation, radar activation, and backshell separation (BSS). At this point, the vehicle started its powered descent phase, during which the descent stage, acting as a sky-crane, lowered the rover using a bridle approximately 7 m long. After rover touchdown, the descent stage executed a fly-away to set down sufficiently far from the rover landing site to avoid the possibility of damage to the rover or contamination of the area around the rover landing site. Because the descent stage's "landing" was uncontrolled in attitude and velocity – destroying the stage, there was no expectation of further DTE X-band radiation being received from the DSDST and the TWTA.

While slowing on the parachute, the system prepared the propulsion subsystem, separated the heat shield, and began using the TDS to acquire a landing solution. (Note: A change from the 2009 mission plan was that the mobility deployment of the wheels was sequenced to occur during the sky crane maneuver in the final seconds before touchdown).

To achieve a soft controlled landing, the EDL system had to be able to accurately measure altitude and three-axis velocity (that is, horizontal and vertical velocity) beginning at several kilometers and continuing all the way down to a few meters above the surface. The TDS was designed to provide these measurements starting at heat shield jettison all the way to rover touchdown.

8.1.6.1 DTE Prime to Entry; Both DTE and Relay via MRO after Entry

Planning for communications during EDL had to be complete before landing site selection or knowledge of the specific launch date. Communications design and use had to be sufficient to allow a reasonable chance to determine what happened (using data reconstruction) in the event of an EDL failure. These mandates had been in place by Headquarters at the National Aeronautics and Space Administration (NASA) since the Mars Polar Lander failure of 1998.

Due to limitations on the range and view angles to the Mars orbiters ("relay assets"), relay during MSL EDL cannot cover the entire time from CSS to landing + 1 minute. Since the majority of important events would occur after

entry, the preparation for EDL included phasing of the orbiters in their orbits to optimize a relay link from entry to landing + 1 minute. The mission design baseline was that X-band DTE should provide the coverage during the period from CSS to entry, a time when, by comparison to the after-entry period, relatively few events occur. Nevertheless DTE coverage from CSS to landing + 1 minute is desirable. The period of maximum heating was expected to create a plasma envelope sufficient to produce a link dropout at UHF relay frequencies (but not at X-band), making DTE via a plasma-penetrating frequency highly desirable during this period.

In addition to the plasma blackout period, there were several short intervals during EDL when link dropouts for both relay and DTE were accounted for in the planning. Table 8-6 lists the most important dropout periods, the cause for each dropout, and the dropout's expected and actual duration.

Table 8-6. Periods of UHF or DTE dropouts between CSS and landing [11].

Event	RF link	Cause	LOS start relative to Entry (E), actual	LOS duration, used in EDL planning	Actual duration seen in EDL
CSS	X-band	Switch to PLGA and blockage by CS	E – 600 s, sequenced	1 s	7 s (including PLGA blockage)
Turn to Entry	X-band	Switch to TLGA	E – 20 s, sequenced	1 s	4 s
Plasma Blackout	UHF	Surrounding plasma envelope	E + 40 s	25 s to 100 s	40 s (carrier), 58 s (data)
Parachute Deploy	X-band	TLGA blockage due to Sabot	E + 260 s	75 s, worst case	No dropout, but high Doppler
Backshell Deploy	Both	Change to DUHF and DLGA, blockage	E + 375 s	1 s to 6 s	6 s (UHF Txr off)
Rover Separation	UHF	Change to RUHF, blockage	E + 410 s	1 s to 6 s	6 s (UHF Txr off)

The "parachute deploy" row of the table mentions a temporary blockage of the X-band DTE from the parachute deployment sabot[10] Figure 8-21 shows the MSL sabot in action during deployment of a parachute mass model from its canister during a ground test. The sabot is the device about a third of the way from the bottom of the picture. It is partially wrapped in a capture bag, a loose

[10] The term sabot referred originally to a device used in a firearm to hurl a projectile, such as a bullet, that is smaller than the bore diameter, or requires the projectile to be held in a precise position.

web of straps designed to keep it contained. The parachute mass model is at the top of the picture. Testing verified the movement of the sabot during parachute deployment to be quite violent, and there was a concern that when the sabot fell back to the top of the parachute canister it could impact and damage the PLGA. At backshell deployment, a steep-angled and very dynamic maneuver was performed by the powered descent vehicle to "divert" the spacecraft away from the parachute and backshell. This maneuver briefly created high Doppler rates and unusual attitudes that could cause a dropout in addition to the blockage and UHF antenna switch shown in the table.

8.1.6.2 Full-DTE EDL Communications

As discussed previously, full-DTE EDL communications is considered desirable as backup to the relay link after entry until landing + 1 minute. This so-called full-DTE coverage could not be guaranteed for both trajectory types and all landing sites. While the type II trajectory did offer full-DTE coverage for the four primary landing sites, only the northern landing site (Mawrth Vallis at 24 deg N) had full-DTE coverage for the type I trajectory.

The calculated end of DTE for the potential landing sites and cruise trajectory types and launch dates varied considerably, as early as a couple of minutes after entry to nearly as late as landing + 1 minute. For expected (nominal) communications performance and the actual type I launch on November 26, 2011, with a landing at Gale Crater on August 6, 2012, the X-band DTE loss of signal (LOS) was planned to be 2 minutes before touchdown, MRO UHF relay LOS to be 6 minutes after touchdown, and Odyssey LOS to be one minute after that.

The project relied on delay-free "bent pipe" UHF relay via the Mars Odyssey orbiter to provide immediate confirmation of a successful landing. Odyssey executed a turn to point in the right direction beforehand to listen to Curiosity during the landing. Without this Odyssey relay, a successful landing could not have been confirmed until more than 2 hours later from playback of MRO-recorded relay data from MSL.

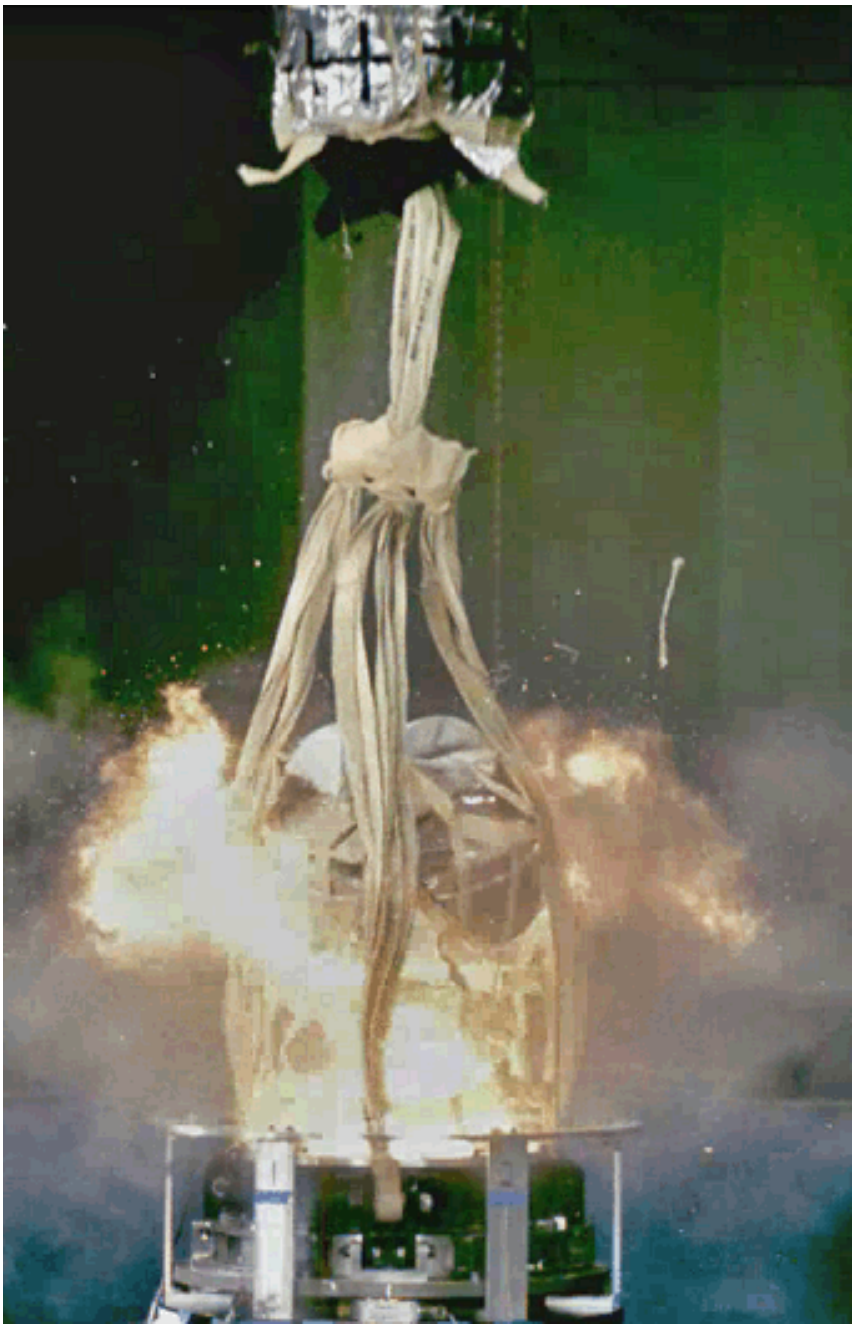

Fig. 8-21. Sabot, shown during ground parachute deployment test.

The baseline sequence for using the X-band EDL antennas was to start with the PLGA (which points along the spacecraft –Z axis from CSS to entry), and then the TLGA (which points along the average tilt angle and, therefore, close to the anti-velocity vector after turn to entry) at entry. Figure 8-22 illustrates the view angles for the antennas during EDL to the Gale Crater landing site (at 4.5 deg S), for the 2011 launch. A plot of the –Z axis views would show considerably greater variation after entry due to the guided entry maneuvers (banking turns); however, using the TLGA minimized the effects of these variations in angle.

8.1.6.3 Surface Phase

The minimum surface operations duration requirement for a successful MSL mission is one Martian year (669 Martian sols or 687 24-hr Earth days). The Earth geometry during the surface mission at Gale Crater is shown in Fig. 8-23. The Mars-Earth range (blue curve, left axis) varies between 0.6 and 2.4 astronomical units (AU) (0.9 and 3.6×10^8 km, respectively). MSL landed at an Earth–Mars range of 1.7 AU (2.5×10^8 km).

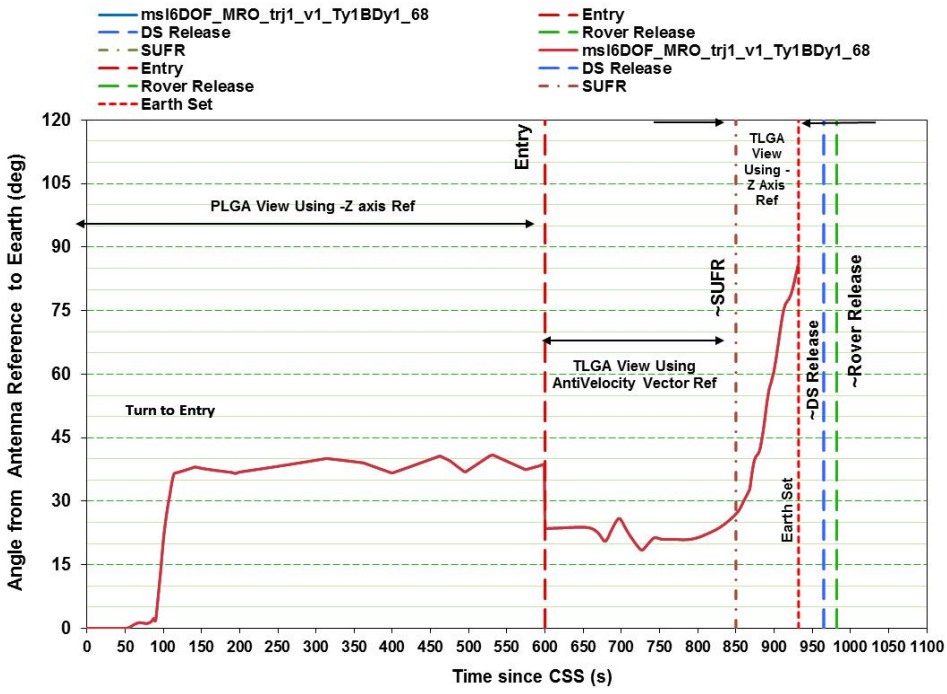

Fig. 8-22. Example DTE view angle (combination of anti-velocity and Z axis) during EDL (2011 launch data, Gale site).

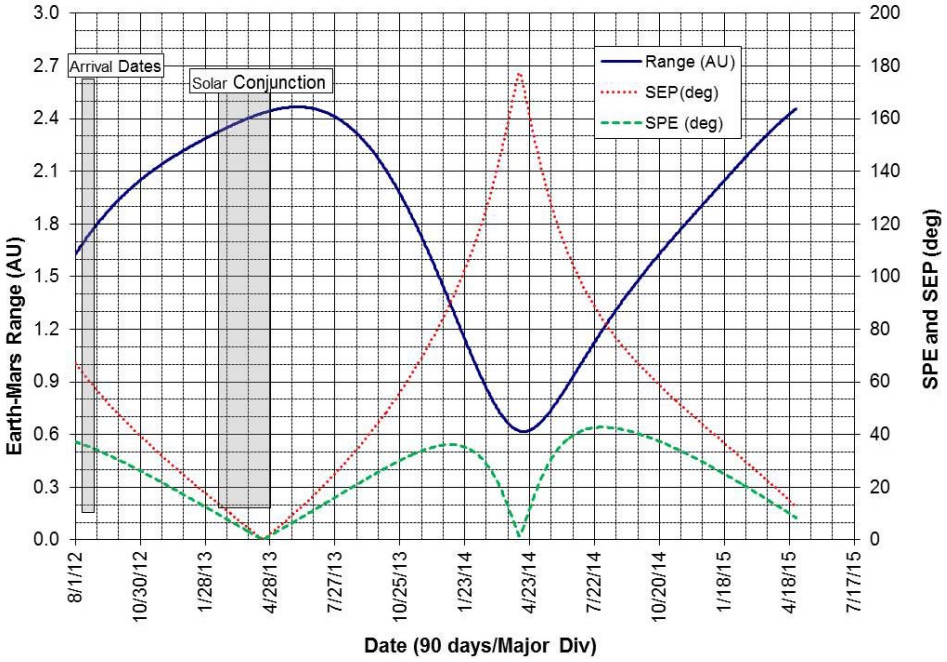

Fig. 8-23. MSL geometry during surface operations.

Figures 8-24, 8-25, and 8-26 were developed to show the surface operational environment as a function of landing site latitude in 15-degree increments from 30 deg N to 30 deg S. Gale Crater is 4.5 deg S, thus well approximated by the solid line labeled Equator. Fig. 8-24 shows how the Earth rise time varies by approximately 5 hours during 1 Martian year. Fig. 8-25 shows that the Earth set-time has a similar variation. The rise and set times are in Mars Local True Solar Time (LTST). [12][11]

[11] Because the orbit of Mars around the Sun is not perfectly circular and the planet does not rotate about an axis perpendicular to its orbit plane, there is a seasonally variable discrepancy between the even advance of an artificially defined mean solar time [12] and of the true solar time corresponding to the actual planet-centered position of the Sun in its sky. By analogy with the 24 time zones on Earth, Mars Mean Solar time is defined on the Mars prime meridian as Mars Time Coordinated, or MTC, by analogy to the terrestrial UTC (Universal Time Coordinated). Again by analogy with the Earth, local solar time at the selected location is defined in terms of similarly constructed "Mars time zones". These Mars time zones are exactly 15 deg wide and centered on successive 15-deg multiples of longitude, at 0 deg, 15 deg, 30 deg, etc.

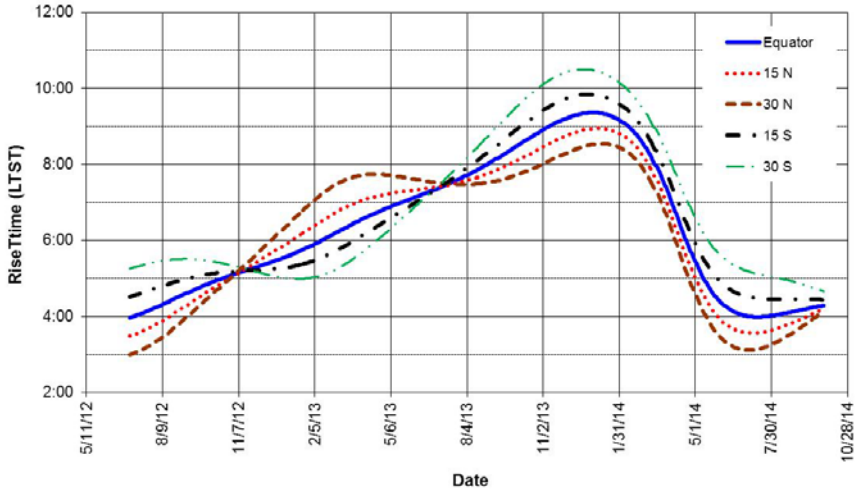

Fig. 8-24. Earth rise vs. date, for different MSL landing sites.

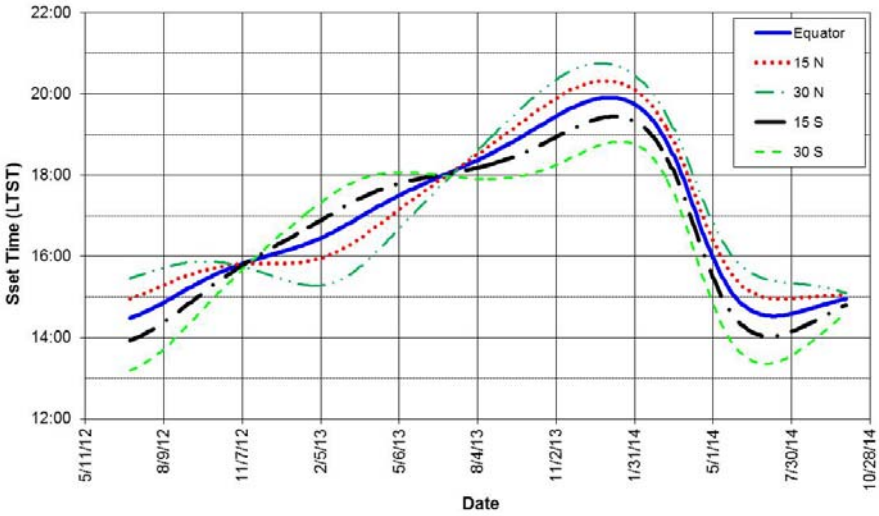

Fig. 8-25. Earth rise time for different MSL landing latitudes.

The duration per day that the Earth is visible (assuming a 10-deg land mask and zero rover tilt) is shown in Fig. 8-26. This duration (8 to 13 hours) is for the Earth, not for any one DSN site on the rotating Earth. Disregarding any constraints in DSN scheduling and uplink/downlink operations, the figure shows the maximum possible time per day available to uplink commands (via a direct from Earth [DFE]) link and to get telemetry data (via a DTE link).

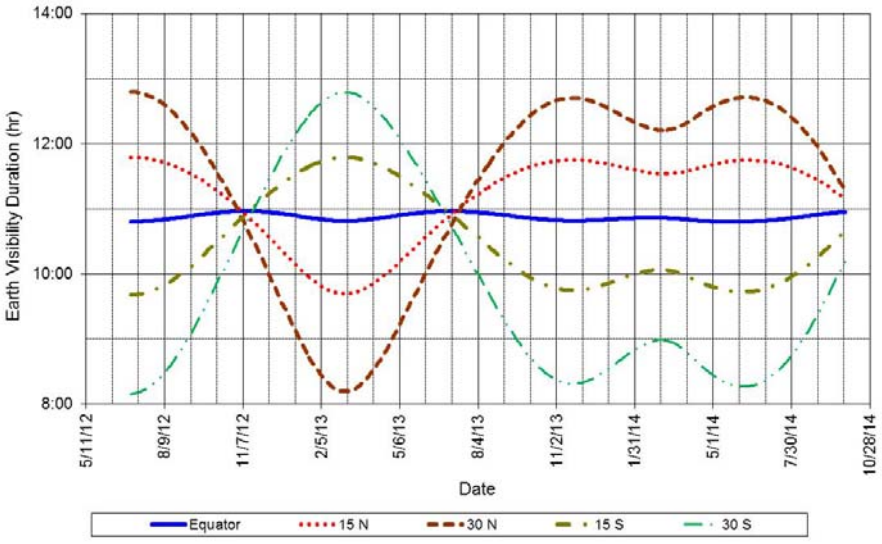

Fig. 8-26. Earth visibility duration vs. date (MSL surface mission, assumes 10-deg land mask and no lander tilt).

MSL relays UHF signals with the Mars Reconnaissance Orbiter (MRO) and Odyssey. Odyssey (launched in 2001) and MRO (launched in 2005) are referred to as the Mars Relay assets available during the MSL surface mission. Table 8-7 summarizes the classical orbital elements for the relay orbiters[12].

Figure 8-27 shows the amount of time per sol that MRO is above an elevation of 10 deg vs. the latitude of the rover's landing site. With MSL near the Martian Equator as it is for Gale Crater, the time MRO is above 10-deg elevation is approximately 13 minutes total, divided between two passes per sol.

Figure 8-28 gives the breakdown of visibility time for each 10-deg elevation step. For a landing site between 45 deg S and 45 deg N (which includes all four candidate sites), the percentage of time is approximately independent of latitude. It is seen that more than half the time is spent between 10 deg and 20 deg elevation and that the time spent progressively decreases until it is just one quarter of one percent for elevations between 80 and 90 deg. This implies

[12] See http://en.wikipedia.org/wiki/Orbital_elements for definitions of Orbital Elements as used in celestial mechanics. Six parameters (Keplerian elements) are necessary to unambiguously define an arbitrary and unperturbed orbit. In Table 8-7, the epoch defines a reference time when the sixth parameter, the mean anomaly (the position of the orbiter along its ellipse) is equal to zero.

that, on average, a broader antenna pattern, which provides significant coverage at low elevation angles, is advantageous, while high gain in the zenith direction is generally not useful.

Table 8-7. Orbital elements for relay orbiters.

Parameter	Odyssey	MRO
Semi-Major Axis (km)	3788.1479	3648.606
Eccentricity	0.0108616	0.012176
Inclination (deg)	92.894	92.655
Longitude of Ascending Node	235.4908	–10.695
Argument of Periapsis (deg)	267.5309	–90.003
Epoch	01-Jan-2006 00:01:00	07-Dec-2006 01:00:00

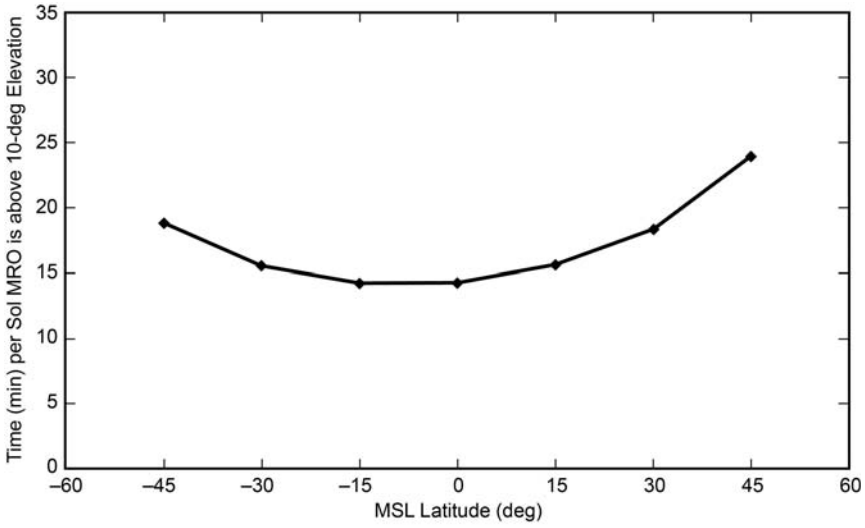

Fig. 8-27. Time (min) per sol MRO is above 10 deg elevation vs. MSL latitude.

8.1.7 Flight System Description

The flight system (Fig. 8-3) consists of an Earth–Mars cruise spacecraft, entry, descent, and-landing (EDL) system, and a mobile science rover with an integrated instrument package. In the figure, the MSL EDL instrumentation (MEDLI) [13] is an instrumentation suite installed in the heat shield of the Mars Science Laboratory's (MSL) Entry Vehicle to gather data on the atmosphere and on aerothermal, Thermal Protection System (TPS), and aerodynamic characteristics of the MSL Entry Vehicle during entry and descent providing engineering data for future Mars missions.

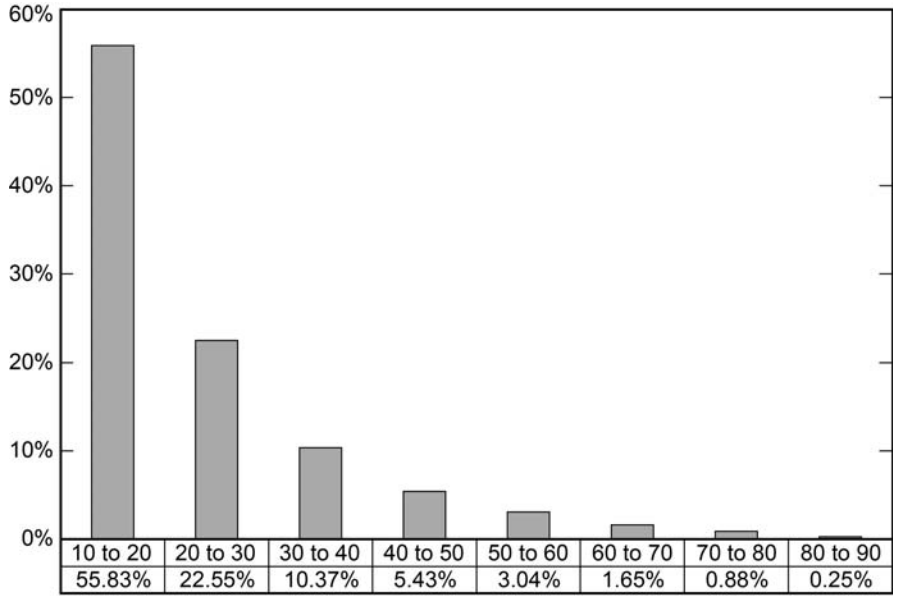

Fig. 8-28. Percentage of time spent by MRO between 10-deg steps in elevation.

During Cruise, the spacecraft was spin-stabilized (2 rpm); with the spin about the Z axis. In Fig. 8-3, the –Z axis is in the plane of the figure, extending at the top center of the figure.

The EDL system consisted of a mid-1970s Viking-derived aeroshell structure and propulsion system for a precision guided entry and soft landing. The soft landing was new for MSL and contrasted with the airbag designs used by the mid-1990s Mars Pathfinder (MPF) mission [14][13] and the early 2000s MER mission. Figure 8-29 is a view of the MSL rover in its fully deployed configuration.

Table 8-8 provides a top-level comparison of MSL and MER. MER telecommunication, including telecom subsystem mass and power draw, is described in Taylor et al. 2005 [9]. The MSL telecom subsystem, including mass and power draw, is described in Section 8.2.

[13] Mars Pathfinder, launched in December 1996 and landed July 1997, consisted of a lander and the Sojourner rover. MPF was originally designed as a technology demonstration of a way to deliver an instrumented lander and a free-ranging robotic rover to the surface. It accomplished this goal. Both vehicles outlived their design lives on Mars, the Pathfinder lander by nearly three times and the rover by 12 times.

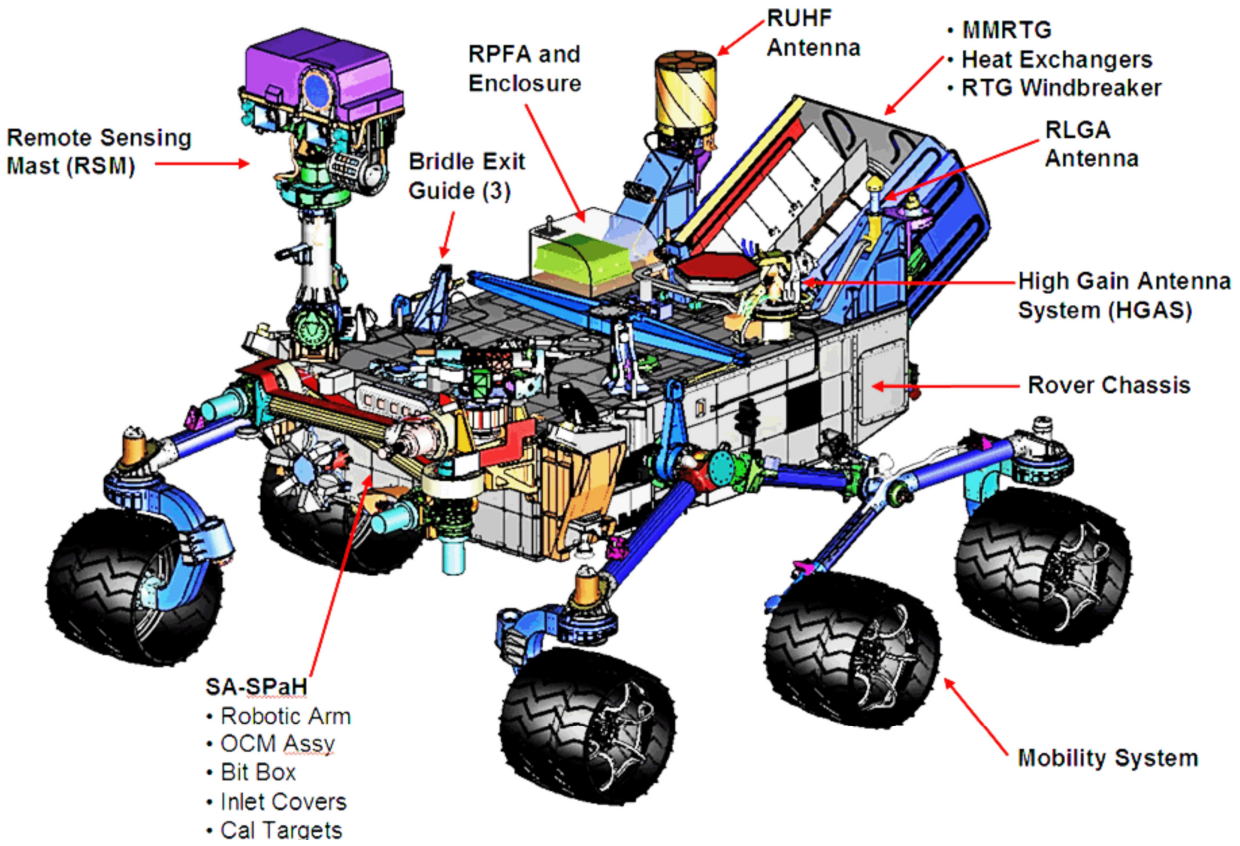

Fig. 8-29. External view of the MSL rover (OCM = organic check material, SA-SPaH = sample acquisition-sample preparation and handling).

Table 8-8. Comparison between MSL and MER.

	MSL	MER
LV/Launch Mass	Atlas V/4000 kg	Delta II/1050 kg
Design Mission Life	1 yr maximum cruise (actual cruise took 9 months) /1 Martian year surface	7 month cruise/3 month surface
Telecom Redundancy	Significant telecom redundancy/Single Mission	Limited telecom redundancy/Dual Mission
	One rover. Telecom includes a small deep space transponder (SDST) and a TWTA on the Descent Stage and an SDST and a solid-state power amplifier (SSPA) on the rover (for X-Band). The rover also has two UHF radios.	2 rovers. Each rover has 1 SDST and 2 SSPAs (X-Band), and one UHF radio
Payload	10 instruments (84 kg)	5 instrument (~9 kg)
Sample Acquisition	Arm + rock abrasion tool (RAT) + Powdering Corer + Scoop	Arm + RAT
EDL System	Guided Entry/Sky Crane	MPF Heritage/Airbags
Heat-shield Diameter	4.5 m	2.65 m
EDL Comm	Partial UHF + partial DTE or full DTE	DTE + partial UHF
Rover Mass	850 kg (allocation)	170 kg (actual)
Rover Range	>20 km designed	1 km (design) and > 37 km (actual so far for Opportunity) and 7.7 km (for Spirit)
Surface Power	MM RTG/2500 Whr/sol	Solar/<900 Whr/sol
Surface Comm	X-Band DTE + UHF	X-Band DTE + UHF

8.1.7.1 Engineering Subsystems and Functions

The following description of the engineering subsystems related to telecom is from the MSL Mission Plan [15].

Chassis. The chassis is the central part of the rover, accommodating the flight system elements. In addition to the structural integration of components, the structural system serves as a significant part of the thermal control of the vehicle, with insulation, thermal coupling of the payload mounting panel and the Multi-Mission Radioisotope Thermoelectric Generator (MMRTG) heat exchangers. The chassis core forms the shell of the warm electronics box (WEB); panels internal to this are used to mount the flight system avionics and payload avionics. Similar to MER, the active telecom components (SDST, SSPA, and Electra UHF radios) are in the WEB.

Mobility. The rover is a scaled-up version of the six-wheel drive, four-wheel steering system from MER, utilizing the rocker-bogie configuration. Based on the center of mass, the vehicle is required to withstand a tilt of at least 50 deg in any direction without overturning. During descent, this number was slightly higher, as the mast had not yet deployed. Fault protection limits the rover from exceeding 30-deg tilts. The design of the rocker-bogie allows traverse over (meaning the wheel moves over) objects approximately as large as the wheel diameter. Each wheel has cleats and is independently actuated and geared, providing for climbing in soft sand and scrambling over rocks. Each front and rear wheel can be independently steered, allowing the vehicle to turn in place as well as execute arcing turns.

Power (surface operations). Rover power is primarily provided by the MMRTG, which is required to generate a constant 110 W at the start of the prime mission (though the current best estimate predicted by the Department of Energy (DOE) was approximately 110 W at the start of surface phase), decaying to approximately 104 W at the end of the 1-Mars-year mission.

Peak power from the rover activities easily exceeds the MMRTG capability, however, and the rover has two 42 amp-hour (A-hr) batteries to allow for all activities. The 2009 launch requirements for performance of the battery were that it should provide as much as 555 W-hr per sol for 670 cycles, given a starting condition of 100 percent state of charge (SOC). Such a deep discharge (555 W-hr) was not intended to occur more than once per sol. In light of the 2009 to 2011 launch slip, and after review of the surface power situation, the 555 W-hr figure was deemed not sufficient. Consequently, among other Rover changes, was a larger battery capacity than the original 20 amp-hour batteries.

Guidance, Navigation, and Control (GNC). During cruise, EDL, and surface operations, the telecom antenna orientation relative to Earth depended on GNC. The MSL Cruise Guidance and Control Subsystem made extensive use of heritage hardware and flight software algorithms from the MER and MPF missions. Three-axis inertial attitude and spin rate were determined onboard in real time using an internally redundant star scanner and one of two 4-head Sun sensors. During cruise, the flight system was spin-stabilized about the spacecraft Z axis at 2 rpm. Eight thrusters arranged in two clusters were used as actuators to control spin rate, “turn” the spacecraft (by precessing the spacecraft spin axis), and perform axial or lateral trajectory correction maneuvers (TCMs).

From the perspective of navigation, the onset of EDL and the events leading up to it were of critical importance to mission success. The EDL system differed from those used for other mission functions in that it did not require an interactive, ground-generated mission plan. On MSL, the landing radar is book

kept as part of GNC. During the entire phase, the vehicle acted autonomously, based on pre-loaded software and parameters. Late parameter updates to be commanded from Earth were in the plan but each update was cancelled when the most recent navigation data and telemetry determined it was not necessary.

Thermal Control (surface operations). The rover was to be capable of landing between 45 deg N and 45 deg S and, accordingly, the thermal control system was designed to accommodate a wide variety of climates and temperatures. Across these latitudes, Mars surface temperatures can reach as high as +40 deg C and as low as –127 deg C (the freezing point of carbon dioxide [CO_2] at Martian atmospheric pressures), with daily thermal cycles as great as 145 deg C. At any latitude, the thermal system could achieve a minimum of 6 hours per sol at which the rover avionics mounting plate (RAMP) and, specifically, the Payload Mounting Module (PMP) would stay at 20 deg C or higher. In extreme cases (for example, at latitudes beyond 30 deg, such as winter at 45 deg S), the RAMP temperature must be maintained above –40 deg C throughout the sol. In addition, the thermal design also limits the daily thermal cycle to ± 30 deg C. Over the majority of the Martian year, at any latitude, the thermal system will be warming the rover. The thermal system achieves this in several ways: passively, through the dissipation of heat from internal components; by electrical heaters strategically placed on key components; and by using the rover heat rejection system (HRS). The HRS is a set of redundant integrated pump assemblies and a fluid loop that runs throughout the WEB that serves to minimize thermal gradients across the rover. The fluid loop actually serves the additional purpose of rejecting heat when the rover has become too warm, but it also can gather waste heat from the MMRTG, by pumping fluid through two heat exchangers mounted alongside the MMRTG. (Because MSL has a surface cooling loop that was not present on MER, the MSL hardware temperatures vary less than they do on MER.)

Rover Avionics. The avionics have been responsible for the command, data handling, power regulation, power distribution, and pyro functions for all mission phases (including cruise and EDL). Rover avionics have served these functions during the surface phase. At the heart of the avionics are the rover compute elements (RCEs), redundant computers which have operated one at a time, with the spare held in cold backup (except during EDL where the redundant computer acted as a hot backup). Each RCE contains a central processor (a radiation-hardened PowerPC 750 architecture system) communicating with peripheral devices using other cards connected on a compact peripheral component interconnect (cPCI) backplane interface and providing central memory storage for mission data and telemetry of 32 gigabits via a non-volatile memory/camera (NVMCAM) card. In addition to the RCEs, power switching and analog input/output are provided by the redundant rover

power and analog modules (RPAMs) connected to the RCEs via MIL-STD-1553 [16] data bus connection[14,15].

Flight Software. The software in the main computer of the rover executes a control loop that monitors the status of the flight system during all phases, checks for the presence of commands to execute, maintains a buffer of telemetry for transmission, performs communication functions (manages "comm. windows" through the communications behavior manager), and checks the overall health of the spacecraft. Central control of the entire flight system is under control of the flight software running in the RCE (the same architecture as was used for the MER mission). On the surface, activities such as imaging, driving, or instrument operations are performed under commands transmitted in a command sequence to the rover from the flight team. The rover generates constant engineering, housekeeping, and analysis (EH&A) telemetry and episodic event reports (EVRs) that are stored for eventual transmission.

Prelaunch testing showed that it was possible that other activities could generate or be affected by radio frequency interference while the rover is communicating. Though such interference with the Electra UHF radio has been seen since EDL on the MRO orbiter, none has been seen on the rover. Should any mutual interference occur during later surface operations, the flight software will ensure that incompatible activities do not run during communication windows.

Communications Behavior. The rover telecom subsystem is used to send and receive command sequences, data, telemetry, and flight-software updates. The behavior of the telecom subsystem is controlled by the interaction of flight software, ground sequences, and a set of parameter tables that define the state of telecom hardware and that control the settings and timing of communication windows. Communication windows ("comm. windows") will be sequenced whenever it is desired to communicate with the rover. Windows must fit within scheduled DSN availability and planned relay orbiter passes. A window is defined as an interval of time that contains all the activities directly associated

---

[14] One hardware element of the avionics that must be powered continuously on the surface is the MSL remote engineering unit (MREU) in the RPAM. The MREU in each RPAM is redundantly connected to the two Electra Lite transponders (ELTs). An ELT may receive a "hail" from an Orbiter at any time requesting the rover to wake up.

[15] MIL-STD 1553 is a standard published by the United States Department of Defense that defines the mechanical, electrical and functional characteristics of a serial data bus.

with preparation and execution of a communication session. During surface operations, the ground system will coordinate with the DSN and the MRO project to determine a set of desired communication windows.

Communication window information is stored in two tables on the rover: the primary table and the high-priority table. The primary table can hold as many as 256 communication windows and is used for standard operations. A high-priority table can be used in the event of rover anomaly resolution or for other purposes. When communication windows are loaded into the high-priority table, they take precedence over any windows defined in the primary table. This allows new communication windows to effectively replace selected onboard windows, should the need arise, without affecting the entire set of previously planned communication events. One routine use of high priority windows is to start two varieties of carrier-only "beep" DTEs. The flight software starts a nominal beep if the daily X-band DFE has been successful and the new sequence begins execution normally; otherwise the existing sequence continues execution and starts a run-out beep. Either of these beeps is a high priority window that is started at a known time.

8.1.7.2 Payload (Science Instruments)

The rover carries the largest science payload suite landed on Mars to date, with instruments sponsored by NASA and others contributed by international partners. The following, also from the Mission Plan [15], is a summary/listing of the MSL science instrumentation.

The instruments are roughly divided into four categories:

1) Remote Sensing (2):
   - Mastcam: Multi-spectral, stereo imaging, as well as video
   - ChemCam: (Chemistry and Mineralogy) Remote spectroscopy of rocks and soils from laser ablation; remote microscopic imagery
2) In-Situ (2):
   - Mars Hand Lens Imager (MAHLI): Color microscopic imager
   - Alpha-Particle X-ray Spectrometer (APXS): spectroscopy of soil and rocks using X-ray fluorescence and particle-induced X-ray emission
3) Analytical (2):
   - CheMin: Mineralogical analysis of acquired samples of rock and soil using X-ray diffraction
   - Sample Analysis at Mars (SAM): Chemical and isotopic analysis of acquired samples of rock, soil, or atmosphere (including organics)

using a mass spectrometer, gas chromatographs, and a tunable laser spectrometer

4) Environmental (4):
   - Radiation Assessment Detector (RAD): Detect and measure natural high-energy radiation
   - Mars Descent Imager (MARDI): High-resolution color video of descent
   - Dynamic Albedo of Neutrons (DAN): Detect and analyze hydrogen in the near-subsurface of Mars
   - Rover Environmental Monitoring Station (REMS): To monitor the meteorology and ultraviolet (UV) environment near the rover

8.2 Telecom Subsystem Overview

The X-band subsystem (with DSDST, RSDST, TWTA, and SSPA as the active elements) was primary for cruise through EDL and is also used for DFEs, DTEs, and beeps during surface communications.

Figure 8-30 is a block diagram of the X-band portion of the telecom subsystem, and Figure 8-31 is a block diagram of the UHF portion. Table 8-9 and Table 8-10, respectively, define X-band and UHF terms used in these two figures.

Table 8-9. Acronyms and abbreviations in X-band telecom block diagram.

Term	Definition	Term	Definition	Term	Definition
Assy	Assembly	L	Left circular polarization	RLGA	Rover low gain antenna
ATN	Attenuator	LPF	Low pass filter	SDST	Small deep space transponder
Com	Common	MGA	Medium gain antenna	SSPA	Solid state power amplifier
D-	Descent	Pol	Polarizer	TLGA	Tilted low gain antenna
Ex	Exciter	P-	Parachute	TWTA	Traveling wave tube amplifier
HGA	High gain antenna	R-	Rover	Tx	Transmit
HGAG	High gain antenna gimbal	R	Right circular polarization	W	Watt
Iso	Isolator	Rx	Receive	WTS	Waveguide transfer switch

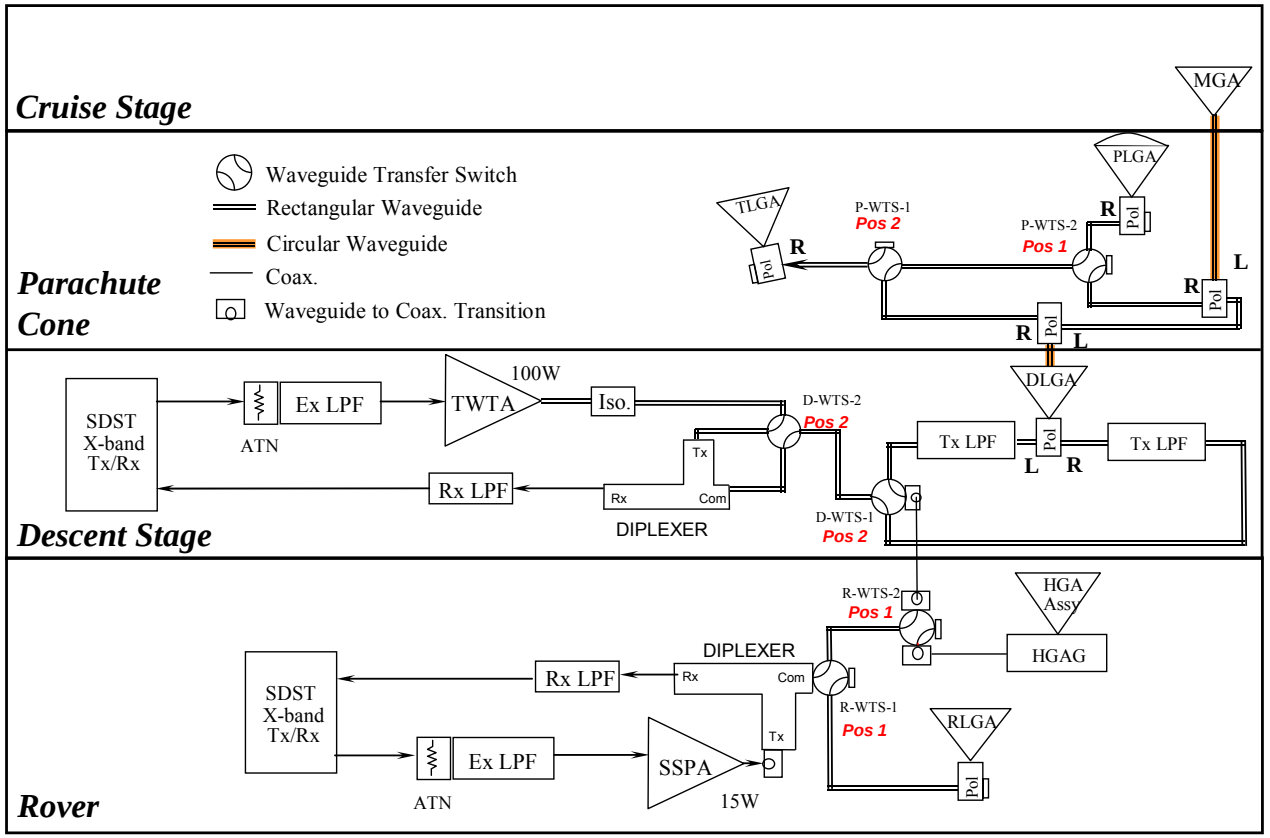

Fig. 8-30. MSL X-band subsystem launch configuration block diagram.

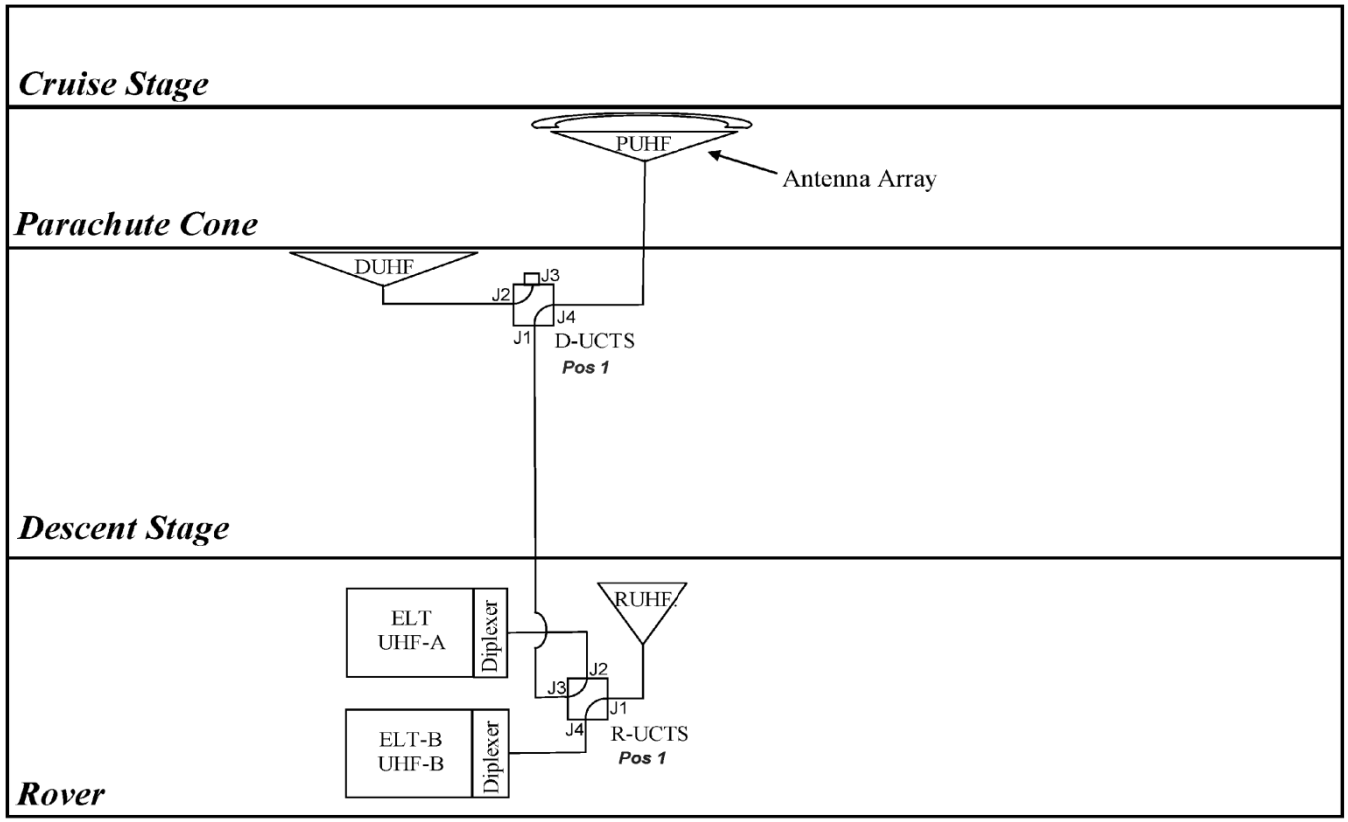

Fig. 8-31. UHF subsystem launch configuration block diagram.

Table 8-10. Acronyms and abbreviations in UHF telecom block diagram.

Term	Definition	Term	Definition	Term	Definition
DUHF	Descent UHF antenna	J-	Jack (connector)	R-	Rover
D-	Descent	Pos	Position	RUHF	Rover UHF antenna
ELT	Electra Lite transponder	PUHF	Parachute UHF antenna	UCTS	UHF coaxial transfer switch

The four layers in Fig. 8-30 and Fig. 8-31 are called slices or stages. Each stage has an X-band antenna or two, with active X-band telecom equipment on two stages (the descent stage and the rover). Each stage except Cruise has a UHF antenna, but the UHF active elements are in the rover. The terms “Pos1” and “Pos2” in the figures define the switch positions at launch.

This complex series of EDL telecom events (involving multiple successive configurations of both X-band and UHF) is shown in Fig. 8-32. Refer back to Figs. 8-16, 8-17, and 8-19 for pictorials of the EDL events at the spacecraft level.

The DSDST and the RSDST are, respectively, the SDSTs on the descent stage and the rover.

8.2.1 Telecom for Launch, Cruise, and into EDL

The descent stage and the rover each has a small deep space transponder (SDST) [17] and a transmitter (a 100-W output TWTA on the descent stage and a 15 W output SSPA on the rover).

The nominal cruise configuration used the X-band radio (DSDST and TWTA) on the descent stage due to its lower line losses and higher output power. A backup switching arrangement would have allowed X-band to be routed to and from the X-band radio (RSDST and SSPA) on the rover. Being able to use either the TWTA or the SSPA provided functional redundancy during cruise. This redundancy proved not to be required, though the SDST and the SSPA on the rover were verified “alive” during cruise by two power on/power off test sequences of about a half hour duration each. The primary cruise SDST and TWTA continued to provide the operational RF signals during the aliveness tests.

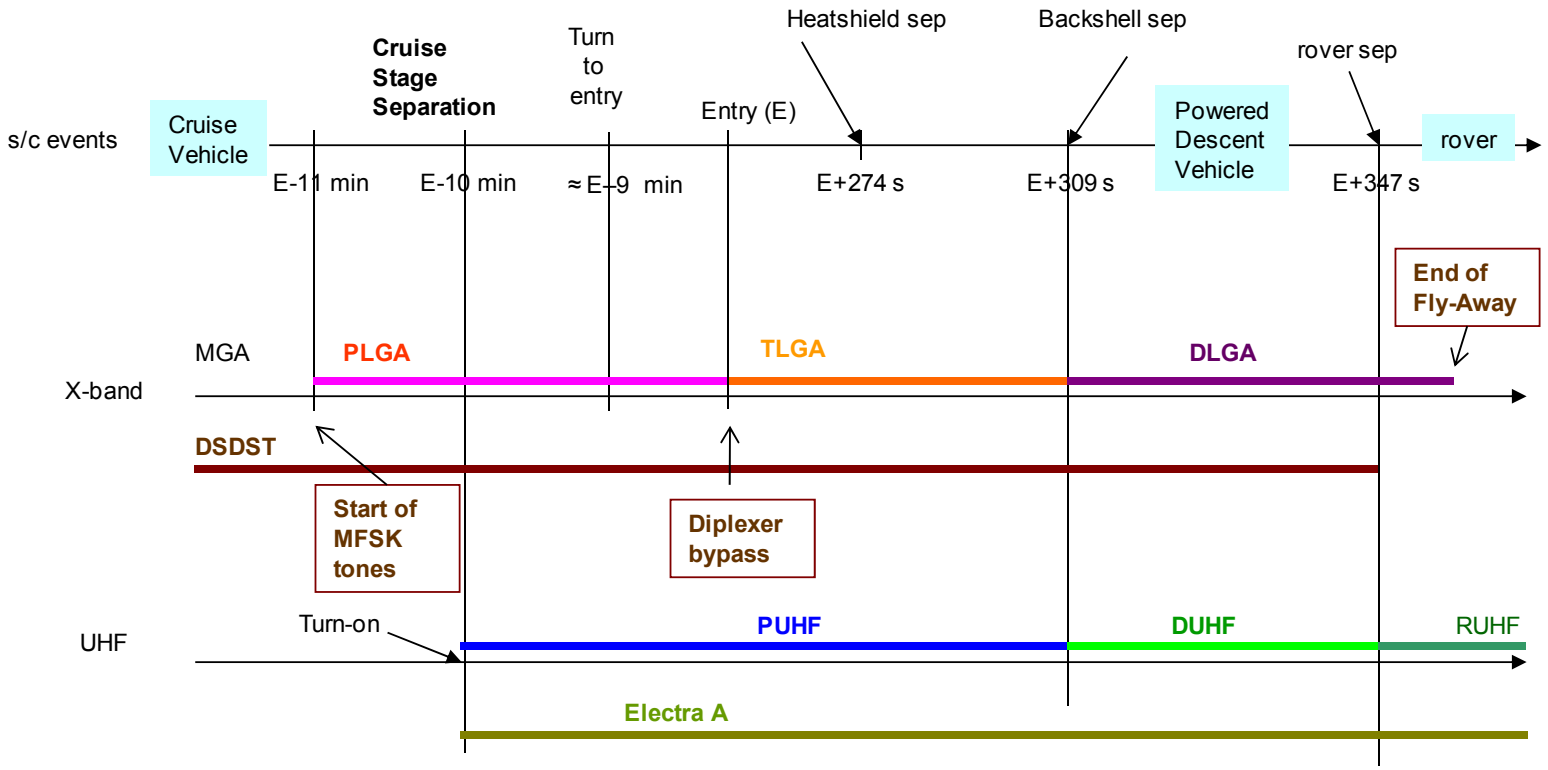

Fig. 8-32. X-band and UHF sequence during EDL.

The X-band MGA and PLGA antennas used during cruise and the first part of EDL are shown in the top two slices of Fig. 8-30 The MGA provided greater gain and a smaller beamwidth; the PLGA provided a larger beamwidth, but less gain. At any given time, one antenna was selected; that antenna simultaneously received uplink from the DSN and transmitted downlink to the DSN.

When EDL started, the EDL-main sequence sequenced CSS to occur; this ejected the top slice (the cruise stage) along with the MGA. The sequence continued, sequentially selecting the PLGA, the TLGA, and the DLGA with only downlink communications required. At the atmospheric entry interface, the sequence bypassed the diplexer in the descent stage to avoid critical-pressure high-power coronal discharge. Activating this bypass had the incidental advantage of decreasing transmit line loss somewhat.

During the banking maneuvers (Fig. 8-18), the TLGA provided the best downlink to the Earth. The original plan was to switch back to the PLGA just before parachute deployment, after the so-called "Straighten Up and Fly Right" (SUFR) maneuver, when the –Z axis and the anti-velocity vector were more co-aligned. However, because there was a good chance the parachute sabot could impact the PLGA at parachute deployment, it was decided to stay on the TLGA to maximize the likelihood of continuing the DTE link during parachute descent.

When backshell separation occurred, the second slice (parachute cone) broke away, taking the TLGA with it. For the remainder of the powered descent, the DLGA carried the downlink. No switching was needed to be on the DLGA. Because the DLGA was part of the waveguide run up to the parachute cone hardware, the DLGA began radiating upon the ejection of the backshell.

The powered descent vehicle phase concluded with rover separation and sky-crane operations. Upon touchdown, the bridle was cut and the descent stage flew away. Because they were on the descent stage, we lost effective use of the DSDST, the TWTA, and the DLGA. By now out of sight of the Earth, the SDST and TWTA continued to transmit through the DLGA until the descent stage crashed on the surface at the end of the "fly-away phase." The rover X-band system (the RSDST and SSPA) was not scheduled to operate for the first time until after the end of EDL.

The UHF block diagram is shown in Fig. 8-31. Table 8-10 defines the terms used in the figure. The two active elements are functionally redundant Electra Lite Transponders (ELT), with either ELT-A or ELT-B selected for use.

The MSL ELT is derived from the Electra UHF transponder (EUT) used on the MRO. Except for two non-radiating "aliveness" checkouts during cruise, the first use of the UHF was in the EDL phase, after cruise stage separation.

During EDL, all three UHF antennas were used: the PUHF from CSS until backshell deployment, the DUHF during powered descent, and the RUHF during and after the sky-crane stage (for the period from post landing + 1 minute through end of the surface mission).

The descent UHF coaxial transfer switch (D-UTCS) selected between the DUHF and the PUHF antennas. The rover UHF coaxial transfer switch (R-UTCS) selected between the rover UHF antenna (RUHF) and either of the descent antennas.

During surface operations, UHF is the primary mode of returning large volumes of data to the Earth (via orbiter relay). Only the RUHF is used during surface operations.

8.2.2 Surface Operations

The surface telecom system uses three antennas: two for X-band DTE/DFE and a UHF antenna for relay to an orbiting asset. Figure 8-29 shows the X-band and UHF antennas mounted on the rover deck.

The X-band antennas are the rover low-gain antenna (RLGA) and the high-gain antenna (HGA). The HGA is used for DFE commanding, DTE telemetry, and HGA beeps. The RLGA is used for low-rate (contingency) DFE commanding and RLGA beeps. The downlink signal level achievable using the RLGA is too low for DTE telemetry.

The HGA sits on a two-degree-of-freedom gimbal and is 0.28 m in diameter. The pointing accuracy requirement for the HGA is 5 deg, including rover attitude knowledge. Relative to the peak gain at boresight, the downlink gain is about 4 dB lower and the uplink gain about 3 dB lower, at 5 deg off boresight.

8.2.2.1 X-Band

8.2.2.1.1 Downlink (DTE). As an RF amplifier, the SSPA receives its X-band RF input signal from the RSDST and generates 15 W RF output. The basic telecom requirement for surface operations on the HGA is to provide a downlink capability of at least 176 bits per second (bps) to a 34-m station.

8.2.2.1.2 Uplink (DFE). The HGA is typically used for a DFE command session each sol. Depending on Earth-Mars distance, uplink rates are 1 kbps or

2 kbps. A command session takes 15 minutes, including margin for possible station transmitter delays and for packaging of commands into groups.

In safe mode, commands from the Earth are received via the RLGA, initially at the fault rate of 7.8125 bps. The RLGA is fixed-mounted to the rover and has a broad pattern. The RLGA provides link capability to command at the fault rate or higher depending on Earth-rover distance.

8.2.2.2 UHF

The primary data path for surface operations is via the UHF relay system, using the Mars orbiting assets (MRO or Odyssey[16]). The primary relay communications is via MRO, with two passes a day to return science and playback engineering data from the surface. Communications through Odyssey provides for additional data return or if MRO is unavailable, as long as there is DSN time for data return from Odyssey and sufficient energy to support UHF operations with Odyssey during the sol.

The UHF subsystem includes a pair of Electra-Lite radios. The Electra-Lite radio is a smaller version of the Electra radio flown on MRO. The MSL Electra-Lite/MRO Electra link can function using an adaptive data rate (ADR) scheme. In the ADR mode, the return link data rate will adjust to variations in signal strength due to antenna patterns, angles, and proximity between MRO and MSL throughout the overflight. In ADR, it is the MRO radio that controls the return data rate, based on its own receiver power telemetry, commanding the lander radio via the forward link to change its return link rate on the fly. The forward rate from MRO remains constant during any relay pass. Section 8.2.4.1 includes UHF frame and coding options.

A single quad-helix antenna designed especially for MSL, the RUHF, is mounted to the rover deck and used with either redundant radio.

The MSL/MRO relay link can also be used in a safe mode. The Electra-Lite radio can communicate a wake-up signal (via low-voltage differential signaling [LVDS]) to the rover avionics upon hearing a “hail” forward link[17] from MRO.

---

[16] The Mars Explorer (MEX) orbiter is also compatible with the Electra lite radio, and it is available as an additional relay path. MEX was launched in 2003 by the European Space Agency.

[17] Forward and return links are used for communications between an orbiter and a lander. The forward link is from an orbiter to a lander. A return link is from a lander to an orbiter. Completing the end-to-end lander-Earth communications paths are the DSN X-band uplink and downlink between the Earth and the orbiter.

This is most useful in a contingency mode, where the rover is effectively asleep with its ELT waiting for a communications possibility. The MSL mission intends to rely on this function as a fault response mode only. For example, a fault response would occur if the spacecraft lost its clock timing and did not know when relay passes were to occur.

The UHF functionality of the Odyssey and MEX orbiters is similar to that of the MRO UHF. However, the Odyssey and MEX radios are not Electras and do not have the adaptive data rate capability.

In some cases, an X-band DTE/DFE link of sufficient duration is not available, most likely because of scheduling contentions for the tracking stations or because the command load is larger than usual. A forward UHF link could be used in these cases to command the rover. Commanding via Odyssey and MRO has been demonstrated with the MER and Phoenix missions and more recently during MSL surface operations.

8.2.3 X-Band Flight Subsystem Description

8.2.3.1 X-Band Interfaces with MSL Control and Data Systems

The data transfer functions from the avionics subsystem to both SDST radios, include:

- Turbo codes that are the baseline for the DTE downlink. The codes have rates of 1/2, 1/3, and 1/6, and they have frame sizes of small (1784 bits) and large (8920 bits).
- Reed Solomon encoding (interleave depth 1 and 5) that can be used for the DTE downlink (in concatenation with convolutional [7, 1/2] coding[18] that is performed by the SDST).

8.2.3.2 X-Band Key Hardware Components

The telecom component descriptions in the following paragraphs are organized by the stages in the Fig. 8-3 graphic. The X-band telecom block diagram (Fig. 8-30) shows the four spacecraft stages ("slices") that contain the X-band

[18] In telecommunication, a convolutional code is a type of error-correcting code in which (a) each m-bit information symbol (each m-bit string) to be encoded is transformed into an n-bit symbol, where m/n is the code rate ($n \geq m$), and (b) the transformation is a function of the last k information symbols, where k is the constraint length of the code (from http://en.wikipedia.org/wiki/Convolutional_code). For MSL, the code parameter values are k = 7, m = 1, and n = 2; the resulting code is abbreviated (7, 1/2).

telecom subsystem elements. These four are Cruise, Backshell or Parachute Cone, Descent, and Rover. The heat shield stage had no telecom components.

8.2.3.2.1 Cruise Stage X-Band Telecom Components

8.2.3.2.1.1 Medium-Gain Antenna. The MGA, called out in Fig. 8-2, was used for mid- to late-cruise communications. The MGA was a build-to-print of the MER MGA, fed by a septum polarizer for circular polarization (CP) operation. The MSL MGA could operate either right-hand or left-hand circularly polarization (RCP or LCP), depending on which side of the polarizer was connected to the receiver or transmitter[19]. RCP was used in the mission.

The MGA, which was attached on the cruise stage, separated from the rest of the X-Band telecom subsystem at Cruise Stage Separation. In the top left drawing of Fig. 8-2, the light blue surface on top of the cruise stage is the annulus-shaped solar array with the MGA at its center.

Table 8-11 states some of the RF characteristics of the MGA.

Table 8-11. MGA RF characteristics.

Parameter	Value
Receive frequency, MHz	7150.8 (DSN channel 4)
Transmit frequency, MHz	8401.4 (DSN channel 4)
Gain, boresight, dB	18.1 ± 0.4 receive 19.2 ± 0.4 transmit
Polarization	RCP or LCP
3 dB-beamwidth, deg	± 10.3 receive ± 9.3 transmit
Axial Ratio, on boresight, dB	1.01 receive; 0.27 transmit
Axial Ratio, 20 deg off boresight, dB	6.29 receive; 7.53 transmit
Design	RF conical

[19] Right-circular polarization (RCP) refers to an electromagnetic wave that propagates such that the tip of the electric field appears from the source to describe a circle in the clockwise direction. Left-circular polarization is the opposite; the tip of the electric field is seen from the source as describing a circle in the counterclockwise direction. A polarizer converts the RF beam traveling through a waveguide to an electromagnetic wave of a specific polarization. In this case the septum polarizer converts a linearly polarized wave in the waveguide run to a circularly polarized wave to be transmitted by the antenna.

Figures 8-33 and 8-34 show uplink and downlink patterns of gain as a function of angle from MGA boresight. These are based on measurements on a MER mock-up. The gain is down 3 dB from its peak at about 10 deg from boresight, as compared with about 5 deg from boresight for the rover HGA. "Beamwidth," commonly defined in terms of a total angular range on both sides of boresight, is double the above numbers.

8.2.3.2.2 Parachute Cone X-Band Telecom Components. The MSL X-band telecom block diagram (Fig. 8-30) shows the telecom components on the Parachute Cone, as well as on three other stages. Note that names beginning with P refer to parachute, those with D to descent, and those with R to rover.

8.2.3.2.2.1 Waveguide Transfer Switches (P-WTS-1 and P-WTS-2): All switching between X-band transponders, power amplifiers, and antennas is with waveguide transfer switches (WTS). The switches are used to connect transmit and receive functions to the proper antennas. On the parachute cone, P-WTS-1 selected the TLGA, and P-WTS-2 selected between PLGA and MGA.

8.2.3.2.2.2 Parachute Low-Gain Antenna: Figure 8-35 shows where the PLGA and the TLGA are installed. The PLGA was used from launch through the first three months of cruise and was also the default antenna for cruise safemode. The PLGA supported MFSK tone transmission over a wide range of pointing angles during EDL communications. The PLGA boresight was aligned along the –Z axis of the spacecraft, as shown in Fig. 8-3.

The design of all MSL X-band low-gain antennas (except for the DLGA) is the same: the PLGA, TLGA, and RLGA were each an open-ended waveguide with chokes and parasitic drooping dipoles. However, the proximity effects of spacecraft components near each LGA resulted in their individual patterns being quite different from one another.

The parasitic dipoles have the effect of broadening the pattern, as compared to the MER design. Figures 8-36 and 8-37 show, respectively, the uplink and downlink patterns of the PLGA (measured on a spacecraft mock-up). Both the maximum gain over all roll angles (red curve) and the minimum gain (blue) are shown. As the spacecraft spun at the 2 rpm rate during cruise, the peak-to-peak link performance varied by as much as several decibels.

For the very early launch dates with a type II trajectory, antenna angles could have been as large as 120 deg. Until the Type Ib trajectory was chosen for the 2011 launch, the type II cases had to be included in the telecom design and mission design tradeoffs. Communications would have been possible only for

the first few hours after trans-Mars injection, while the range loss was not yet too high.

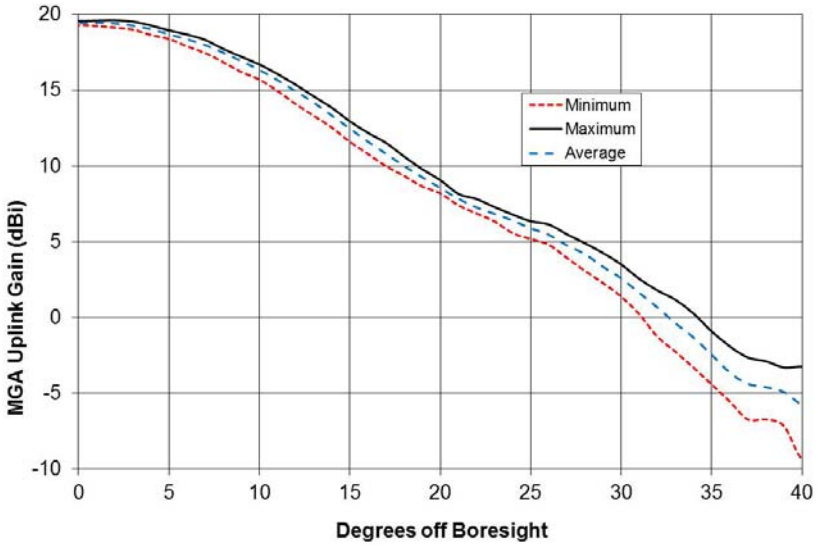

Fig. 8-33. MGA uplink gain.

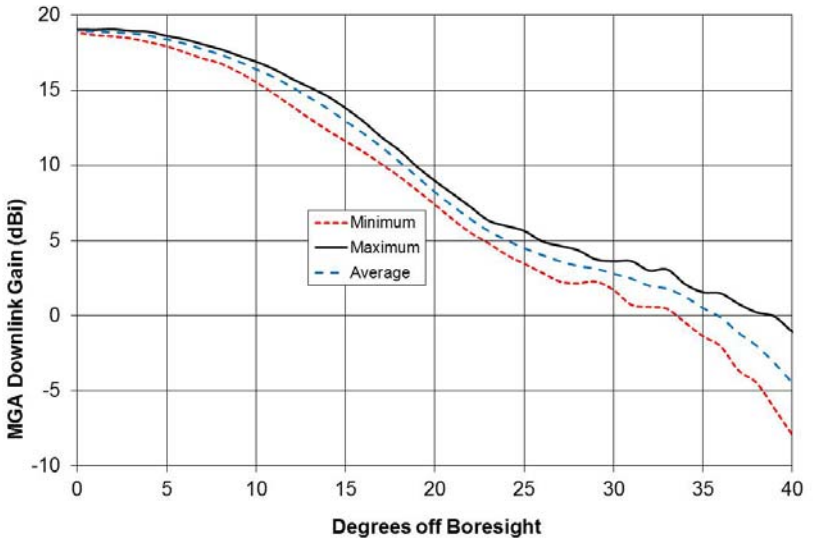

Fig. 8-34. MGA downlink gain.

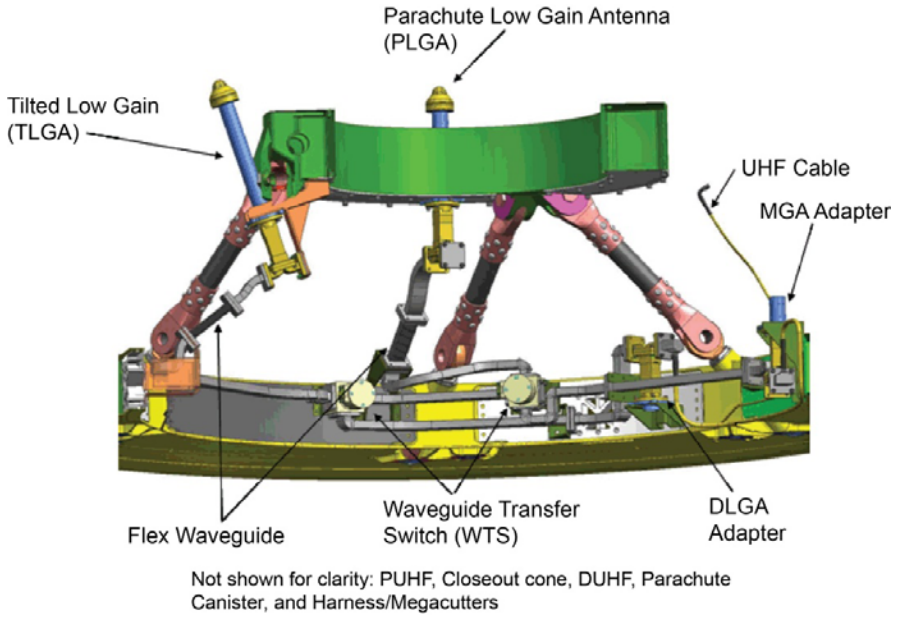

Fig. 8-35. Locations of the low-gain antennas.

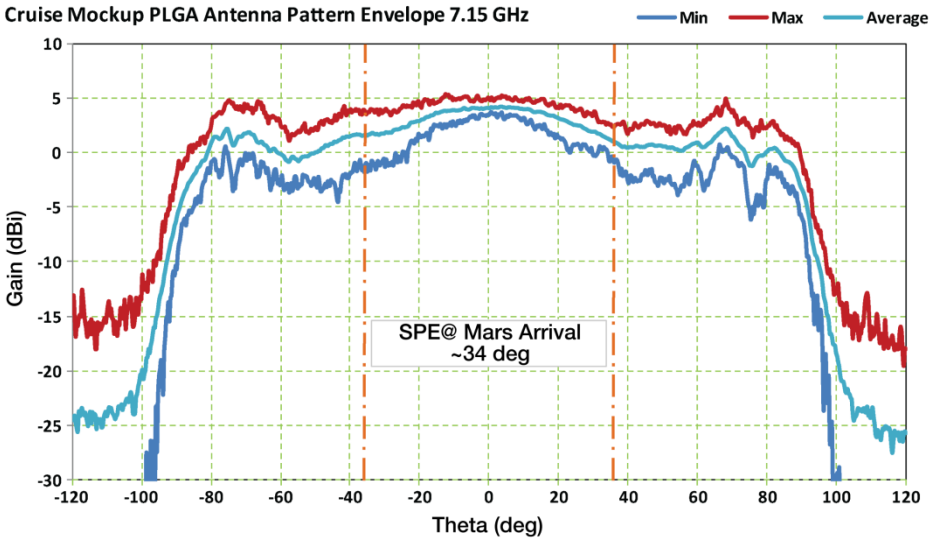

Fig. 8-36. PLGA X-Band uplink gain with spacecraft mock-up, RCP, 4/30/09.

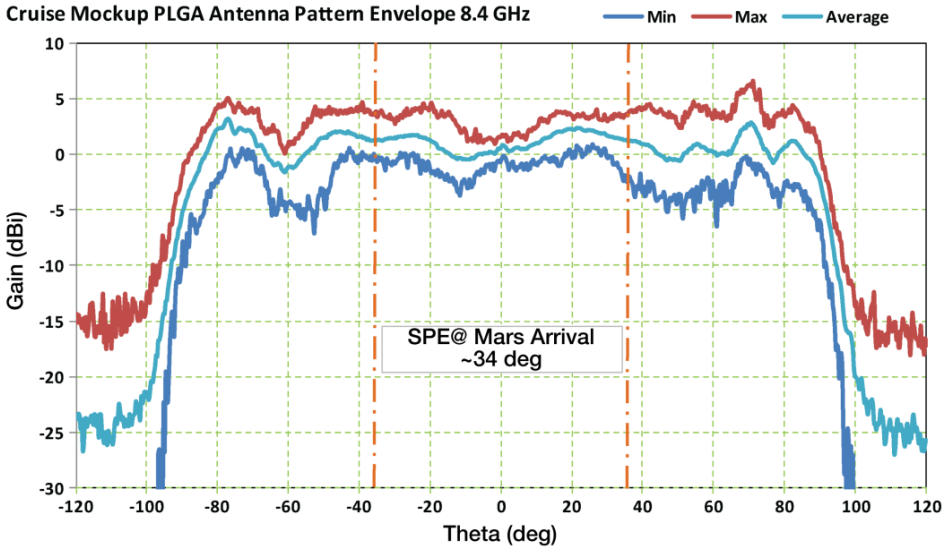

Fig. 8-37. PLGA X-Band downlink gain with spacecraft mock-up, RCP, 4/17/09.

8.2.3.2.2.3 Tilted Low-Gain Antenna: The TLGA had the same design as the PLGA. One difference, however was that the TLGA's boresight was 'tilted' with respect to the spacecraft –Z axis by 17.5 deg, which was chosen to bring it close to the average anti-velocity vector direction during post-entry banking maneuvers. This minimized the span of Earth-to-boresight angles and, therefore, the link-signal level variation during the critical hypersonic and banking phases. Figure 8-18 illustrates the geometry involved for the EDL maneuvers when the TLGA is in use.

8.2.3.2.3 Descent Stage X-Band Telecom Components. The MSL X-band telecom block diagram (Fig. 8-30) shows the telecom components on the Descent stage, as well as on three other stages. Note that names beginning with D- refer to "descent."

The descent stage (DS) contained two active telecom components, the DSDST and the TWTA, as well as the DLGA. In addition, there were several components involved in routing the high-powered TWTA RF output and the much weaker RF input destined for the SDST receiver.

Figure 8-38 shows the overall layout of the DS telecom components. Most were on a telecom plate, shown in a contrasting color and detailed in Fig. 8-39.

Both the TWTA (on the far side of the plate) and the TWTA's electronic power conditioner (EPC) were powered on throughout cruise. These items dissipated

relatively large amounts of spacecraft power as heat to be carried away by the cruise stage thermal control system (heat rejection system [HRS]).

8.2.3.2.3.1 Descent Low-Gain Antenna: The descent low-gain antenna (DLGA) (Fig. 8-40) is an open-ended waveguide with chokes. The relatively broad pattern of the DLGA was expected to suffer significant distortion from interaction with the surrounding structure of the descent stage. The DLGA gain as a function of angle from boresight and its variation was modeled[20] using the General Reflector Antenna Scatter Program (GRASP) antenna scattering software. Figure 8-41 shows the GRASP model used to generate the pattern.

The actual view angles for DTE during the powered descent phase could vary widely, depending on the landing site chosen and descent geometry (such as the large tilt during the divert maneuver). As the landing date and site were not selected until well after the spacecraft design was complete, the antenna design tradeoff included the possible range of boresight view angles. For some trajectories, the Earth would be quite close to the horizon at touchdown and, therefore, the antenna pattern as far as 90 deg from boresight needed to be considered. The resultant pattern in Fig. 8-42 shows that the variation is worst near the 75-deg off-boresight angle.

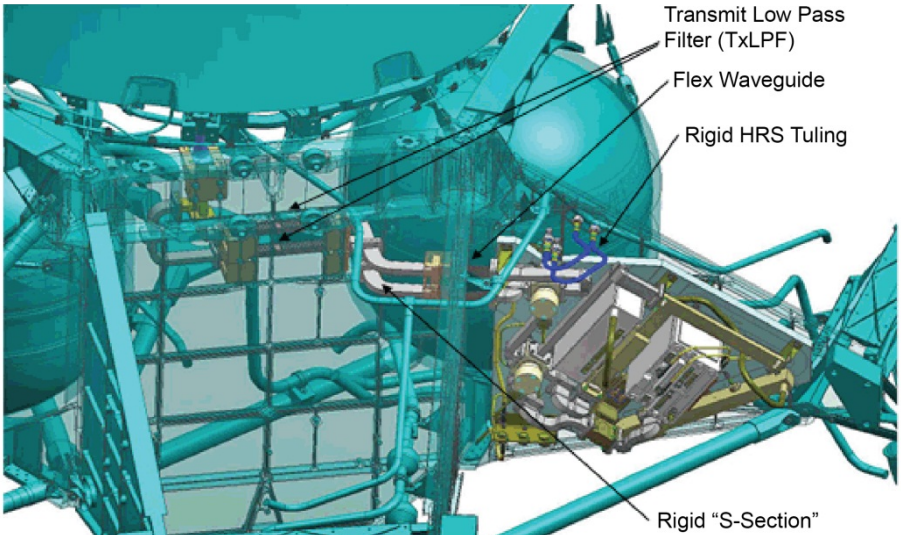

Fig. 8-38. Descent Stage X-band layout.

[20] "DLGA on the Descent Stage: 8.400 GHz." Dan Hoppe, April 21, 2008 (internal MSL project document).

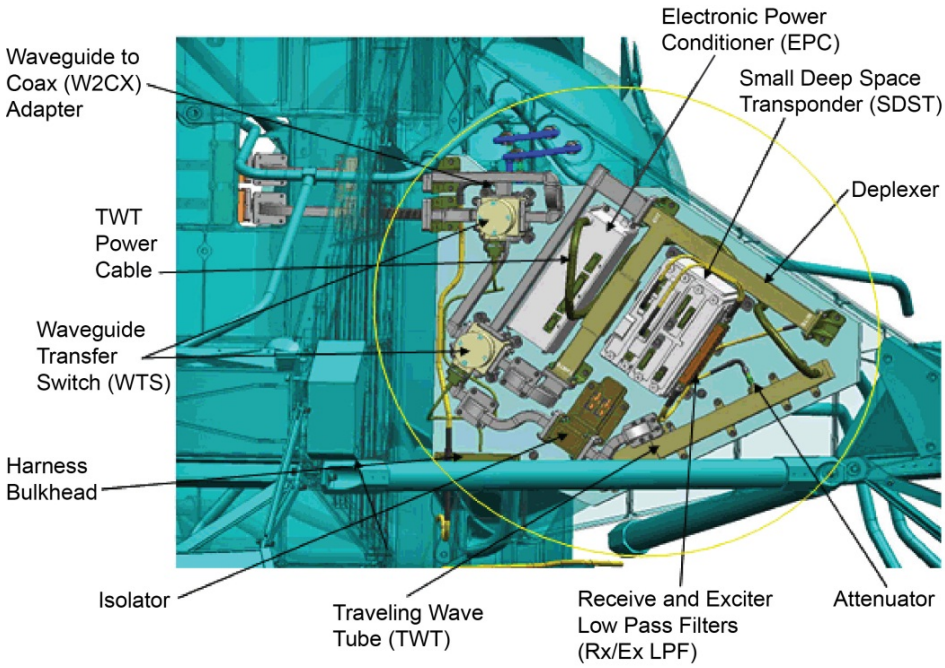

Fig. 8-39. Telecom plate assembly.

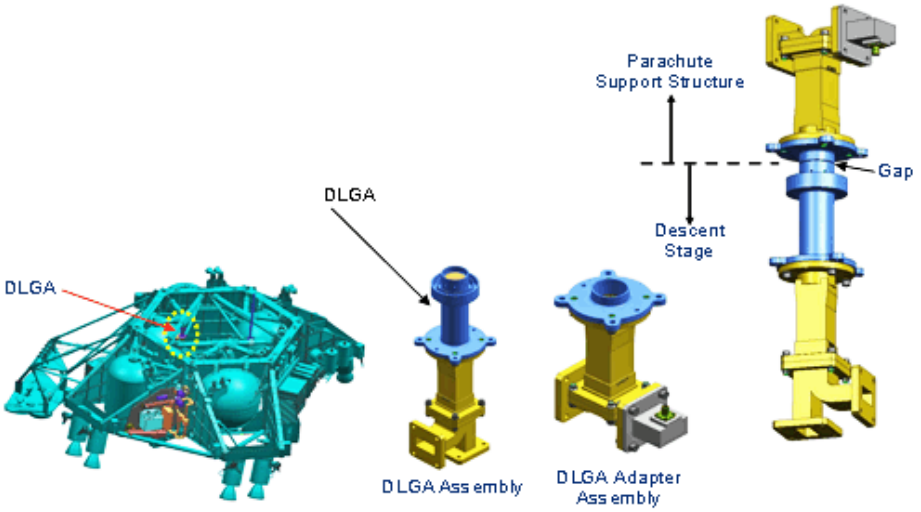

Fig. 8-40. DLGA and DLGA adapter overview.

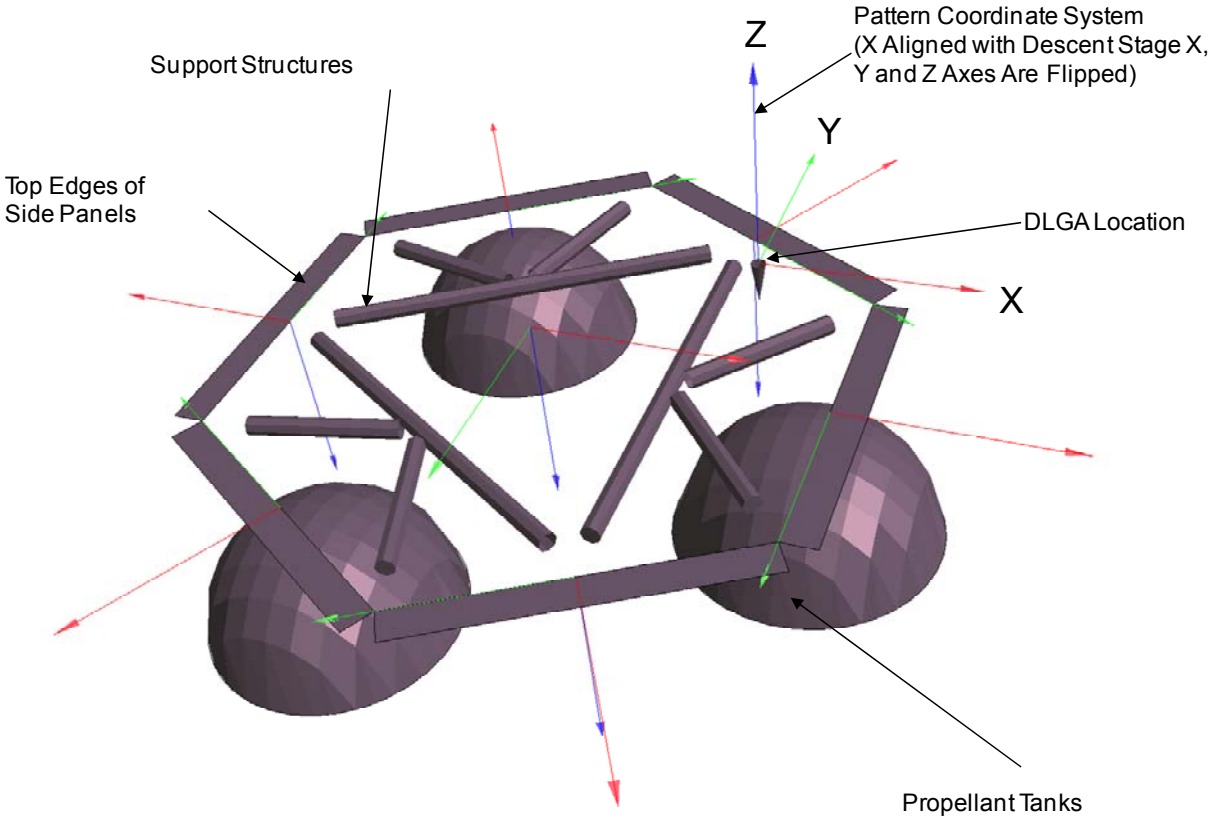

Fig. 8-41. GRASP model for DLGA scattering study.

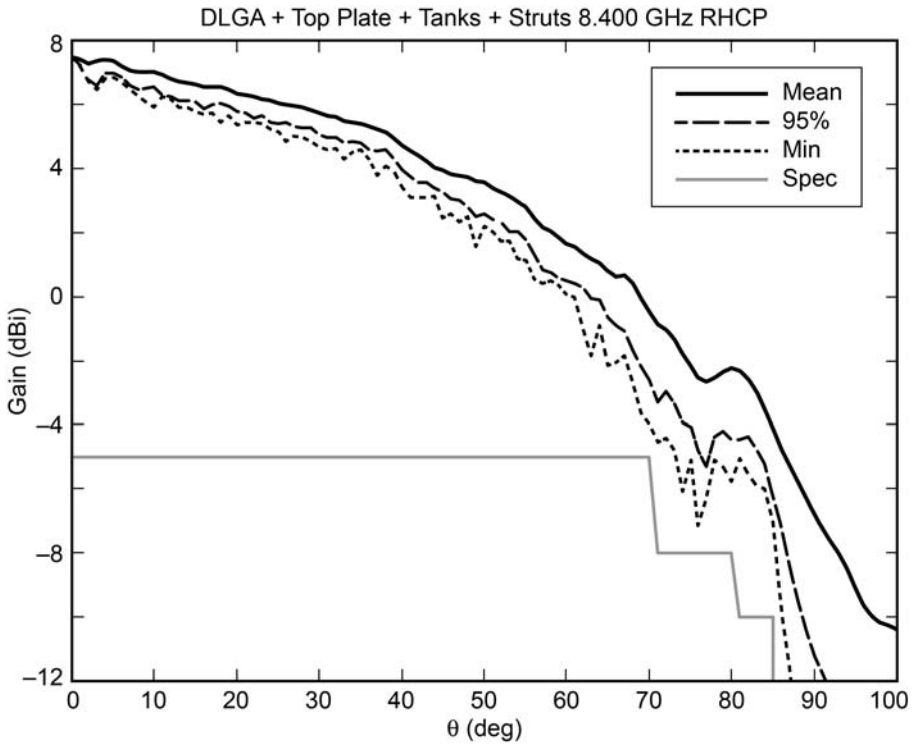

Fig. 8-42. MSL DLGA downlink pattern modeled from GRASP model.

8.2.3.2.3.2 Descent Stage Waveguide Transfer Switches: D-WTS-1 selected one of two polarization signal paths: RCP and LCP.

D-WTS-2 is a "diplexer-bypass" switch, to be used for EDL. Bypassing the diplexer was sequenced during EDL. This avoided coronal breakdown in the diplexer at critical pressure during passage through Mars' atmosphere[21]. Once the diplexer was bypassed, X-band uplink-receive capability was no longer possible, but none was needed.

8.2.3.2.3.3 Traveling Wave Tube Amplifier: The TWTA consisted of two components: the traveling wave tube (TWT) and the electronic power conditioner (EPC) that provided the voltages required by the tube. The TWTA is of MRO heritage.

[21] The power handing capability of the diplexer at critical pressure was found in test to be insufficient for use with the TWTA during EDL. Breakdown occurred at 85 W in test, lower than the 100-W nominal output. The bypass design avoided this problem.

The TWT was specified to provide at least 100 W of RF output to support X-band communications and radiometric requirements during cruise and during EDL until rover separation. The MSL flight unit had RF output of 104.7 W, which is 50.2 dBm (decibels referenced to 1 milliwatt [mW]).

As with other deep-space TWTAs, when the spacecraft bus voltage was first input to the EPC, a warm-up delay (between 200 and 240 s) occurred before the EPC applied high voltage to the TWT. During the delay, the TWTA was prevented from generating RF regardless of the On/Standby Mode control.

Because the TWTA operated with high voltages and high power levels, it was designed with three kinds of internal protection:

1) **Bus Undervoltage Trip**: The undervoltage trip would happen if the spacecraft bus voltage at the EPC input went below 20.5 V ±0.5 V. During the shutdown, period the TWTA indicated status as Under Voltage Trip. The TWTA initiated a start-up sequence when the bus input voltage rose above 21.5 V.
2) **Converter Overcurrent Trip**: The converter overcurrent trip would occur if the high-voltage converter exceeded a safe current value. The TWTA initiated an automatic restart function (ARF). The ARF turned off the electron beam in the TWT. Within 50 ms, the electron beam came back on, and the TWTA returned to nominal operations. If a second trip occurred within 180 seconds, the TWTA would go to the start-up sequence described above. [22]
3) **Helix Current Trip**: The helix overcurrent trip was designed to occur if the TWT body (helix) current exceeds safe values (set by the TWT manufacturer); however, this trip was intentionally disabled for MSL.

8.2.3.2.3.4 X-Band Diplexer: The design of the diplexers in the descent stage and the rover is the same. The diplexers provide for the separation of the receive frequency from the antenna and the transmit frequency to the antenna.

8.2.3.2.3.5 Transmit Low-Pass Filter: Two transmit low pass filters (Tx LPF), branch out of D-WTS-1, one for each polarization.

---

[22] Telemetry played back via UHF after landing indicates that the TWTA tripped off late in EDL. The cessation of RF output was not seen in real time. The X-band link was not prime at the time. Assessment of the playback telemetry was that a converter overcurrent trip occurred, but the data sampling rate was insufficient to prove this. Dynamics (vibration, shock) was the most likely cause of the trip.

The Tx LPF is a waveguide filter and had two purposes:

1) For near-Earth operations, the filter reduced out-of-band emissions from the TWTA. This function is similar to MRO, which also has a 100-W TWTA of the same design.
2) During EDL, the filter reduced TWTA emissions into the landing radar, especially in three frequency bands of 16.7 to 17 GHz, 25.2 to 25.5 GHz, and 33.4 to 34 GHz. The radar center frequency was 35.75 GHz. Tests with the LPF early in 2009 verified that radar operation would not be degraded by TWTA emissions into its sensitive frequency bands.

Table 8-12 documents the RF characteristics of the transmit LPF.

8.2.3.2.3.6 Exciter Low-Pass Filter: This filter attenuated the DSDST exciter broadband spurious emissions. This filter and the Tx LPF worked together to attenuate the overall out-of-band emissions sufficiently at the input to the landing radar.

8.2.3.2.3.7 Receiver Low-Pass Filter: The receiver low-pass filter (Rx LPF, Table 8-13) rejected TWTA power reflected from the diplexer ('ring-around' noise) so the DSDST could detect very weak uplink signals. The SDST threshold is –155 dBm, as contrasted with the TWTA's +50 dBm RF output.

By design, the diplexer passed any signal in the receive band to the receiver while attenuating TWTA output at other frequencies. To complete the job, the Rx LPF attenuated the TWTA output at frequencies lower than the transmit band.

Table 8-12. Transmit low-pass filter RF characteristics.

Parameter	Value
Receive passband* insertion loss	0.2 dB at 7.17.2 GHz
Transmit passband insertion Loss	0.2 dB at 8.35 to 8.5 GHz
Transmit attenuation of the second harmonic (16.7 to 17 GHz)	> 50 dB
Transmit attenuation of the third harmonic (25.0 to 25.4 GHz)	> 35 dB
Transmit attenuation of the fourth harmonic (33.4 to 34 GHz)	> 30 dB
Group delay variation, over 1 MHz in receive (7.1–7.2 GHz) and transmit (8.354–8.5 GHz) passbands (*)	1 nanosecond (ns)

* A passband is the portion of the spectrum, between limiting frequencies. This portion is sent through with minimum relative loss or maximum relative gain by a filtering device.

Table 8-13. Receive low-pass filter RF characteristics.

Parameter	Value
Insertion loss	< 0.2 dB at 7.1 GHz
Transmit attenuation	> 70 dB

8.2.3.2.3.8 Waveguide: The waveguide between the TWTA isolator output and D-WTS-2 was redesigned to cut off TWTA emissions in the receive band that could "sneak back" into the SDST. The redesign was necessitated by the addition of the diplexer bypass switch D-WTS-2. Addition of the switch had introduced a new sneak path that allowed TWTA noise at the receive frequency band into the diplexer receive arm.

8.2.3.2.3.9 Descent Stage SDST: The SDSTs in the descent stage and the rover were both of the same "group buy III" design. The DSDST and RSDST transponders are discussed together in the next section.

8.2.3.2.4 Rover X-Band Telecom Components. The X-band telecom block diagram (Fig. 8-30) shows the telecom components on the rover stage as used during surface operations, as well as on three other stages. Note that names beginning with R refer to components on the rover.

The figure shows that the rover has two active components (the RSDST and the SSPA), two antennas (RLGA and HGA), the gimbal to point the HGA, and several microwave components (filters, etc.). Figure 8-43 shows the overall placement of the rover's X-band and UHF components, and Fig. 8-44 provides detail regarding the components. The UCXS in Fig. 8-43 is a UHF coaxial transfer switch.

8.2.3.2.4.1 Rover Waveguide Transfer Switches: The rover waveguide transfer switches have the designators R-WTS-1 and R-WTS-2. In the X-Band telecom block diagram (Fig. 8-30), position 1 of R-WTS-1 selects the RLGA.

R-WTS-2 selects between the HGA and the "through-path" that connected the RSDST with antennas in the cruise stage or the parachute cone. This WTS was first switched to select the HGA in Sol 1 and will not be switched again.

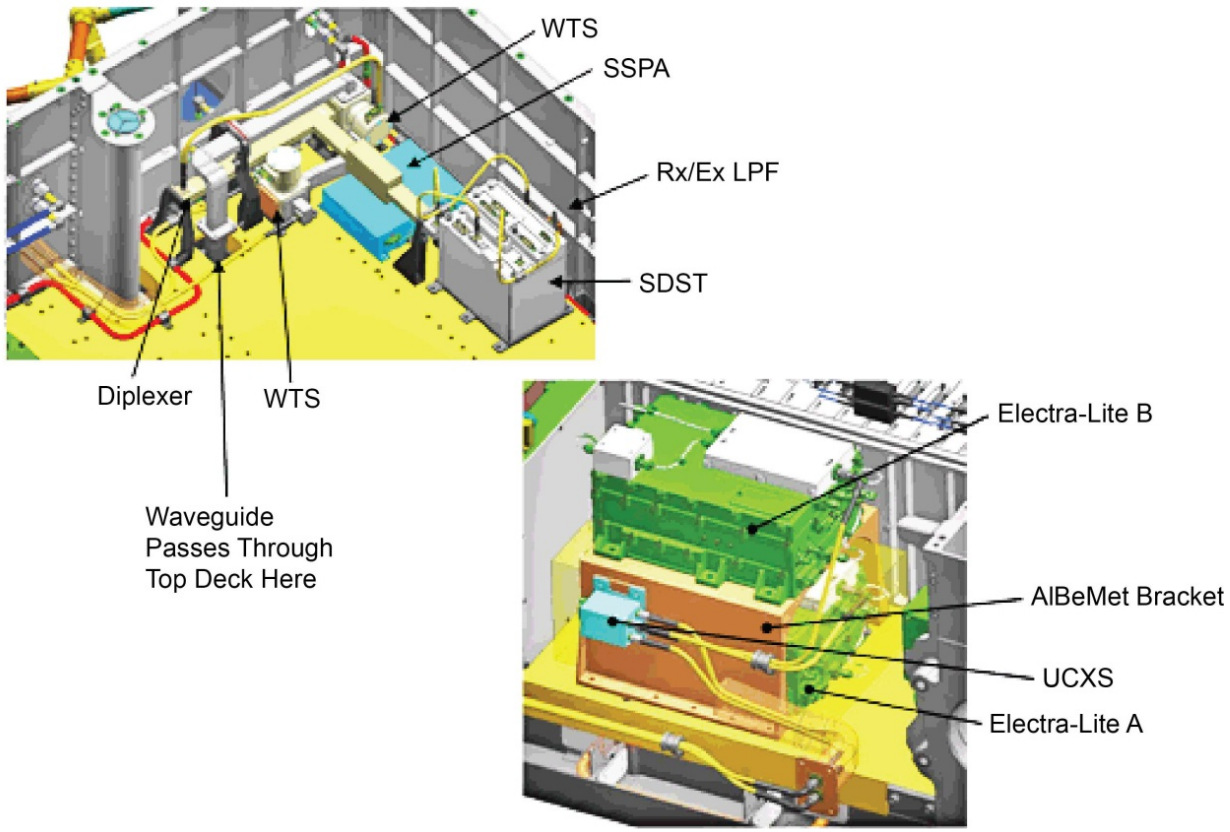

Fig. 8-43. Rover telecom internal layout showing overall placement of the X-band and UHF components.

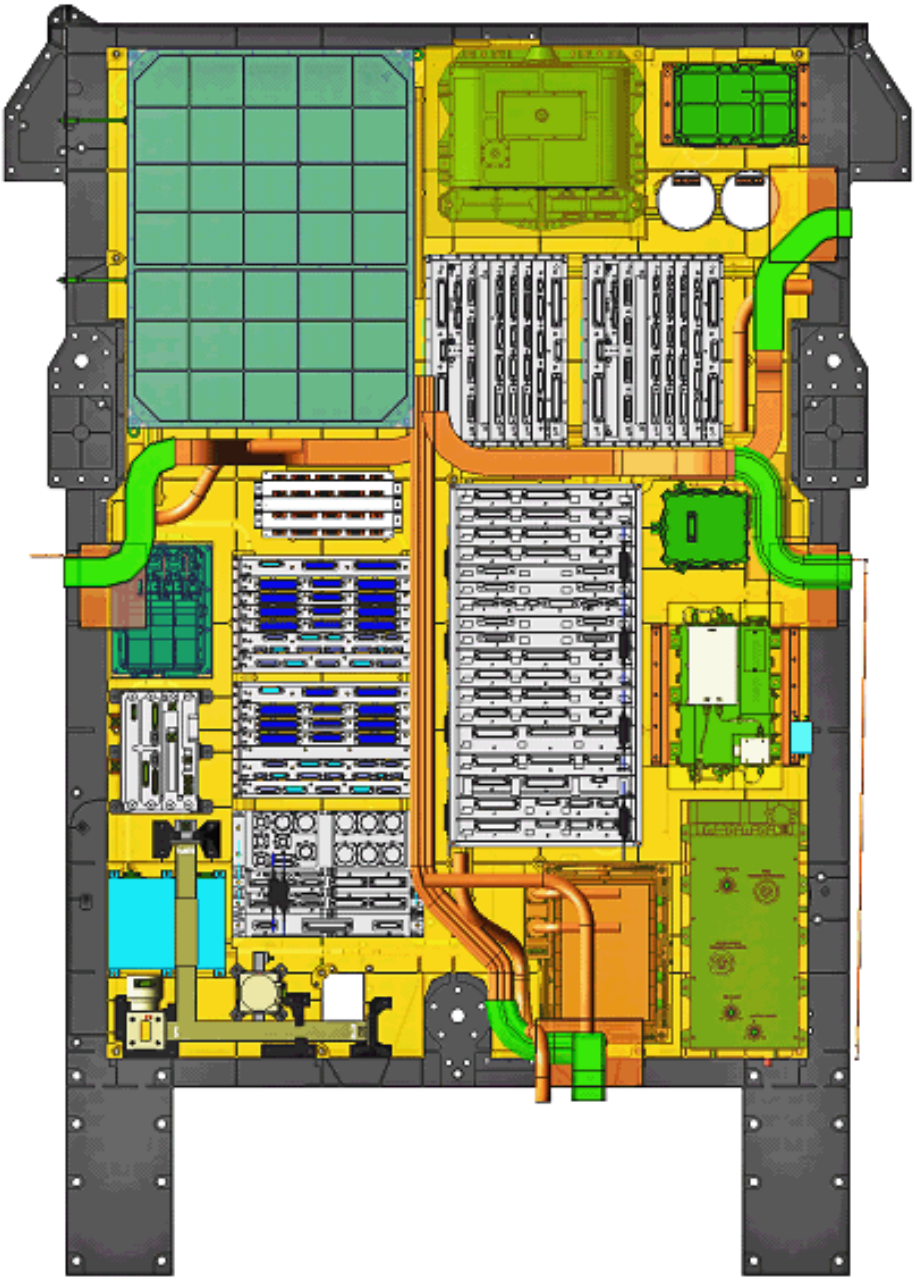

Fig. 8-44. Rover detailed internal layout.

8.2.3.2.4.2 Rover Low-Gain Antenna: The RLGA is of the same design as the PLGA and TLGA. Fault protection selects the RLGA for safe-mode communications on the surface. Depending on Earth-Mars distance, the RLGA can also support a low-rate uplink transmitted at 18 kW from a 34-m or a 70-m antenna in case the HGA is not functional or its view of the Earth during a DFE would be obstructed by terrain or occluded by objects on the rover.

A simplified analysis [18] was performed prior to the critical design review (CDR) to evaluate the RLGA pattern using the WIPL-D commercial high-frequency electromagnetic modeling software package [19] (WI = wires, PL = plates, D = dielectrics). Only a few key components were included in the model since the structure is large compared to the wavelength (see Fig. 8-45). The pre-CDR analysis, with the pattern shown in Fig. 8-46, includes ground-plane effects. The patterns are relatively smooth; however, the worst-case variations are quite high, on the order of 10 dB over a very small percentage of the coverage region. Figure 8-47 compares the pre-CDR gain pattern for the MSL RLGA with the design and with the minimum gain value for the MER RLGA.

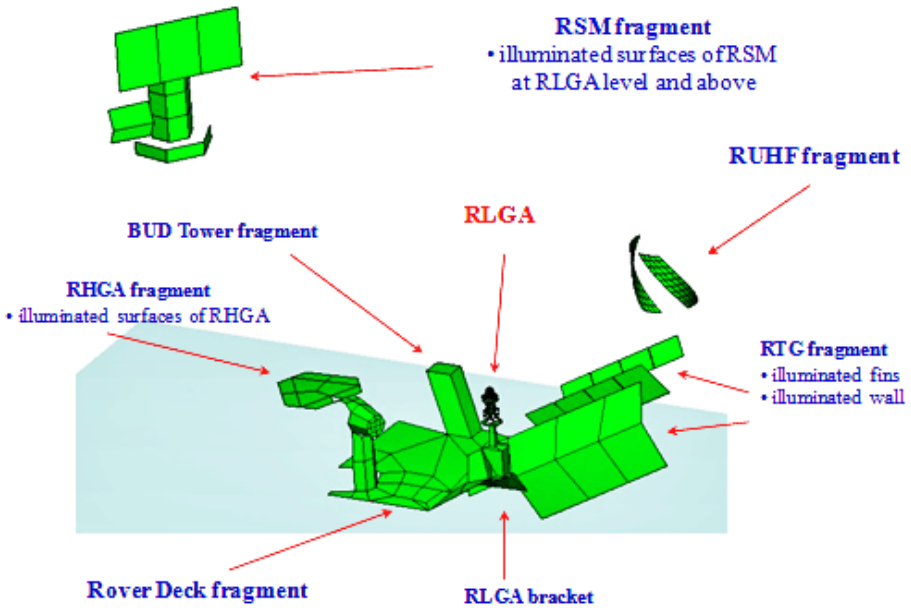

Fig. 8-45. WIPL-D model of RLGA on rover deck.

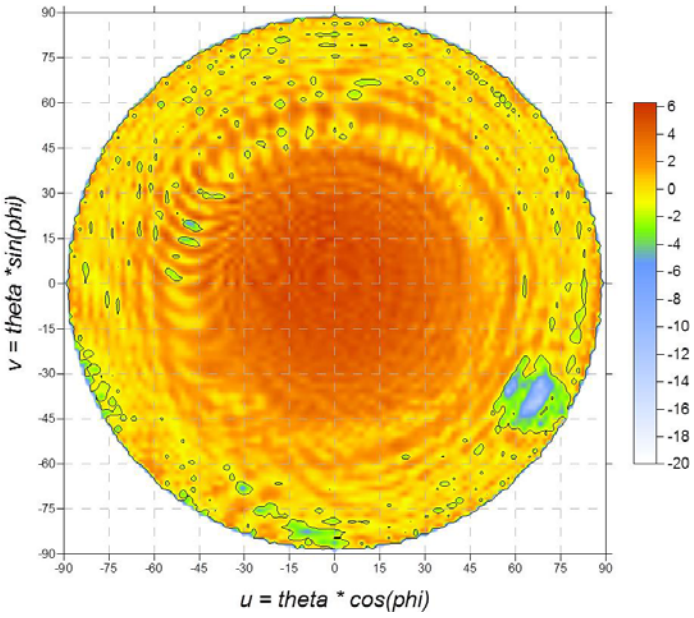

(a) Rx RLGA with groundplane effects, RCP 7.15 GHz

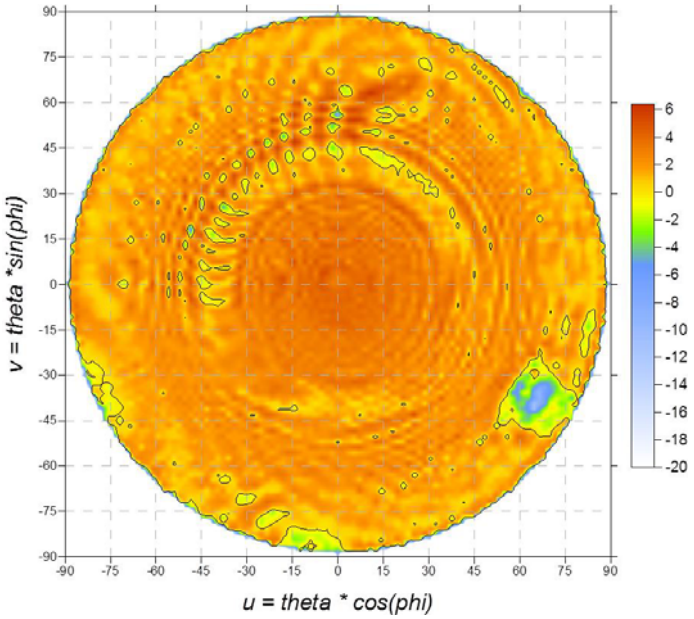

(b) Tx RLGA with groundplane effects, RCP 8.4 GHz

Fig. 8-46. RLGA patterns modeled by WIPL-D (includes ground-plane effects) for (a) 7.15 GHz and (b) 8.4 GHz.

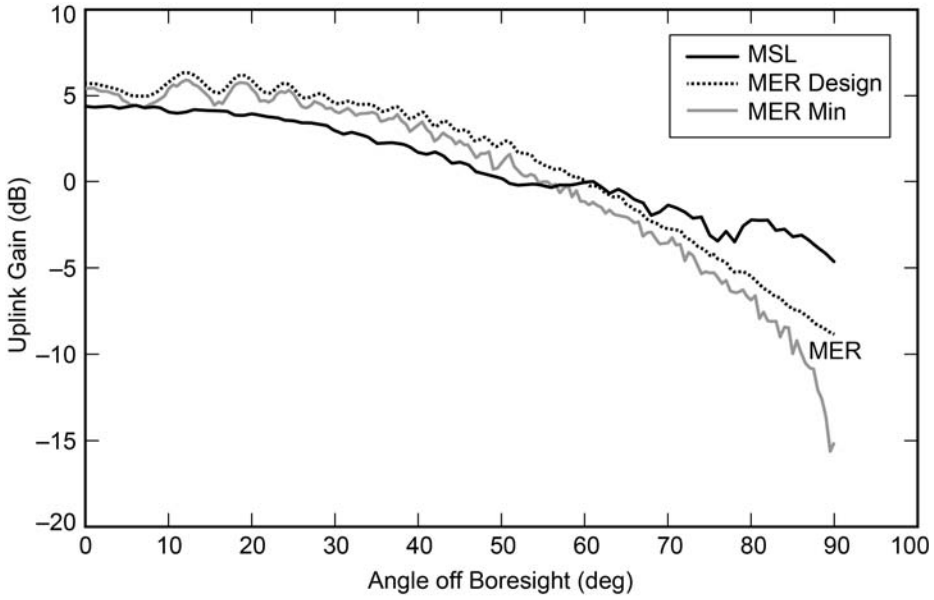

Fig. 8-47. Free-space uplink gain comparison between MER RLGA and MSL RLGA.

8.2.3.2.4.3 High-Gain Antenna: The HGA is mounted on a two-axis gimbal (Fig. 8-48) located on top of the rover deck. The 48-element microstrip patch HGA radiating element is the six-sided flat structure to the left. The antenna was provided by the European Aeronautic Defense and Space Company (EADS CASA ESPACIO).

The HGA was deployed after the rover landed. Table 8-14 provides the rover HGA RF characteristics.

Note that Table 8-14 separates out the "circuit loss" in the gimbals from the antenna gain.

Figures 8-49 and 8-50 show the measured uplink directivity (gain relative to the gain at boresight) at a frequency of 7145 MHz. Similarly, Figs. 8-51 and 8-52 show the measured downlink directivity at a frequency of (8395 MHz). The measured frequencies are representative of the MSL X-band frequencies.

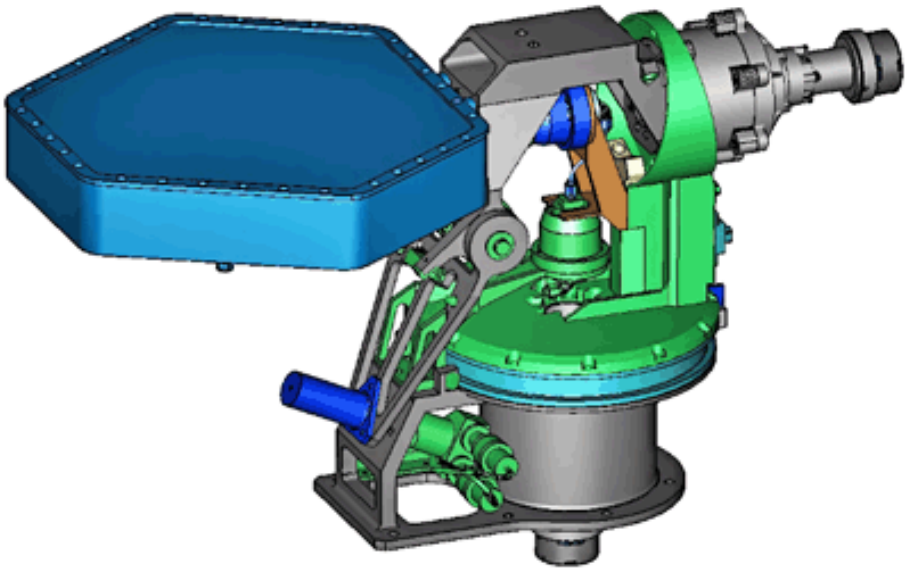

Fig. 8-48. HGA and gimbal assembly.

Table 8-14. Rover HGA RF characteristics.

Parameter		Value	Conditions
Dimensions	cm	25.5 by 29.4	
Transmit gain	dBi	25.5	0 deg off boresight
		24.1	2 deg off boresight
		20.4	5 deg off boresight
Receive gain	dBi	20.2	0 deg off boresight
		19.7	2 deg off boresight
		17.3	5 deg off boresight
Loss in gimbals	dB	1.2 dB	
Polarization		RCP	
Transmit axial ratio		3.0 dB	Within 5 deg from boresight
Receive axial ratio		2.4 dB	Within 5 deg from boresight

In the patterns, theta is the angle from boresight, with the boresight planned to be Earthpointed. The multiple curves apparent in the sidelobes of the patterns represent cuts at 0, 45, 90, and 135 deg around phi, the axis orthogonal to theta.

The expanded Fig. 8-50 and Fig. 8-52 show primarily the main lobe, with the main lobe's pattern similar at each phi. The figures show that the HGA has good main lobe symmetry over the full range of phi and that the main lobe meets the required gain (shown as the rectangles beneath the main lobe).

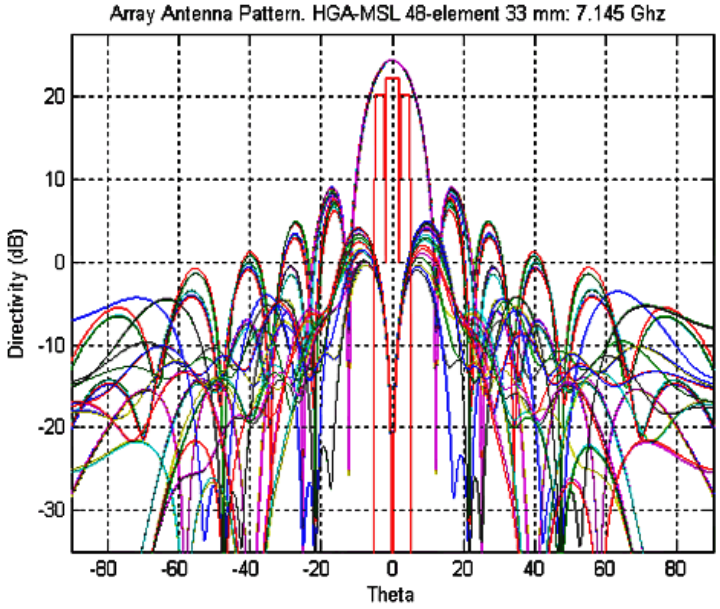

Fig. 8-49. HGA uplink directivity showing first several sidelobes.

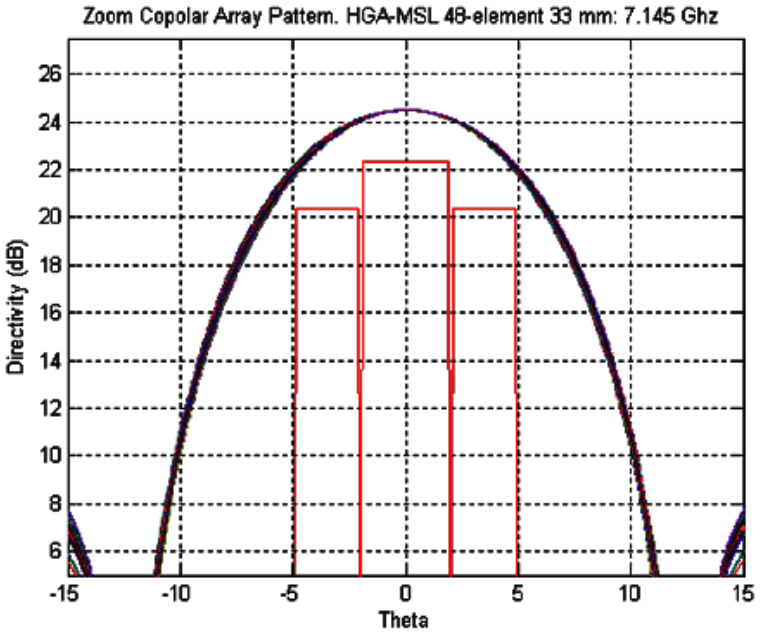

Fig. 8-50. Detail of the uplink main lobe HGA directivity.

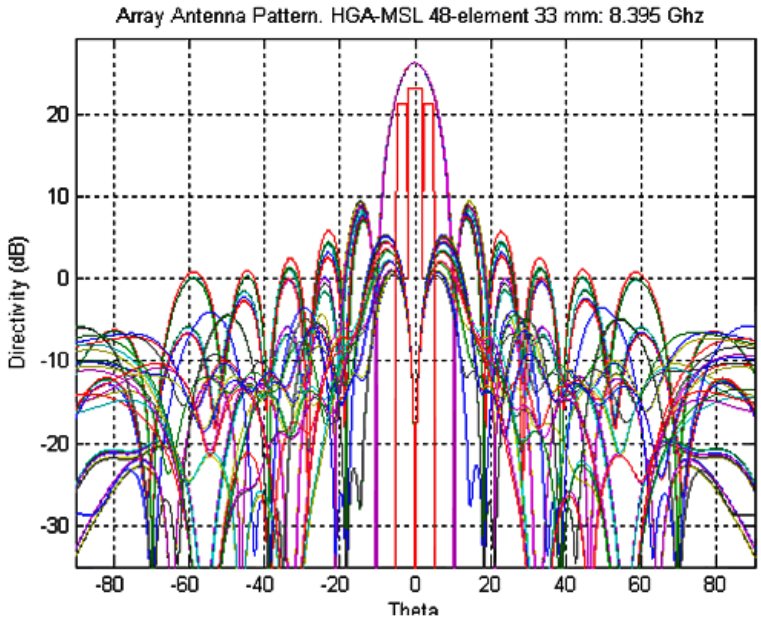

Fig. 8-51. HGA downlink directivity showing first several sidelobes.

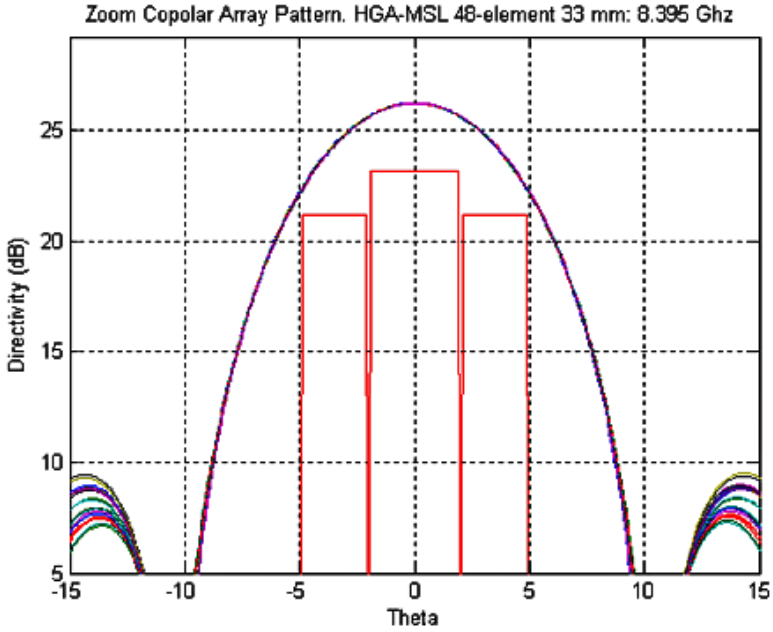

Fig. 8-52. Detail of HGA main lobe downlink directivity.

8.2.3.2.4.4 Rover Diplexer: The design of the descent-state diplexer and the rover diplexer is the same. A diplexer provides for the frequency separation of the receive signal coming from and the transmit signal going to the antenna.

8.2.3.2.4.5 Rover Small Deep Space Transponder: This paragraph describes the rover SDST (shown in some figures as RSDST) and the identical descent SDST (DSDST). During cruise, DSDST provided the X-band links, and RSDST was powered off except during two brief "aliveness" tests. In surface operations, RSDST provides the X-band links.

To distinguish from earlier SDST designs, the MSL SDST is in the "Group Buy III." Relative to earlier designs used on MER and MRO, Group III transponders have two major improvements. First, a problem has been fixed with the digital-to-analog converter in the receiver tracking loop (the "DAC glitch")[23]. This makes receiver acquisition of a swept uplink carrier frequency at any temperature easier than on previous projects. Second, Group III transponders have much less coherent leakage compared to the one used on MER-A (Spirit). As a result, the receiver static phase error (SPE) does not drift when the receiver is not locked. This also makes uplink carrier sweep frequencies easier to plan compared to MER.

Figure 8-53 shows a Group III SDST.

The SDST is composed of four different modules: the digital processing module (DPM), the downconverter module[24], the power module, and the exciter module.

[23] When the digital representation of the receive frequency changes from a mixture of 1s and 0s to nearly all 0s, this can cause a voltage spike at the analog output in earlier designs. This spike, more prominent at cold temperatures, can knock an already acquired SDST receiver out of lock on the uplink, particularly with sweeps in the positive direction.

[24] In a receiver, a downconverter is used to transform the signal from the passband back to the baseband for further processing. Baseband refers to the original frequency spectrum of the signal before modulation or up-conversion.

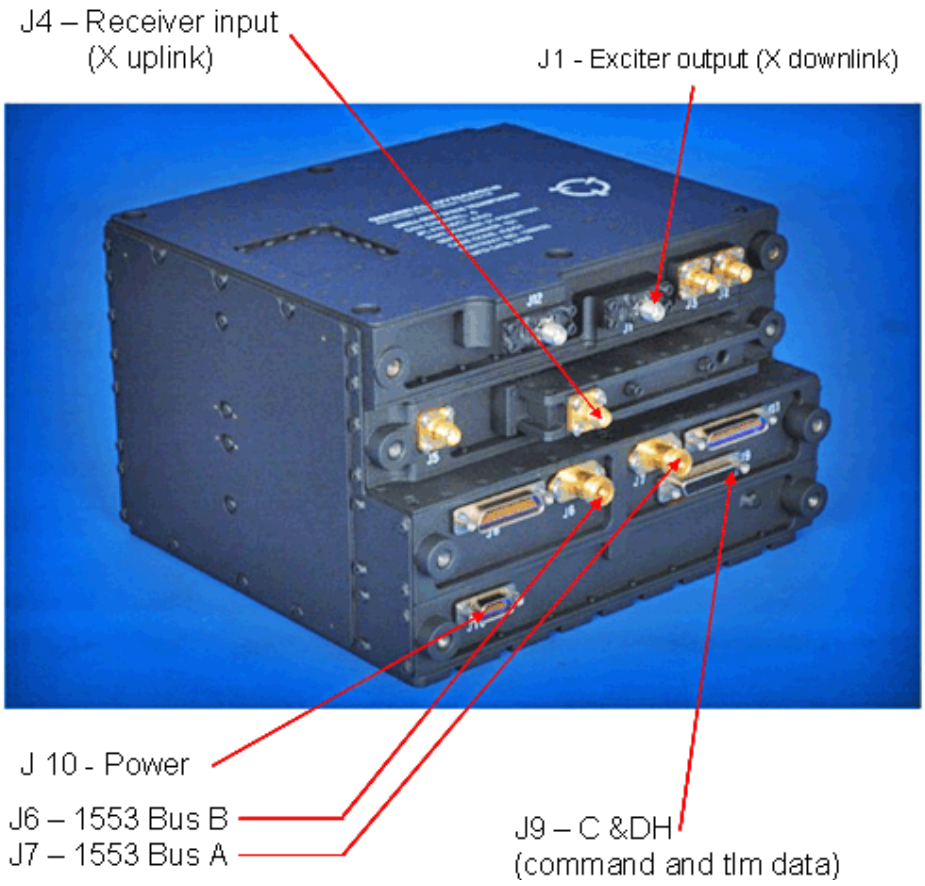

Fig. 8-53. Group III small deep space transponder.

The DPM has three main functions:

1. Convolutionally encode the data (if "coding" is enabled by 1553 control).

2. Provide X-band baseband telemetry and ranging signals to the exciter module.

3. Convert the analog output of the downconverter module into binary data.

Each SDST has two oscillators that can drive the downlink: a voltage-controlled crystal oscillator (VCXO) whose frequency is controlled by the loop's error voltage and is, therefore, related to the uplink frequency transmitted to the rover; and an auxiliary oscillator (aux osc) for which the

frequency is generated on board and, therefore, varies with temperature (and to a lesser extent, atmospheric pressure).

The power converter module provides a set of steady voltages to the other SDST modules.

The downconverter module takes the 7.150-GHz received uplink signal and converts it to an intermediate frequency (IF) signal at 4/3 F1 [20][25]. The uplink signal, which may be modulated with command and ranging waveforms, gets sampled by an analog-to-digital converter (ADC) at the input of the digital processor module. These samples are provided to three "channels" to use the old analog terminology:

1. The carrier channel (for uplink carrier tracking).

2. The command channel (for demodulating the command signal).

3. The ranging channel.

The command channel has a ± 2 kHz bandpass filter centered around 2 kHz.

The ranging samples of the baseband uplink are put through a DAC to produce an analog signal. The resulting analog signal is a "turn-around" ranging waveform that modulates the downlink carrier.

Table 8-15 lists some of the SDST requirements relevant to the uplink (receive) telecom link performance. The SDST functional specification [17] provides a more complete listing.

The exciter's RF power output to the SSPA or the TWTA can be an unmodulated or modulated carrier. In surface operations, the RSDST downlink is either unmodulated (beep) or modulated by telemetry only (DTE). During cruise, the DSDST exciter module phase modulated the downlink carrier with telemetry and (if selected) either of two waveforms used for navigation.

1. Telemetry (from the DPM; this is a binary phase shift key (BPSK)-modulated square-wave subcarrier).

---

[25] In SDST nomenclature, F1 is the fundamental frequency from which the uplink and downlink frequencies are derived. For example, the X-band downlink is 880 times F1, and the X-band uplink is 749 times F1. For MSL, operating on X-band channel 4, F1 will be approximately 9.59 MHz. The VCXO output is at two times F1.

Table 8-15. SDST receive functional characteristics.

SDST Receive Parameter	Value
Receive signal maximum power	–70 dBm (maximum to meet other performance specs) +10 dBm (maximum to cause no damage)
Carrier loop threshold bandwidth	Two bandwidth (BW) settings: 20 ± 2 Hz at receiver threshold (varies with carrier loop signal to noise ratio (SNR); max bandwidth is ~120 Hz at strong signal, 100 dB SNR) 50 Hz ± 5 Hz at receiver threshold (used in DSDST in launch phase, not planned for RSDST surface operations)
Noise Figure	< 3.2 dB over temperature, aging, and radiation, 2.1 dB typical at beginning of life (BoL), room temp
Carrier Tracking Threshold at BLF and 0-dB loop signal-to-noise ratio	–157.7 dBm typical –155.0 dBm worst case
Data Rates	7.8125 to 4000 bps

2. Turn-around ranging (analog, from the DPM, after its D/A converter).

3. Differential one-way ranging (DOR) (analog, a 2 F1 [~19 MHz] sinewave continuous wave (CW) signal, generated in the exciter module). In this case, CW refers to an analog signal as opposed to a discrete-time signal.

Table 8-16 lists some of the SDST requirements relevant to the downlink (transmit) telecom link performance; see [17] for more.

8.2.3.2.4.6 Rover Receiver Low-Pass Filter: The rover Rx LPF is of the same design as the descent stage Rx LPF. The filter rejects SSPA 'ring-around' noise (power reflected from the diplexer) so that the RSDST can detect very weak uplink signals.

8.2.3.2.4.7 Solid State Power Amplifier: The MSL SSPA is of the same design as the MER units. Figure 8-54 is an SSPA block diagram (© 2005 IEEE). The X-band SSPA consists of a solid-state RF amplifier, an electronic power converter (EPC), mode control and telemetry circuitry, and input and output isolators. Table 8-17 shows key characteristics. More detail, diagrams, and photographs of the MER SSPA are in Ref. 21.

8.2.3.3 Functional Redundancy (Rover as Backup to Descent Stage)

The MSL RF switch complement allowed the RSDST to act as a back-up to the DSDST during cruise. The downside is that the rover has a weaker transmitter (15-W SSPA rather than the 100-W TWTA) and more circuit losses.

Table 8-16. SDST exciter characteristics at 880f1.

X-Band 880f1 Transmit Parameter	Value
Output power level of X-band exciter	13.0 + 3/–2 dBm over temperature, tolerance, end of life, radiation
Phase noise	<–20 dBc/Hz @ 1 Hz (aux osc mode)
Aux Osc short term frequency stability	0.06 ppm at any constant temp from 10°C to 40°C (1 sec integration measured at 5 minute intervals over 30-min span)
NCO subcarrier tone short term stability	1 ppm (as of July 2009)
NCO subcarrier tone long-term stability	50 ppm (as of July 2009)
Harmonics	<–50 dBc
In-band and out-of-band spurious	<–50 dBc
Minimum symbol rate	0 symbols per second (sps) for subcarrier; 2000 sps for direct modulation
Maximum symbol rate	Filtered mode: 4.4 million symbols per second (Msps) Wideband (unfiltered) mode: > 4.4 Msps
Modulation Index accuracy	±10%
Ranging modulation indices (peak)	4.375, 8.75, 17.5, 35, 70 deg
Ranging modulation Index accuracy	±10%
Ranging modulation index stability (over temp., radiation, and EOL)	< ±20%
Ranging delay variation over flight acceptance (FA) temperature range	< 20 ns typical
DOR modulation index (peak)	70 deg nominal
DOR modulation index accuracy	± 10%
DOR modulation Index stability (over temp., radiation, and EOL)	< ±25%
Telemetry Modulation Index	0 to 138 degrees (128 steps, approximately 1.1 degrees per step)

The difference between rover and descent stage downlink capability is about 9 dB in effective isotropic radiated power (EIRP). Except for the power difference all downlink functions were available through either path. Note that there is no provision to bypass the diplexer in the rover. The diplexer could have handled the SSPA RF power output at critical pressure during EDL and does handle it on the surface.

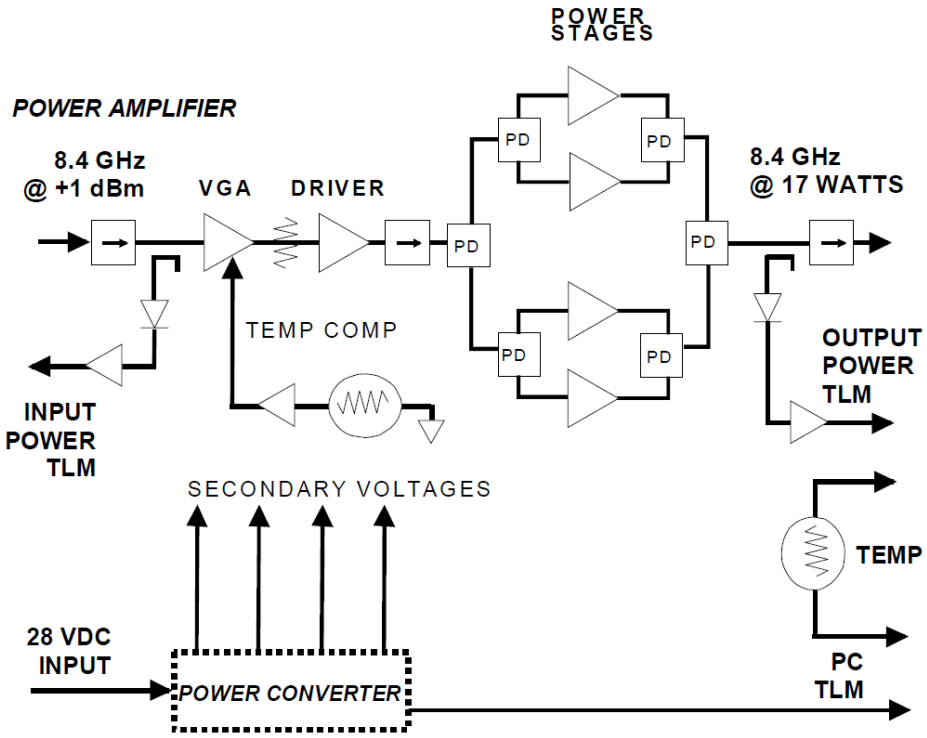

Fig. 8-54. MSL SSPA block diagram (PD = passive device in power amplifier, VGA =variable gain amplifier).

Table 8-17. SSPA key characteristics.

Parameter	Value
Frequency Range	8.395–8.455 GHz
Output Power (RF)	15 W
DC Input Power	55 W nominal, 64 W max
Output voltage standing wave ratio (VSWR)	1.5:1 max

8.2.3.4 Encoding Modes/Frame Sizes

The X-band downlink has three Turbo codes (1/2, 1/3, and 1/6); the data rates range from 10 bps to 62,500 bps. RF spectrum management bandwidth limitations to prevent interference between missions preclude the use of the combination of 62,500 bps bit rate with turbo 1/6 coding. That combination would produce too high a symbol rate; for Mars missions, the symbol rate is limited to 300,000 sps.

An effort was made to reduce the telemetry frame size (1784 bits) at low rates while keeping some coding efficiency. MSL can use an interleave depth of 1,

whereas MER had only an interleave depth of 5. From these values, the effective information rate (the ratio of information bits in a frame to total bits) on MER was 1760/3040 = 0.58; on MSL it is 1784/2072 = 0.86, an improvement of 1.7 dB. The improved efficiency means MSL has significantly less frame overhead than MER at 10 and 40 bps.

8.2.4 UHF Flight Subsystem Description

8.2.4.1 UHF Interfaces with MSL Control and Data Systems

The Electra-Lite (ELT, used for UHF relay) differs from the SDST (used for X-band DTE/DFE) in that the transmitted data rate is controlled by the radio, not the multi mission system architectural platform (MSAP) telecommunications interface board (MTIF). The MTIF clocks data into the ELT internal buffer. When the buffer-fill threshold (a settable parameter) is passed, the ELT forces the data flow control line high and the MTIF stops clocking in data until the line drops again. MSL selected three ELT buffer fill rates as baseline:

- 8250 Hz used for low transmit data rates to minimize latency (primarily for use during EDL), with a telemetry frame size of 1784 bits.
- 33,000 Hz used for transmit data rates between 2 kbps to 32 kbps (primarily for safe-mode low-latency applications), with a telemetry frame size of 1784.
- 2,062,500 Hz for normal operations, with a telemetry frame size of 8920 bits. This fill rate can keep up with even the highest transmit rates of 2 Mbps.

Two kinds of data encoding are possible for the UHF links:

1) Reed Solomon encoding (interleave depth 1 and 5) for unreliable (bit-stream or non-Proximity-1 protocol) MSL-to-Orbiter communications.
2) Checksum-frame for nominal reliable (Proximity-1) mode UHF return link (EDL and surface operations).

The ELT has redundant uplink (command) and downlink (telemetry) LVDS interfaces that are cross-strapped to the MTIF card (each MTIF has four command/telemetry ports). The active downlink port on the telecom side must be selected via a 1553 command. Both uplink ports in ELT are always active.

The rover bus controller (BC) on the MTIF controls the primary 1553 bus. ELTs are connected via the remote terminal (RT). The MTIF resides in the rover computer element (RCE).

8.2.4.2 UHF Key Hardware Components

Refer to Fig. 8-31 for the UHF components on the parachute cone, the descent stage, and the rover, as discussed in the next three sections.

8.2.4.2.1 Parachute Cone UHF Telecom Components

8.2.4.2.1.1 Parachute UHF Antenna (PUHF): The PUHF was used only from the CSS to the backshell deployment portion of EDL. Refer to Fig. 8-16 for this part of EDL. The antenna provided communication with relay orbiters over a wide range of view angles. If a major spacecraft failure such as an event resulting in a tumbling attitude had occurred, the antenna would have permitted reconstruction data to be received in all but the most extreme attitudes.

The PUHF (see Fig. 8-55) was a wrap-around antenna of the type used previously on launch vehicles and during the Phoenix lander EDL. It was designed and manufactured by Haigh-Faar of New Hampshire, in close cooperation with JPL.

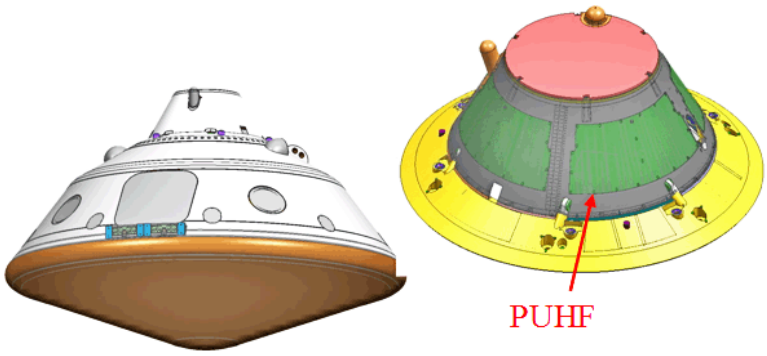

Fig. 8-55. PUHF antenna mounted on parachute cone.

The antenna consisted of four segments individually mounted on the parachute cone, and connected via a one- to-four power divider. Each segment had two radiating patch antenna elements, making a total of eight radiating patch antennas in a conical array.

Excitation of the antenna was via a coaxial cable between the descent stage switch D-UCTS and the one- to-four power divider mounted on the inside of the parachute cone. The pattern was semi-omnidirectional, roughly azimuthally symmetric, with a null aligned with the spacecraft –Z axis. Pattern cuts for a full 0 to 360 degrees in theta (red labels), for different phi angles (rotation about the –Z axis) overlaid, are shown in Fig. 8-56.

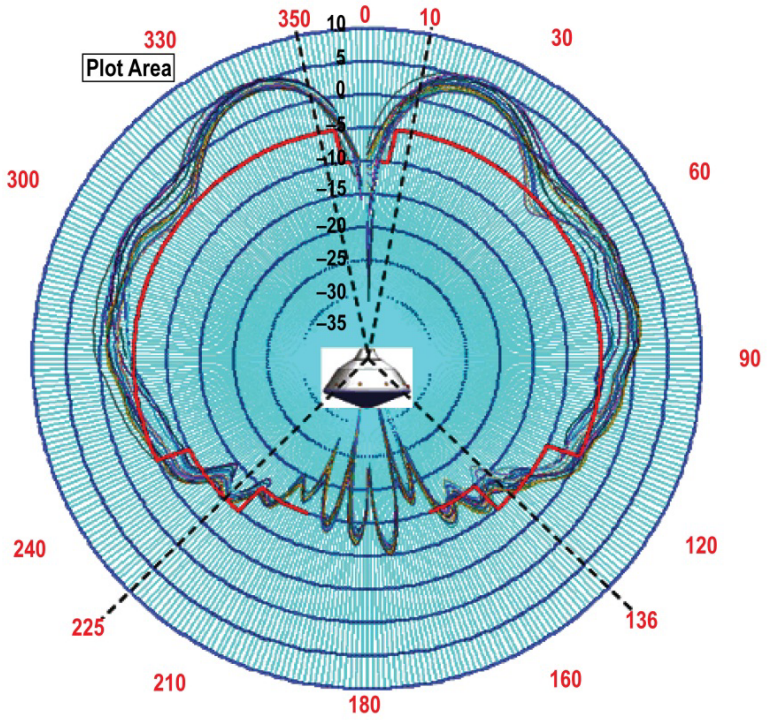

Fig. 8-56. PUHF antenna required and measured radiation pattern (angles and curves as defined in text).

The figure is a polar plot with angle from the reference direction around the plot's circumference and the gain increasing radially outward. The reference direction is the –Z axis (theta = 0 deg) at the top of the figure. Theta angles are labeled in red 0 to 360 degrees clockwise. Gain is labeled from –35 dBi near the center of the plot to +10 dBi at the outer edge.

The several colored curves in this figure plot gain vs. theta. They are analogous to the curves for the HGA in Figs. 8-49 through 8-52. However, the HGA figures are rectangular plots with theta on the X-axis and gain on the Y-axis.

- Required gain: indicated by the thicker red curve.
- PUHF measured gain: indicated by the remaining six curves. Each curve shows the gain vs. theta at a fixed phi (0, 30, 60, 90, 120, or 150 deg).

The figure shows that the PUHF gain pattern generally met the requirement (measured gain greater than required gain) for the range of theta angles specified. Over most theta angles, the six phi curves do not differ from each other by more than 6 dB. The antenna had a narrow but deep null along the –Z

axis, and its performance within about 20 deg of the +Z axis was highly variable with small changes in pointing angle.

8.2.4.2.2 Descent Stage UHF Telecom Components. The UHF components on the descent stage are the D-UTS switch and the DUHF antenna (plus connecting cables). The DUHF (Fig. 8-57) is a sleeve dipole design that provides an azimuthally symmetric pattern.

As shown in Fig. 8-58, the DUHF transmit pattern was significantly affected by the descent stage hardware [22]. Scattering from the descent stage distorted and moved the dipole null from along the –Z axis. The pattern coverage, however, was sufficient to close the link to the relay assets during the critical few minutes of powered descent and sky crane activity.

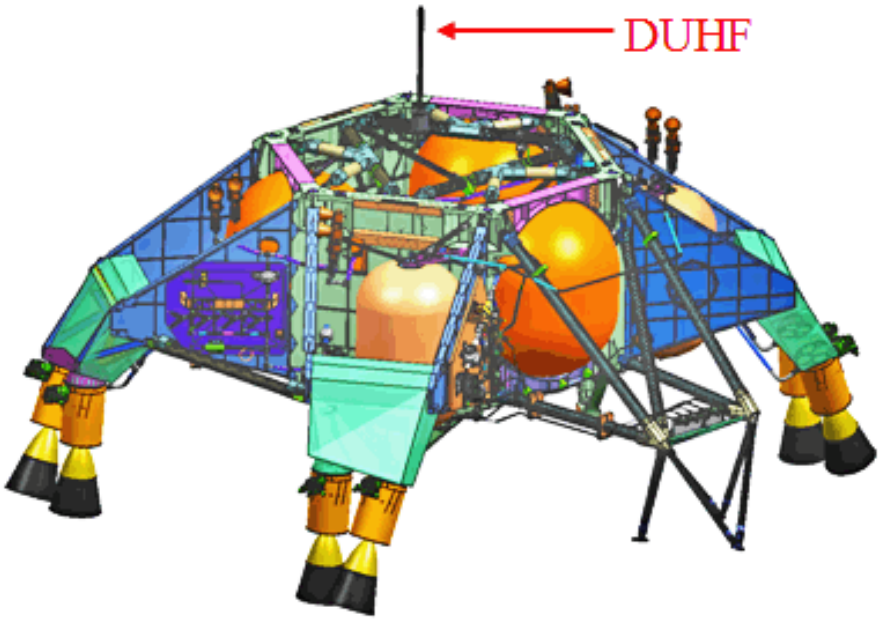

Fig. 8-57. DUHF antenna mounted on descent stage.

The D-UTCS was used to switch from the PUHF to the DUHF at backshell deployment. To avoid "hot switching" of the D-UCTS, UHF transmission was stopped briefly while the switch actuated.

The antenna cable from the parachute cone (where the PUHF was mounted) to the descent stage (DUHF) and the antenna cable from the descent stage to the rover (RUHF) passed through the mega-cutters. The two cables were severed at backshell separation and rover deployment, respectively.

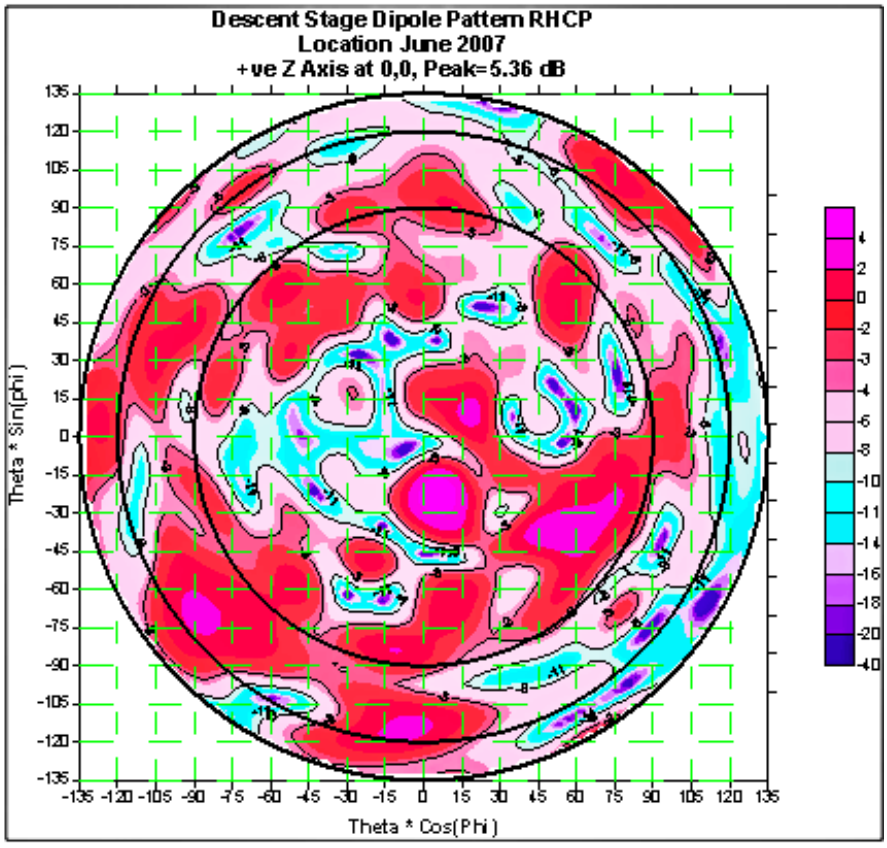

Fig. 8-58. Transmit pattern for DUHF antenna mounted on descent stage.

8.2.4.2.3 Rover UHF Telecom Components. The Electra-Lite radios are mounted inside the rover WEB, as shown in Fig. 8-59. ELT-A and ELT-B are redundant radios. ELT-A has been in use since EDL, and this use will continue unless there is a problem with it. The ELT-B radio is mounted on a bracket (made from AlBeMet[26]) above the ELT-A radio. The R-UCTS mounts on the side of the bracket. Because there is extra thermal isolation of the ELT-B due to the bracket, ELT-B would run warmer than ELT-A during return-link

[26] AlBeMet is the trade name held by the Brush Wellman Company for a beryllium and aluminum composite material derived by a powder metallurgy process. AlBeMet is formed by heating fine beryllium and aluminum powder under high pressure to form a uniform material. These alloys are significantly less dense than aluminum. (http://en.wikipedia.org/wiki/AlBeMet)

transmission. ELT-B thermal control would only be an issue if ELT-B was required for a long overflight, and the WEB thermal environment was severe.

The RUHF is a quadrafiler helix antenna specially designed for the MSL mission. It is used for all of the surface activities in the mission and was used during the last portion of EDL. Figure 8-60 shows the RUHF mounted on the rover. Figure 8-61 shows a detailed view of the antenna itself.

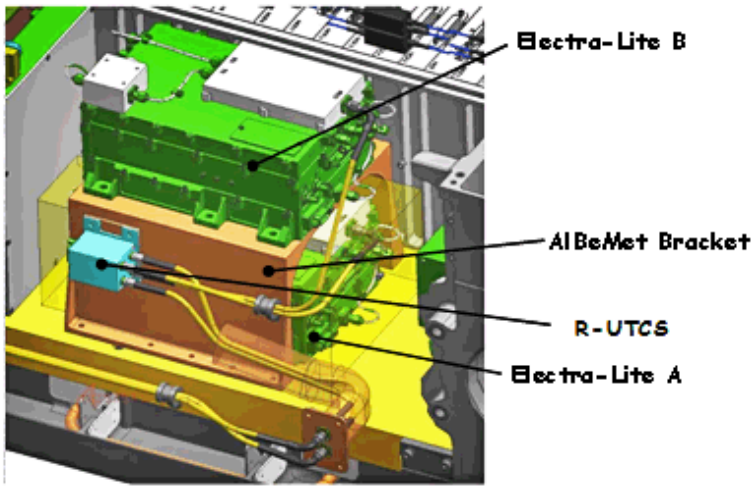

Fig. 8-59. UHF hardware in rover WEB.

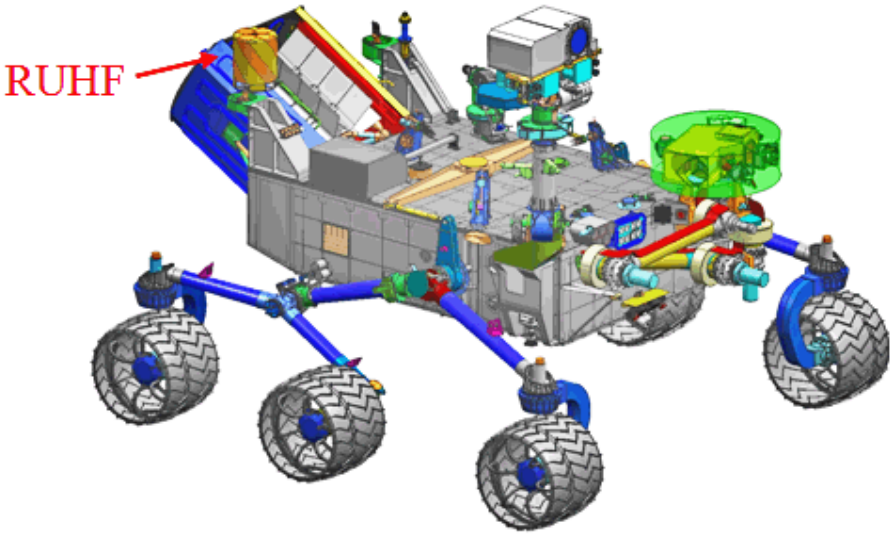

Fig. 8-60. RUHF antenna mounted on rover.

Fig. 8-61. MSL RUHF Quadrafiler helix antenna.

The EDL sequence commanded the R-UTCS to switch UHF from the DUHF to the RUHF for the sky crane activity (Fig. 8-62). During this activity, the RUHF was shadowed partially and to a varying degree by the descent stage above it. In this sketch, the term BUD refers to the bridle, umbilical, descent rate limiter device.

To study the effects on the pattern, we performed an analysis using WIPL-D at three representative heights (distances) below the descent stage (as illustrated in Fig. 8-62). The results at the 401 MHz return link frequency are shown in the three parts of Fig. 8-63. It is evident from the top part that, as expected, the RHUF pattern shows much distortion initially (when the rover is still close to the descent stage (1 m away). Near the end of the sky crane deployment (7.5 m away from the descent stage), the bottom part of the figure shows a pattern similar to the surface pattern. (The surface pattern at 401 MHz is in Fig. 8-66.)

After the landing, the broad pattern of the RUHF has provided coverage at RCP over most of the sky to very low on the horizon.

A WIPL-D analysis [19] was performed early in the telecom development to assess the pattern distortion in surface operations due to the rover deck, the RTG, and other objects in close proximity to the antenna. At the UHF frequencies, most of the deck and its payload can be considered close to the antenna. Fig. 8-64 shows the WIPL-D model.

Knowledge of the RUHF performance on the Martian surface is critical to the mission. The RHUF 437 MHz forward link pattern and the 401 MHz return link pattern were measured using an MSL mockup in a fashion similar to the measurements made for the Phoenix lander mission [23]. These measurement patterns are included in the data volume prediction tool used by the flight team for planning sol-to-sol activities.

Figures 8-65 and 8-66 show the analysis results, including ground effects [24], for the return and forward links, respectively. The patterns are significantly better than the corresponding MER UHF monopole patterns, with no deep nulls except at the low elevation angles near the horizon.

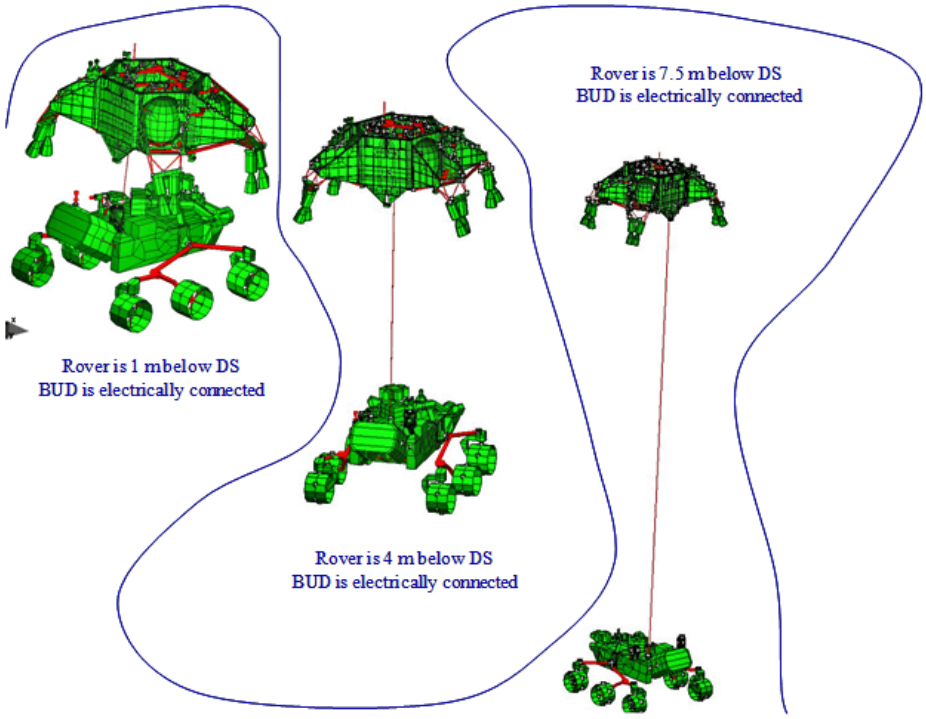

Fig. 8-62. RUHF pattern study for sky crane.

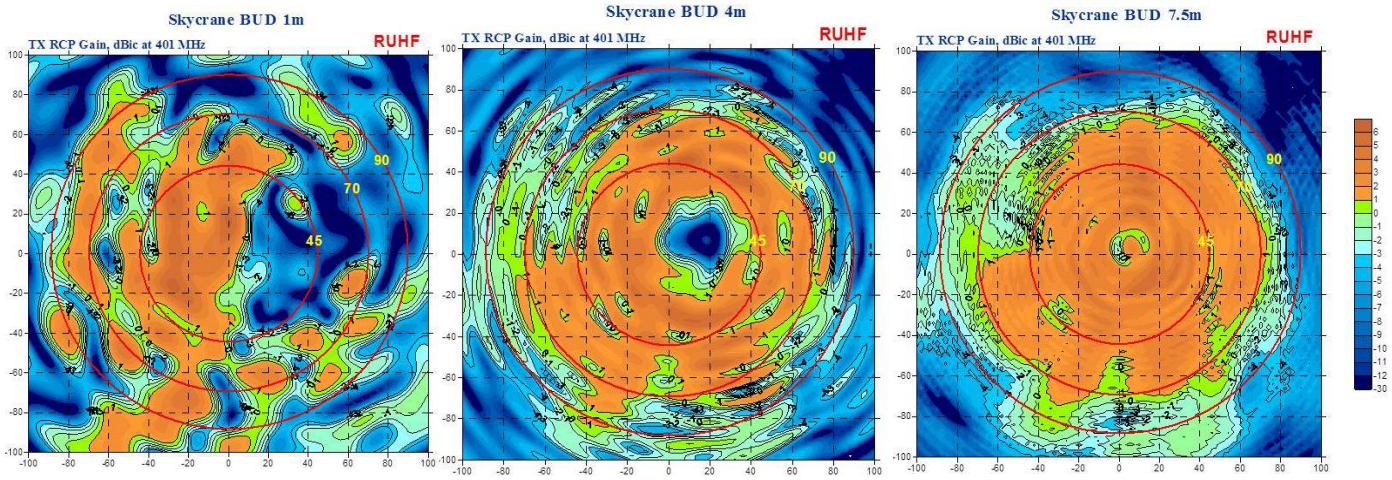

Fig. 8-63. RUHF pattern analysis results for sky crane BUD 1 m, 4 m, and 7.5 m.

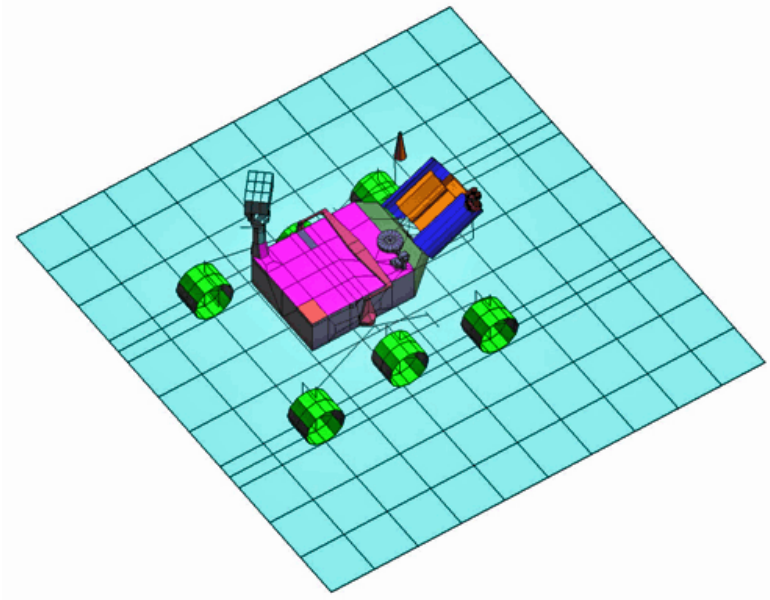

Fig. 8-64. WIPL-D model for RUHF pattern analysis.

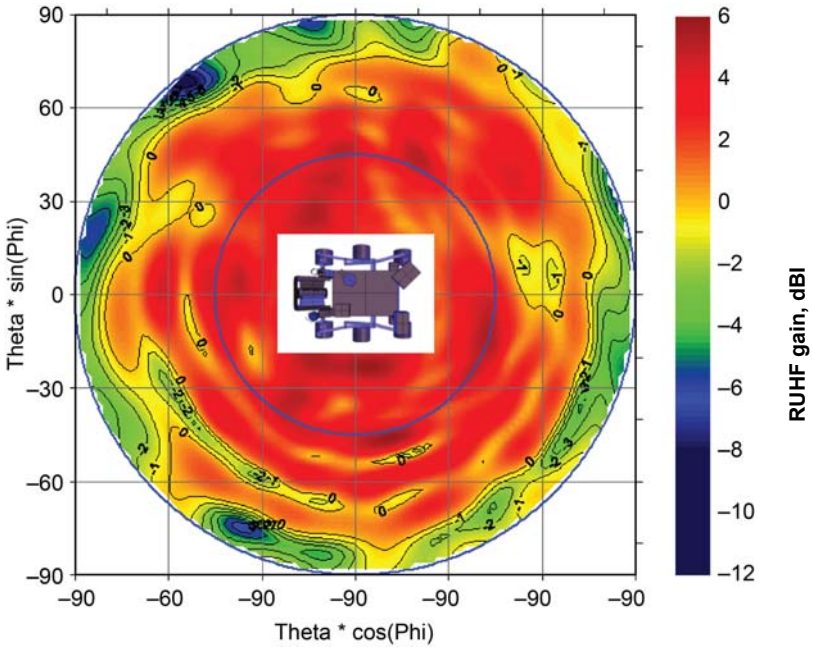

Fig. 8-65. Surface RUHF antenna pattern, Rx.

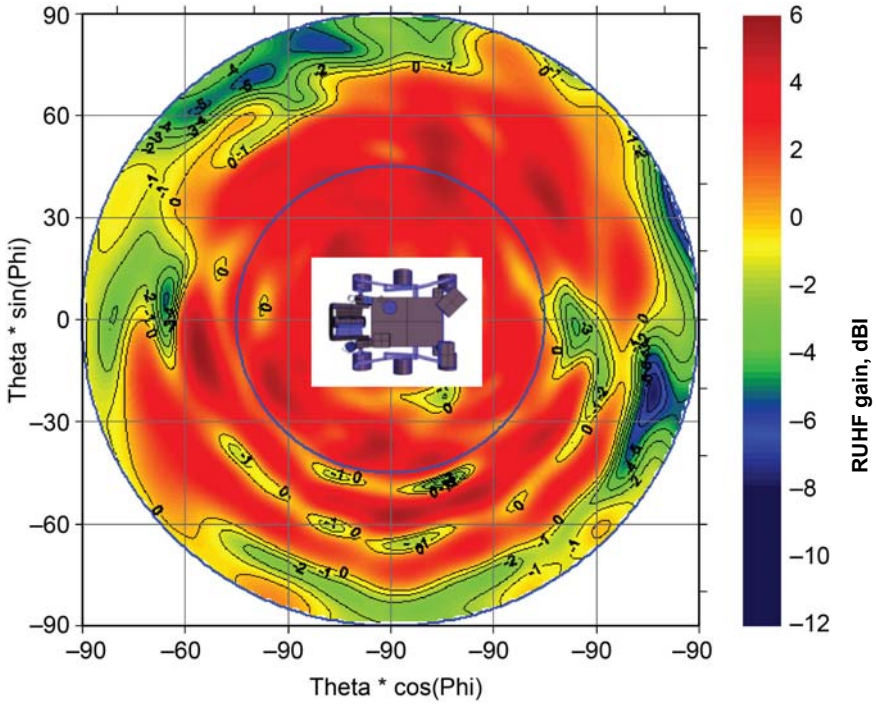

Fig. 8-66. Surface RUHF antenna pattern, Tx.

8.2.4.2.3.1 Electra-Lite Radios: The dual-redundant Electra-Lite radios (ELT-A and ELT-B) implement the functions for relay communications with the Mars Odyssey and MRO orbiters (and other compatible orbiters such as MEX). ELT-A has provided the rover UHF communications for EDL and all surface operations so far, with ELT-B tested for "aliveness" during cruise, but currently standing by.

The ELT is a variant of the JPL Electra style software defined radio (SDR that is intended for use in landers. The name Electra-Lite refers mainly to a reduced weight relative to the standard Electra and also to a lower power consumption. The only function not present in the ELT is a half-duplex mode signal path. The ELT provides full capability in all the other radio functions of the standard Electra, and Ref. 25 provides more detail on the Electra and Electra-Lite radios.

Unlike the MSL X-band subsystem with its transponders and its separate power amplifiers (TWTA or SSPA) and diplexers, each ELT has an integrated transponder, power amplifier, and diplexer. The UHF RF power delivered to the antenna from the diplexer is greater than 8.5 W.

The flight radio FM-002 (ELT-A) is shown in Fig. 8-67.

The downlink and uplink operational parameters are summarized in the next two subsections, followed by information on the Prox-1 parameters, buffer data management, and other ELT functions.

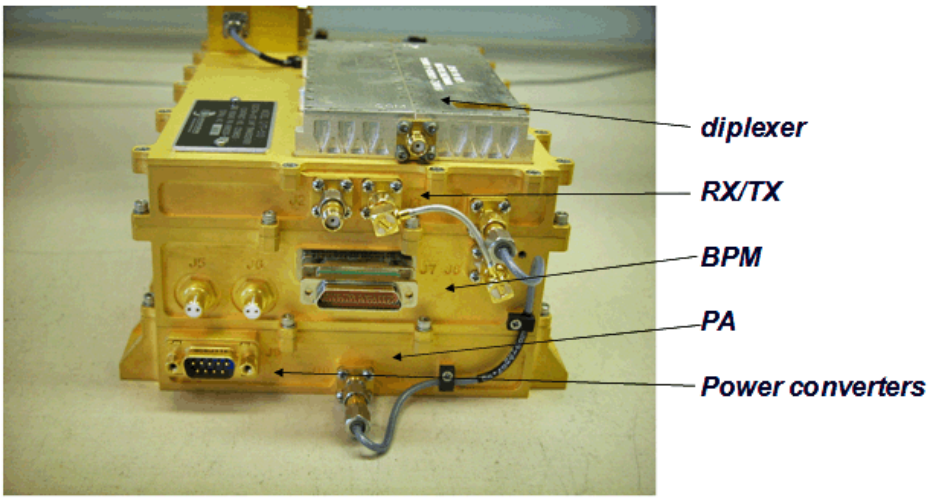

Fig. 8-67. Electra-Lite FM-002.

8.2.4.2.3.1.1 ELT Downlink: Downlink is the link from MSL to the orbiter, also referred as the return link.

- Downlink rates from 2 kbps to 2048 kbps are available. The CE505 radio onboard Odyssey can only support rates of 8, 32, 128, and 256 kbps. The nominal return link with MRO uses suppressed carrier modulation with adaptive data rates (ADR) during a relay pass (overflight). Odyssey links must use residual carrier with a single data rate for each relay pass. Which data rate or the ADR mode (allows for multiple data rates) is used is determined by the "hail" by the orbiter.
- Throughput efficiencies at either the MRO or MSL end of the link, or both, limit the effective maximum rate to approximately 1.35 Mbps, depending on whether there is significant forward data being sent by MRO.
- Bypass and (7,1/2) convolutional coding.
- As defined by the Consultative Committee for Space Data Systems (CCSDS) Proximity-1 standard [26], three frequency channels are available: Channel 0: 401.585625 MHz; Channel 1: 404.4 MHz; or Channel 2: 397.5 MHz. Which channel the ELT uses is determined by the hailing from the orbiter.

  - Channel 0 was the baseline at the time of landing and is the only one compatible with Odyssey (so is used with Odyssey).
  - With MRO, however, relay operations during the early sols confirmed the presence of return link electromagnetic interference / electromagnetic compatibility (EMI/EMC) issues with the preferred MRO science instrument operating modes. From in-flight link characterization and performance tests between MSL and MRO, we found the best return link frequency to MRO was 391 MHz. This assessment also included antenna patterns and gains.
- Modulation: Residual Carrier with fixed modulation index (with biphase-L baseband modulation), and suppressed carrier (with non-return to zero, NRZ).
- Coherency enabled/disabled.

8.2.4.2.3.1.2 ELT Uplink: Uplink is the link to MSL from the orbiter, also referred as the forward link. The planned nominal forward link with MRO will use residual carrier modulation at 32 kbps. Odyssey links must use residual carrier.

- Uplink rates are from 2 to 256 kbps.
  - The following UHF uplink rates can be used by MSL: 2, 8, 16, 32, 64, 128, 256 kbps.
  - Only 8 and 32 kbps is supported by Odyssey.
- Bypass and (7,1/2) convolutional coding.
- Three CCSDS standard [26] frequency channels: 0: 437.1 MHz, 1: 435.6 MHz, 2: 439.2 MHz.
  - Channel 0 is the baseline and used for the forward link from both Odyssey and MRO.
  - There are no EMI/EMC issues identified with MRO with the use of Channel 0 for the forward link.
- Modulation: Residual carrier with fixed modulation index (with byphase-L), and suppressed carrier (with NRZ).

8.2.4.2.3.1.3 Proximity-1 Parameters (Forward and Return Links).

- Sequence controlled (reliable) link is the nominal protocol.
- Bit stream (unreliable) mode that bypasses the Proximity-1 protocol was used for EDL and is available for off-nominal conditions in surface operations.
- The adaptive data rate mode (ADR), avaliable when relaying between MRO and MSL, takes advantage of the ability of the Proximity-1

protocol to command different data rates on the fly. (ADR is available only with the MRO radio, not with Odyssey. Also with MSL only the return link data rates are being changed this way; the baseline forward rate between MRO and MSL is fixed at 32 kbps.)

- The baseline hailing interaction data rate for MSL is 8 kbps.

8.2.4.2.3.1.4 Buffer Data Management (Forward and Return Links)

- ELT provides a transmit (downlink) flow control signal to the MTIF using an additional LVDS line ("ready for data") so that the ELT transmit buffer does not overflow. Flight software (FSW) can also set various buffer parameters (buffer depth and two watermarks) to control the latency in the transmit link.
- On the MSL receive (forward link) side, there is no flow control. The content of the Proximity-1 transfer frame data field is sent out of the LVDS line as soon as the frame is validated.

8.2.4.2.3.1.5 Other ELT Functions

- Collection of Proximity-1 time-packets via the 1553B interface is nominally planned for every overflight.
- Collection of radiometric data via 1553B is nominally done only in troubleshooting scenarios.
- Wake signaling is baselined for use only in a fault-protection situation. Send "spacecraft wake-up" signal to LVDS upon receipt of Proximity-1 hail from an orbiter.

8.2.4.2.3.1.6 UHF Coaxial Transfer Switches (D-UCTS and R-UCTS): The coaxial transfer switches (in the Fig. 8-31 UHF block diagram) were used to switch between the antennas during EDL. The switch in the rover stage selected the radio to either the descent stage switch or to the RUHF antenna. During surface operations this switch selects between ELT-A and ELT-B.

These coaxial switches are double-port double-throw (position 1 and position 2) switches, manufactured by Sector Microwave. The switches have a port-to-port isolation of > 60 dB and a maximum insertion loss of 0.2 dB. Their switching time is < 50 ms. They are rated to handle as much as 15 W of RF power, with a maximum return loss of –20 dB.

8.2.5 Terminal Descent Sensor (Landing Radar) Description

The MSL terminal descent sensor (TDS), used only during the last part of the EDL activity, was a six-beam Ka-band pulse-Doppler radar designed to measure the three-axis velocity and altitude of the spacecraft from about 100 m/s and 4 km altitude until rover touchdown [27]. Specifically, the radar

provided line-of-sight velocity and range for each radar beam to the spacecraft's navigation filter, to compute the three-axis velocity and altitude of the descent stage.

Figure 8-68 is a system overview block diagram of the TDS. Table 8-18 details the TDS high-level performance and physical characteristics. Chapin (2011) [27] provides the high-level sensor specifications and physical characteristics of the TDS.

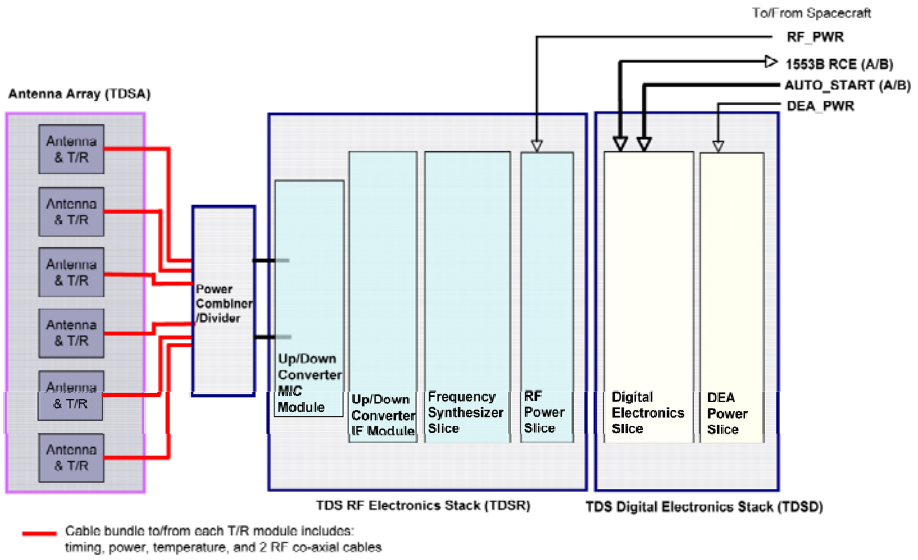

Fig. 8-68. System overview block diagram of the TDS (T/R = transmit/receive, TRM = transmit/receive module).

Table 8-18. TDS high level characteristics.

Parameter or condition	Value
Center frequency	36 GHz
Antenna beamwidth	3 deg
Transmit power (per beam)	2 W
Pulse width	4 to 16 ns
Altitude above Mars	6 to 3500 m
Velocity of descent stage	200 m/s maximum
Spacecraft bus power	30 W
Transmitting	120 W
Mass	25 kg
Dimensions	1.3 × 0.5 × 0.4 m

Although the TDS was not book kept during development as part of the telecom subsystem, it transmitted and received RF power. The MSL X-band telecom subsystem as configured for EDL included an exciter low-pass filter and transmitter low-pass filters to ensure that the radar's performance was not degraded by the simultaneous operation of the X-band SDST and TWTA during the powered descent and sky-crane portions of the descent.

The TDS hardware consists of the TDS Digital Stack (TDSD), the TDS RF Stack (TDSR), the RF power combiner and divider, and the antenna (TDSA). The block diagram shows the electrical interfaces among the TDSD, TDSR, and the TDSA.

The TDSA consists of six separate antennas, each with its own front-end filter assembly (FFA) and transmit/receive module (TRM). Figure 8-69 shows the mechanical configuration of the TDS, with the locations of the electronic assemblies and the antennas.

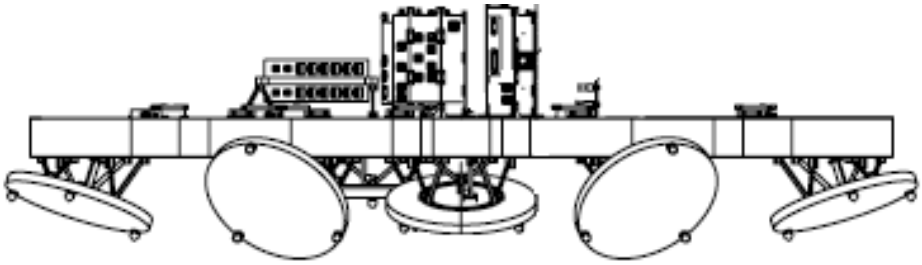

Fig. 8-69. TDS antenna locations and pointing directions.

The TDSD is a stack of two "slices" of electronic assemblies: the digital electronics assembly (DEA) slice and the digital power distribution unit (DPDU) slice.

The TDSR is a stack of four "slices" of electronic assemblies: the RF power distribution unit (RPDU) slice, the frequency synthesizer slice, the up/down converter intermediate frequency (IF) module (UDIM) slice, and the up/down converter microwave integrated circuit (MIC) module (UDMM) slice.

The power slices supplied conditioned direct current (DC) voltages to the electronic assemblies. The frequency synthesizer slice consists mainly of a voltage-controlled oscillator and supporting circuitry that generated the reference frequencies for the DEA slice and the RF electronics. The frequency upconverter generated the Ka-band pulse for the transmitter, and the frequency downconverter module converted the received signal down to video frequency for digitization.

The DEA served as the controller and digital signal processor of the TDS. The DEA consists of a 1553 transceiver chip supporting 1553B command and telemetry transfers and a large (~1 mega gates) reprogrammable field-programmable gate array (FPGA), referred to as the radar processor (RP), for generating timing signals for the TDS and handling all the digital signal processing of radar data. A 12-bit ADC was utilized to digitize radar video signal with a bandwidth as high as 240 MHz. A radiation-hardened scalable processor architecture (SPARC) processor served as the radar controller (RC); this item handled spacecraft commands, time tagging, post-processing, packaging of telemetry messages, and other functions.

The TDS cycled through the antenna beams, making measurements with the six antenna beams one at a time at 20 Hz (50-ms intervals). A limited number of beam sequences were pre-stored in the TDS memory to be recalled by using a beam sequence table ID command. The use of the beam sequence allowed the exclusion of an anomalous beam or a blocked beam.

In Normal mode, the TDS was set up to make line-of-sight velocity and range measurements at 20-Hz rate by cycling through the radar beams according to the specified beam-cycling pattern. The Normal mode of TDS operation included Acquire, Dop1, and Dop2 dwells. A dwell consisted of a group of radar pulses with identical radar parameters. The Dop1 and Dop2 dwells were executed only when a target was detected (valid range) in the Acquire dwell. In Dop1, the TDS determined the Doppler velocity by using the pulse-pair Doppler technique. In Dop2, the TDS used a different inter-pulse period (IPP) to resolve the Doppler velocity ambiguity. We also determined the slant range in Dop2.

8.2.6 MSL Telecom Hardware Mass and Power Summary

8.2.6.1 X-Band Mass

Table 8-19 lists the masses for the major X-band telecom assemblies, as defined in the MSL Mass Equipment List (MEL) [28]. The table is organized by the stages previously defined: cruise, EDL (combined parachute cone and descent), and rover.

8.2.6.2 X-Band Spacecraft Power Consumption

Table 8-20 summarizes the power consumption of the active subsystem elements (SDSTs and power amplifiers) at a nominal bus voltage of 28 V.

The SDST values are indicated for receiver-only operation, receiver and exciter in the non-coherent mode, and receiver and exciter in the coherent mode. The exciter is required for a downlink, and the non-coherent mode also requires the

auxiliary oscillator to be powered. The DSDST was powered during cruise and EDL, and the RSDST is powered for X-band activities in surface operations.

When the TWTA is on, it has two modes: standby (the unit producing no RF output) and operating. When the TWTA is off, it draws no power.

Table 8-19. X-band telecom mass summary.

Spacecraft Stage	X-Band Subsystem Element	Quantity	Unit Mass (kg)	Total Mass (kg)
Cruise	MGA and adapter	1		0.65
EDL backshell	PLGA	1		0.4
	TLGA	1		0.4
	WTS	2	0.45	0.9
	Microwave components			2.8
EDL descent	DLGA	1		0.35
	Microwave components			2.5
EDL descent telecom plate	TWTA	1		2.5
	WTS	2	0.45	0.9
	SDST	1		3.0
	Telecom plate	1		6.6
	Microwave components			2.5
Rover X-band	SDST	1		3.0
	SSPA	1		1.4
	WTS	2	0.45	0.9
	RLGA	1		0.4
	HGA	1		1.4
	HGA gimbal	1		6.6
	Microwave components			3.7
TOTAL				**40.9**

Table 8-20. X-band telecom spacecraft power consumption.

Subassembly	Descent Stage Telecom Subsystem Mode	Nominal Bus Voltage (28.0 V)
DSDST	RX	11.4
	RX + noncoherent TX (TLM only: SAFE_MODE)	14.7
	RX + Coherent TX (TLM Only: CRUISE MODE)	14.4
TWTA	Standby mode (no RF drive) (exciter OFF)	62.4
	Operating (with RF drive) (exciter ON)	175.2
RSDST	RX	11.3
	RX + noncoherent TX (TLM only: SAFE_MODE)	14.8
	RX + coherent TX (TLM only: CRUISE_MODE)	14.2
SSPA	Exciter OFF (no RF drive)	45.1
	Exciter ON	62.9

Throughout cruise and EDL, the DSDST (receiver and exciter) and the TWTA remained powered. For the most part, the TWTA remained in the operating mode, being sequenced to the standby mode only briefly during antenna switches.

During surface operations, only the RSDST receiver is powered on in the background mode or when a DFE is active. The RSDST exciter and the SSPA are also powered on when a DTE or a beep is active.

8.2.6.3 UHF Mass and Power Consumption

The TDS had four power states[27]:

- **Off** – Both power switches from the 28-V spacecraft bus were open (no power to the TDS).
- **Low** – The power switch to the digital power distribution unit (DPDU) was closed while the power switch to the RF power distribution unit (RPDU) remained opened. At this lower power state, only the DEA was powered on, and the RP (Xilinx[28] field programmable gate array [FPGA]) was not running because there was no 1-GHz clock to the FPGA. The power draw in this state was about 30 W.
- **Quiescent** – Both power switches were closed, essentially powering up both the DEA and the RF electronics. The TDS was in standby mode in which the high-power amplifiers in the TRMs were properly biased but not transmitting.
- **Full** – Radar timing was running in the RP and pulsing the TRMs to transmit RF power. The power usage is about 120 W.

---

[27] The TDS was powered off during cruise, except for self-checks when other power modes were active for brief periods. The TDS modes were controlled by an onboard sequence during EDL.

[28] Xilinx, Inc. is the inventor of the field programmable gate array (FPGA). An FPGA is a semiconductor device that can be configured by the customer or designer after manufacturing—hence the name "field-programmable." FPGAs contain programmable logic components called "logic blocks," and a hierarchy of reconfigurable interconnects that allow the blocks to be "wired together"—somewhat like a one-chip programmable breadboard. (http://en.wikipedia.org/wiki/Xilinx and http://en.wikipedia.org/wiki/Field-programmable_gate_array)

8.3 Ground Systems EDL Operations: EDL Data Analysis (EDA)

EDL was a critical and the most anticipated communications mission phase. Obviously, for purposes of redundancy and signal diversity, all possible communications paths were to be used to their fullest extent. Both X-band and UHF were on when they could provide signals to be received. The DSN operated with multiple redundant antennas. MSL transmitted a UHF return link to MRO and Odyssey (and MEX as backup). Also the Parkes Observatory in Australia tracked the UHF carrier.[29]

In addition to the standard closed loop receivers, the DSN antennas were also connected to a special EDL Analysis (EDA[30]) system that performed fast Fourier transform (FFT) signal processing on the signal captured by the open-loop radio science recorder (RSR) receivers.

A NASA Tech Brief [29] documents the MER EDA, which is described as a system of signal-processing software and computer hardware for acquiring status data conveyed by M-FSK tone signals transmitted by a spacecraft during descent to the surface of a remote planet.

MSL undertook an EDA rebuild to use modern computer hardware and the Linux operating system.

8.4 Telecom Subsystem Link Performance

8.4.1 X-Band

8.4.1.1 Cruise Link Performance

Telecom performance prediction and analysis played a major role during cruise and approach. In particular, many of the checkout and subsystem maintenance activities scheduled during these mission phases required relatively high telemetry data rates with the consequent low link margin.

---

[29] On schedule at 05:16 UTC on August 6, the signal was detected. It was slightly stronger than expected. Parkes tracked the descent of the rover until just after the parachute deployment and heat-shield separation. Less than two minutes before scheduled landing, MSL dropped below the Martian horizon, out of sight of Earth. See http://www.parkes.atnf.csiro.au/people/sar049/msl_tracks/edl/ for details.

[30] The EDA was first developed for MER and is described in Chapter 6. The EDA, which has been updated for MSL, is a system for carrier and tone detection and tracking the high Doppler-dynamics and low-SNR of EDL.

During cruise there were five main X-band functions: downlink carrier tracking, uplink command, downlink telemetry, differential one-way ranging (delta-DOR), and turnaround ranging. Because the turnaround ranging signal levels during late cruise were low relative to threshold (especially on the downlink), ranging was the most difficult of the functions to achieve.

For surface operations, the primary X-band functions are uplink command, downlink carrier-only beeps, and downlink telemetry. Because the landing site is well characterized in location, the turnaround ranging and delta-DOR navigation data are not required at the surface, and the two-way Doppler is rarely used.

Sequential ranging is a two-way measurement. Ranging is degraded by three sources of thermal noise:

1. Noise on the uplink (from the finite SNR on the uplink).

2. Noise in the transponder ranging channel.

3. Noise in the station receiver.

Of these, the noise in the ranging channel is the largest contributor because of the channel's bandwidth. The double-sided bandwidth is 3 MHz, adequate to pass a ranging waveform that has a clock-component fundamental frequency of 1 MHz. The receiver noise results from a relatively low spacecraft transmit power and consequently low SNR.

Figure 8-70 shows the ranging P_r/N_0 during cruise for several configurations. There are curves for early-cruise at 34-m stations on the PLGA using either the TWTA or the SSPA, for later cruise at 34-m stations on the MGA using either of these amplifiers, and for 70-m stations late in cruise using the MGA and the TWTA.

MSL had available the following three "improved ranging" techniques to use separately or together as necessary. "Improved ranging" is a mode that can

- Configure the SDST downlink ranging modulation index at 35 deg,
- Set the station uplink ranging mod index to 5 dB carrier suppression, the highest available, and
- Decrease the telemetry modulation index to 45 deg.

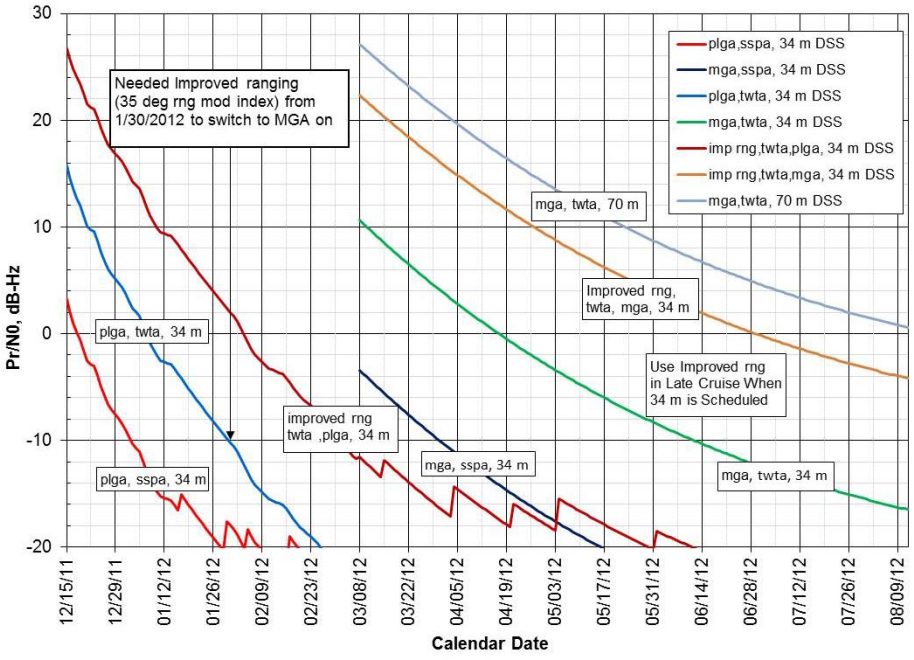

Fig. 8-70. Turnaround ranging P_r/N_0 in cruise for type Ic trajectory (rng = ranging).

Because the X-band system performed normally, only the first was needed, and this reduced telemetry capability (bit rate) very slightly. The second would have reduced command capability (bit rate) and the third would have reduced telemetry capability (bit rate) significantly.

A more drastic form of increasing ranging performance, which fortunately was not required, is called "ranging max". "Ranging max" would have

- Set the SDST ranging modulation index to its highest value of 70 deg and turned off the telemetry modulation, and
- Turned off the station command modulation, with the station ranging mod index set to 5-dB carrier suppression.

The DSN can process ranging samples at signal levels as low as P_r/N_0 of –20 dB-Hz, albeit at the cost of integration times that increase as P_r/N_0 decreases. Figure 8-71 shows the cycle time for the collection of each ranging point as a function of P_r/N_0. This figure is based on a required minimum probability of ranging acquisition of 99% and a one-sigma ranging accuracy of 3 m. Because the cycle time becomes very large as the P_r/N_0 goes below –10 dB-Hz, –10 dB is taken as the ranging threshold. Cycle time is defined in

the ranging module of the *DSN Telecommunications Link Design Handbook* [30].

$$\text{Cycle time in seconds} = T1 + 3 + (L - C)*(T2 + 1)$$

where $T1$ is the integration time of the clock component and

$T2$ is the integration time of each of the other components,

L is the component number of the last (lowest frequency) ambiguity resolving component, and

C is the component number of the range.

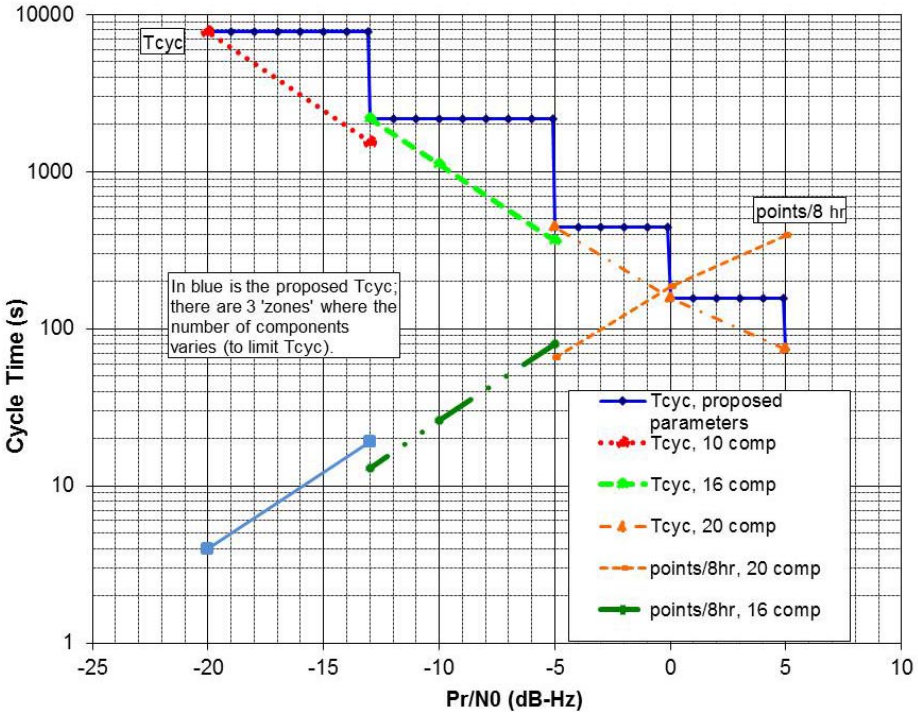

Fig. 8-71. Required ranging cycle time as a function of P_r/N_0.

During the cruise mission phase, the telecom lead on the Spacecraft Team coordinated several times with the Navigation Team lead and with the DSN to define suitable ranging integration times T1 and T2 to use for the next series of tracking passes. These times are not only a function of the changing P_r/N_0 but also of factors such as the change in round-trip light time (RTLT) during a maximum-duration station pass and the ambiguity resolution required.

The P_r/N_0 available at a given time and station/spacecraft geometry and configuration can be increased by:

- Increasing the uplink ranging modulation index
- Lowering the command modulation index by reducing uplink rate (or turning command modulation off)
- Increasing the downlink ranging modulation index
- Lowering the telemetry modulation index (or turning telemetry off)
- Increasing the ground station size from 34 m to a 70 m.

In early cruise, while the spacecraft was on the PLGA, the –Z axis had to be pointed within 80 deg of Earth to provide telecom coverage, as discussed in Section 8.1.3 and shown in Fig. 8-15. Beyond 80 deg, significant scattering off the spacecraft would make antenna pattern modeling for prediction unacceptably unreliable.

About 3 months after launch, due to the increasing Earth–MSL distance, the ranging performance drove a telecom configuration change from the PLGA to the MGA. Pointing requirements on the MGA were significantly tighter than for the MGA, as the Earth had to be within 15 deg of the –Z axis immediately after the transition from the PLGA and to 9 deg later in the cruise. The cruise pointing strategy, in fact, achieved an MGA pointing error of less than 4 deg.

The telecom subsystem capability drove much of the scheduling of station coverage during cruise, as key events required 70-m coverage to satisfy real-time data rate requirements or additional 34-m coverage to return larger data volumes.

Figure 8-72 is a prediction of uplink data rate capability from a 34-m station from launch to Mars arrival. The figure is for a Type Ic launch at window-open (Day 1). The 2-kbps maximum rate shown is the highest that the SDST can support.

Figure 8-73 shows the corresponding set of predictions for the downlink data rates. Part (a) of the figure is capability to a 34-m station, and Part (b) is capability to a 70-m station. MSL can produce telemetry rates up to a maximum of 62.5 kbps, but the highest rate used during cruise was 25 kbps.

The pointing conditions for each antenna in each figure are indicated. Given this pointing, the stair-step fall-off in capability is due to going through thresholds for each bit rate as the Earth-spacecraft distance steadily changes.

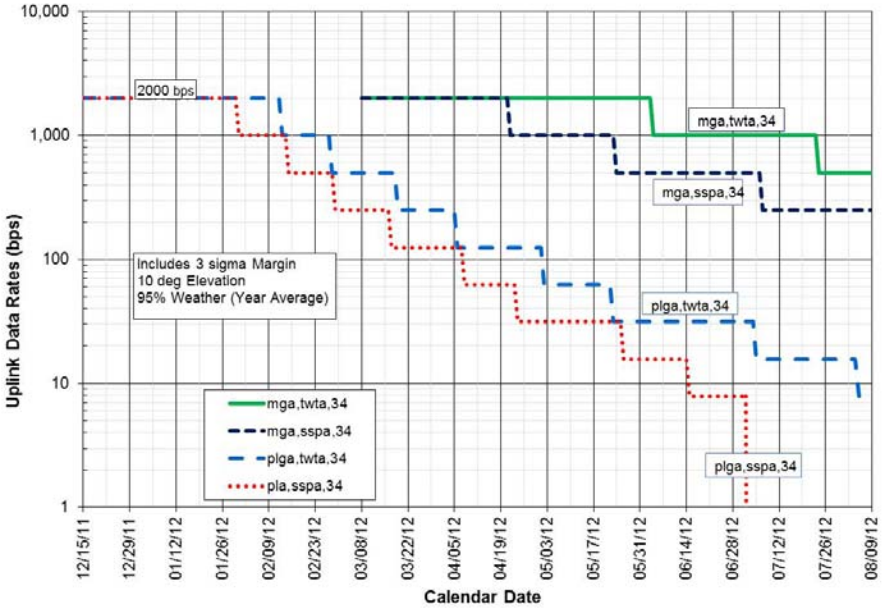

Fig. 8-72. MSL X-band uplink data rates during cruise (after TCM-1, Type Ic trajectory).

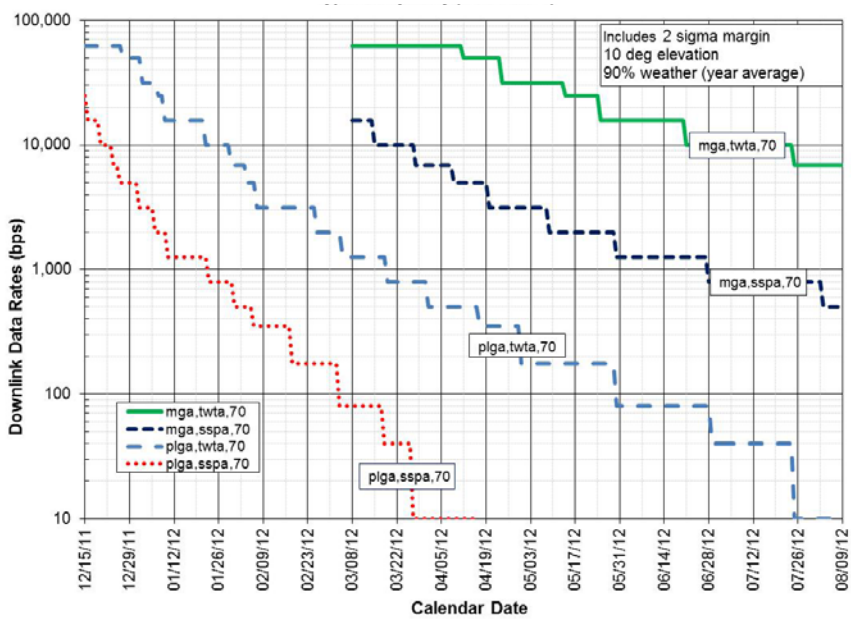

Fig. 8-73. MSL X-band downlink data rates via TWTA during cruise, type Ic trajectory day 1 (after TCM-1).

8.4.1.2 EDL (X-Band) Performance

At a planned time during EDL, the SDST telemetry mode was set to "TLM_OFF," which meant the normal engineering housekeeping, and analysis (EH&A) telemetry data stream no longer modulated the outgoing signal. After that time the X-Band subsystem transmitted information to Earth concerning the state of the spacecraft in the form of a series of discrete frequencies (referred to as MFSK tones or semaphores). Each tone was actually an unmodulated telemetry subcarrier (at a specific frequency) of the normal SDST transmitted signal. Each tone in the series indicated the occurrence of an event or condition. Each timeline segment of EDL had its unique event schedule (parachute deployment, for example), and each segment had a unique set of nominal and off nominal tones. The collection of tones, of which 256 were available, constituted the MFSK dictionary.[31]

The geometry of EDL was challenging for DTE links, with large view angle variations during the descent. The plot in Fig. 8-22 illustrates the type of angle variation that occurred for DTE. Because the RTLT was significantly longer than the EDL duration, EDL had to be entirely pre-programmed. Once the last command was sent, observers on the Earth were simply along for the ride, to observe the signals radioed back after all the actions had already been completed at Mars. Consequently, the real value and purpose of EDL communications (besides public outreach) was to permit reconstruction of what happened in the event of a failure.

To observe EDL as it played out over the varying Earth view angle, we relied on a series of spacecraft low-gain broadbeam antennas: the PLGA, TLGA, and DLGA. Each LGA was essentially an open-ended waveguide antenna, with the PLGA and TLGA having added parasitic dipoles to broaden the beams even more off boresight.

The ground detection system for EDL consisted of the DSN antennas and radio science receivers. They recorded and piped the raw received signal to the EDA

---

[31] Multiple-frequency-shift keying (MFSK) is a variation of frequency-shift keying (FSK) that uses more than two frequencies. MFSK is a form of M-ary orthogonal modulation, where each symbol consists of one element from an alphabet of orthogonal waveforms. M, the size of the alphabet, is usually a power of two so that each symbol represents log2M bits. Like other M-ary orthogonal schemes, the required E_b/N_0 ratio for a given probability of error decreases as M increases without the need for multisymbol coherent detection. In fact, as M approaches infinity the required E_b/N_0 ratio decreases asymptotically to the Shannon limit of –1.6 dB. (http://en.wikipedia.org/wiki/Multiple_frequency-shift_keying)

computers. The EDA did the spectral analysis on the signal and extracted the tones from the noise. Figure 8-74 shows the EDA configuration at a station complex (for example, Goldstone): several RSRs recording data from several antenna assets and feeding data to the EDAs. As the diagram shows, the distribution of signals to the RSRs (dotted lines) was at IF via the full spectrum processing (FSP) subsystem.[32]

We did not need to co-locate the EDAs at the DSN complexes for MSL as was done for MER; instead the connections from the stations to the EDAs were via the network to JPL.

To maximize the number of semaphore tones reliably detected, we planned for as much off-nominal coverage and, therefore, far off-boresight coverage, as possible. Prior to the EDLs of the two MER rovers in January 2004 and again in the early studies for MSL, analysis had been performed to quantify the SNR levels that could be expected to produce acceptable tone detection probabilities. Figure 8-75 shows an example analysis simulation where challenging high Doppler events could cause tones to be missed. (Carrier frequency tracking results are presented using 5-Hz FFT and 1.0-s update with T = 1 s integration with correctly interpolated Doppler profile and the nominal rate search space of ± 40 Hz/s.) For MSL EDL, such events included the parachute deployment and the divert maneuver, when large Doppler rates and high off boresight angles occur.

When the SNR is strong, the job is easy. When the angles are far off boresight or the Doppler environment is challenging (such as when the Doppler rates and higher derivatives are large), the task becomes difficult or, in some cases, impossible. It is possible to array the DSN antennas during EDL to maximize the probability of tone detection if we expected difficulties in detection. DSN antenna arraying was studied for MSL use but determined not necessary.

[32] Distribution of telemetry and Doppler signals is via a separate IF switch to the Downlink Tracking and Telemetry (DTT) subsystem.

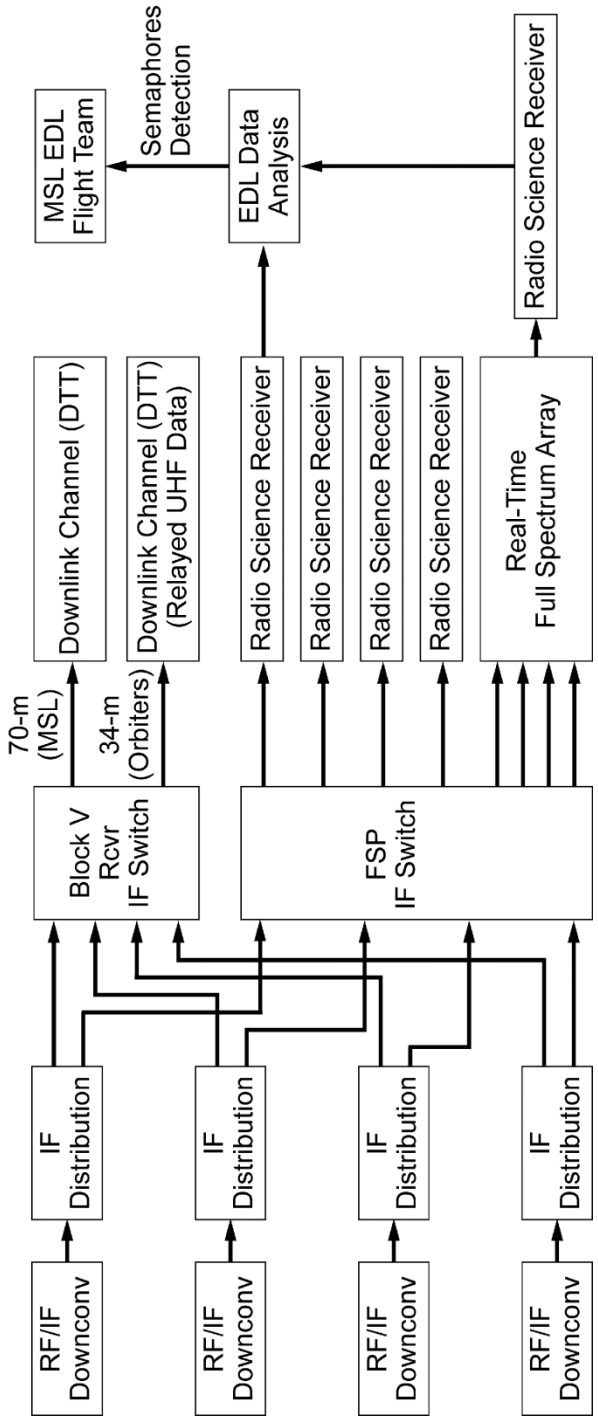

Fig. 8-74. Configuration of EDAs for EDL support.

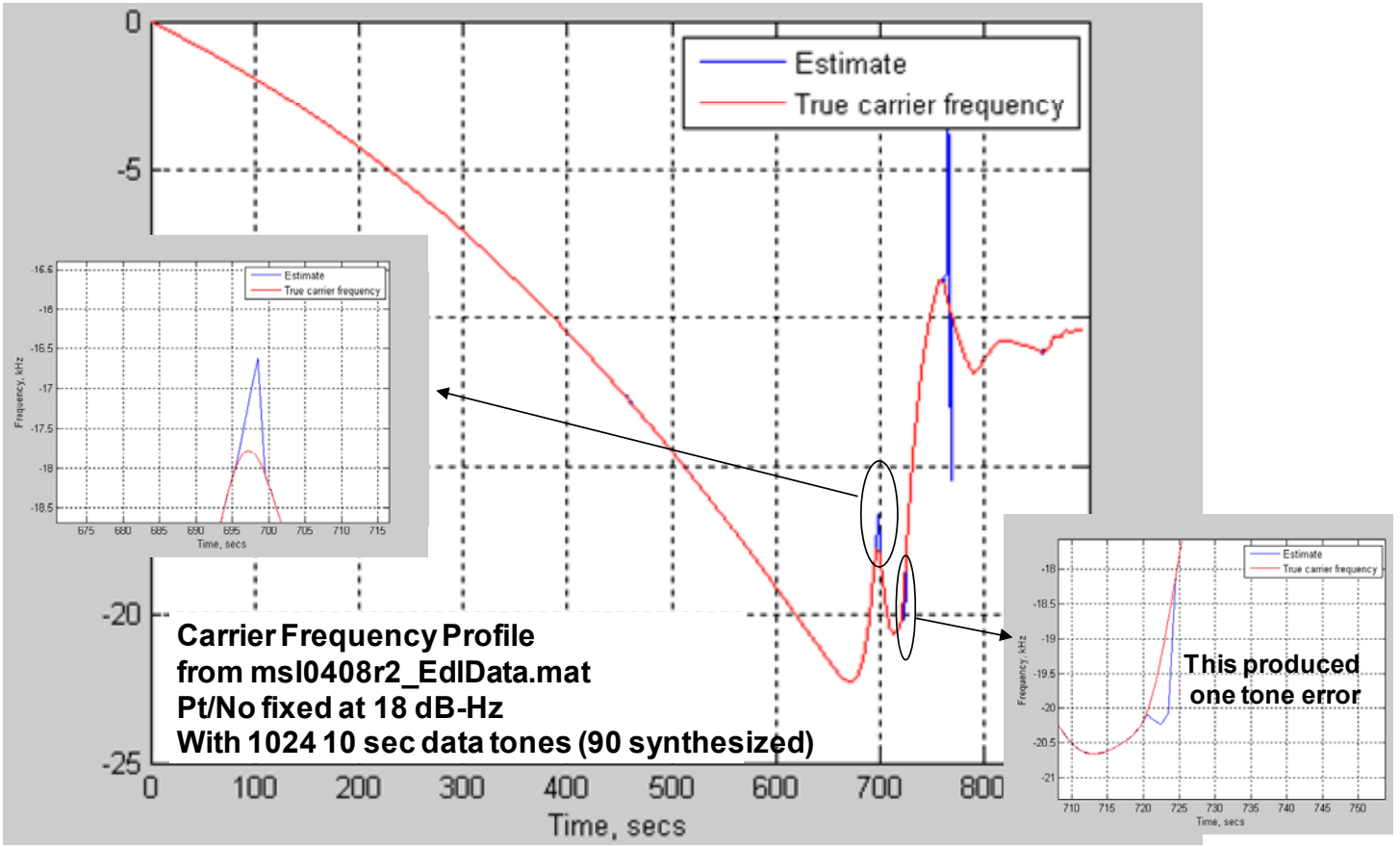

Fig. 8-75. MER EDA analysis example showing missed tone cases. Note: missed tones 70 (690–700 s) and 73 (720–730s).

Nevertheless, in some cases, and assuming nominal entry profile, the DTE signal was predicted to be reasonably strong, such as in the case shown in Fig. 8-76, for the Gale landing site.

In this example, we see the pre-entry period has a sufficiently strong DTE signal, near the 30 dB-Hz level, well above the low dynamics threshold for high-probability correct detection. This period also has very low Doppler rates, and therefore the Doppler predictions, were expected to be accurate. The left halves of Figs. 8-76, 8-77, and 8-78 show, respectively, the signal level, the Doppler frequency, and the Doppler rate during this "low dynamics" period. In this relatively benign environment, DTE was expected to be easily achievable.

In the subsequent "high-dynamics" period, shown in the right halves of these figures, the UHF return link relayed via an orbiter would be the more reliable signal.

After entry, the large deceleration during hypersonic entry produced large Doppler rates and acceleration (shown in Figs. 8-77 and 8-78), and the view angles also became challenging. Reliable X-band DTE provided a separate link for EDL events during the period of UHF plasma blackout, which coincided with the large deceleration period. The DTE reliability, however, depended largely on the accuracy of the profile predictions, for the receiver to be able to compensate for the Doppler changes.

Planning for real-time DTE coverage after landing was ultimately limited by the Earth setting below the horizon at the landing site, the time of which was affected by the launch date. Planned coverage was to landing plus one minute.

8.4.1.3 Surface Performance (X-Band)

Throughout surface operations, the X-band requirements are:

- Data return from the HGA (at least 160 bps at max range, 34-m BWG station, 5-deg HGA pointing error).
- Command capability via the HGA (225 kbps in 20 min, equivalent to a 190 bps uplink rate, via a 34-m, with 5-deg HGA pointing error).
- Emergency command capability via the RLGA (support of safemode 7.8125 bps uplink rate via a 70-m antenna, assuming the Earth is 70 deg off the RLGA boresight).

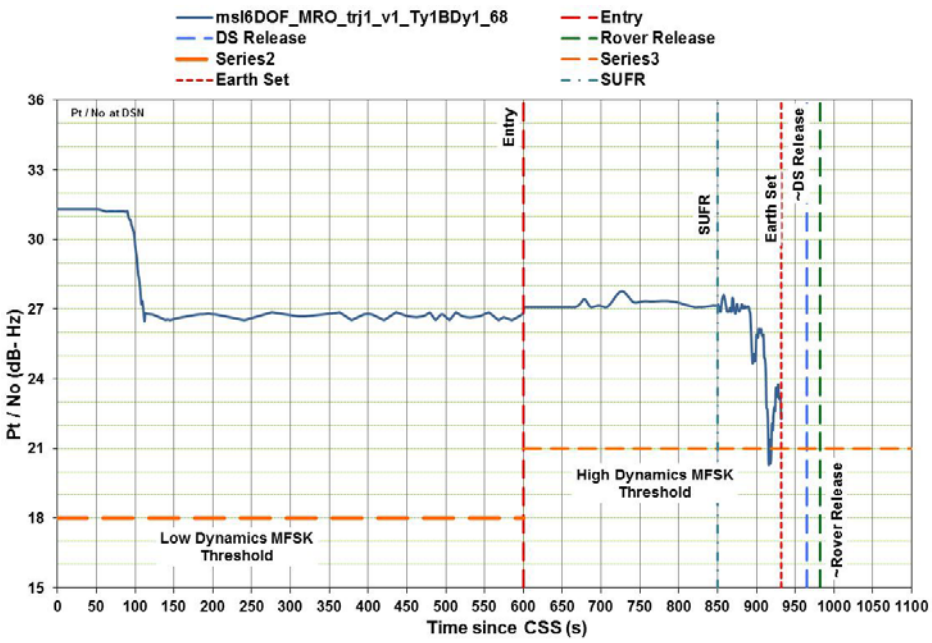

Fig. 8-76. DTE P_t/N_0 at DSN, Gale site, 2011 launch.

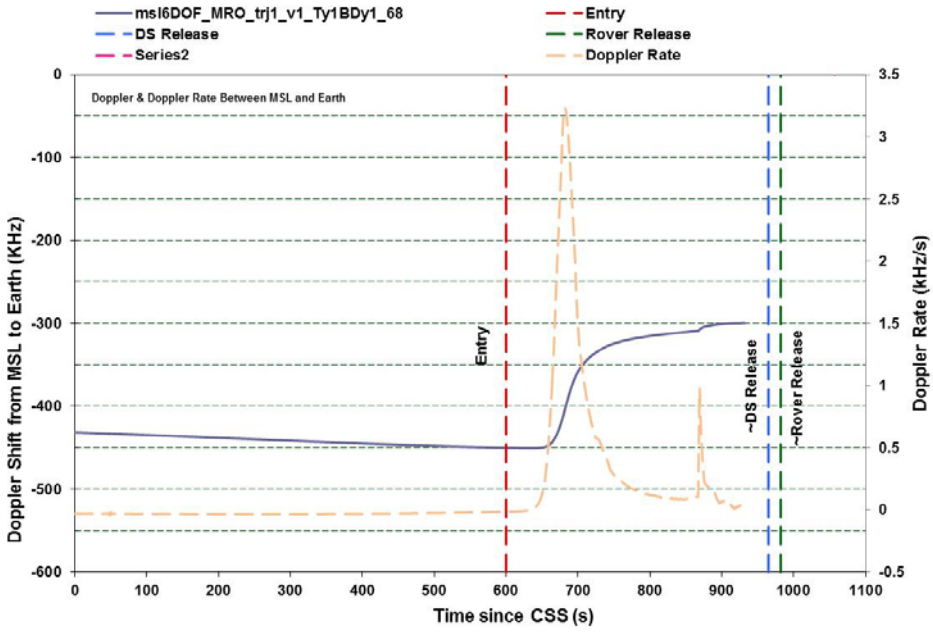

Fig. 8-77. DTE Doppler Frequency Shift and Doppler Rate at DSN, Gale site, 2011 launch.

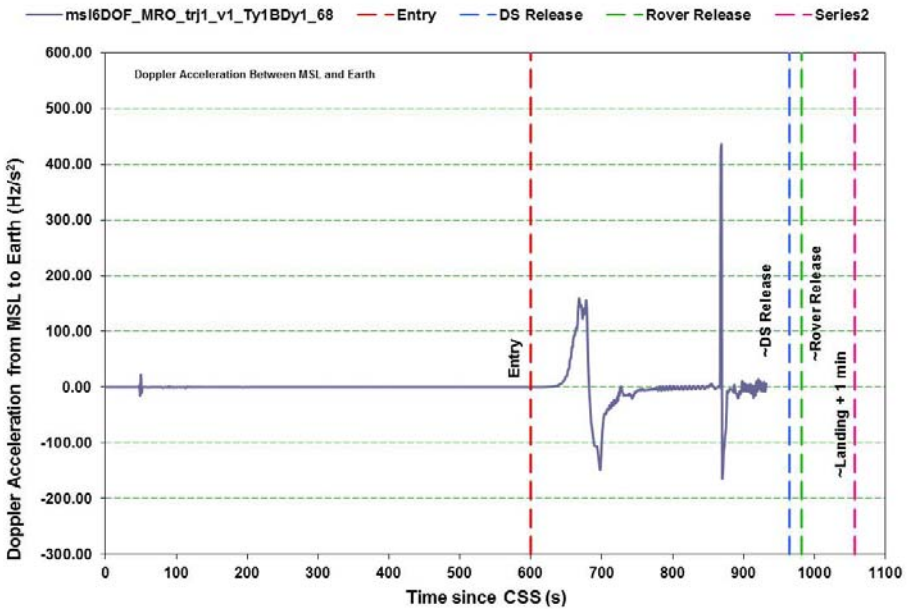

Fig. 8-78. DTE Doppler Acceleration at DSN, Gale site, 2011 launch.

X-band surface communications, unlike cruise, assumes that turnaround ranging is never required—we know where Mars is and have other means of determining more accurately than ranging where the rover is on Mars. Therefore, these DFE command rate capabilities assume only command modulation is on the uplink.

The Telecom Forecaster Predictor (TFP) tool, first operationally used to predict spacecraft-DSN links for the Deep Space 1 mission in 1998, has been since updated for newer missions, including MSL. The first year of surface operations included maximum range and a solar conjunction in April 2013. Excluding the solar conjunction within a Sun–Earth–probe angle of 3 degrees, the requirements above have all been met: 176 bps downlink rate and 1 kbps uplink rate on the HGA, and 7.8125 bps uplink rate on the RLGA.

The X-band DFE is used for transmitting command sequences almost every morning on Mars. X-band DFE communication sessions include allowance for a 7-minute preparation period to set up the communication window and a 10-minute rover activity keep-out afterwards for post-pass processing.

The X-band DTE downlink is used to send limited amounts of engineering data to Earth independent of the relay orbiters. Though the rover can receive DFEs or transmit DTEs independent from each other, the practice is almost always to

open a single communication window per sol, for either a DFE only or a combined DFE/DTE.

X-band communications are often combined into a single pass station pass per sol, with the pass duration made long enough to accommodate verification of DFE commanding. Verification can be via the DTE telemetry that follows, accounting for RTLT. More often, verification is by the station receiving a separate carrier-only "beep" that follows the DFE window.[33] After one year on the surface, the combined DFE/DTE is done about once a week, with the sols in between DTEs having beeps only.

The next three figures are for 2011 mission surface operations, with arrival from a Type Ic cruise trajectory. Figure 8-79 shows how uplink performance varies with time for the HGA and also with off-Earth angle for the RLGA. The DFE command data rate capability for 34-m and HGA never falls below 500 bps. In contrast, the 34-m/RLGA capability dips as low as 15.625 bps at larger Earth–Mars ranges, assuming a 40-deg off-boresight angle and as low as 7.8125 bps at a 70-deg off-boresight angle. With a 70-m station scheduled, the RLGA DFE capability is always at least 31.25 bps, disregarding 70-m antenna aberration effects[34]. Note that the "40-deg" and "70-deg" curves refer to different RLGA off-boresight angles.

---

[33] The beep is the simplest form of providing an X-band downlink capability to send discrete messages (such as "operation normal," or "need help") at the equivalent of very low bit rates. This concept is similar to an EDL-type signaling scheme, but could have much longer integration times than the minimum 10-second interval between semaphores at EDL.

[34] Aberration is the name of an effect resulting from the Earth-Mars geometry. Station antenna pointing toward Mars is optimized for the signal being received on the downlink at a given time. The antenna pointing for an uplink that was transmitted a round trip light time earlier has a slight error when Mars' coordinates (declination and right ascension) are changing. The 70-m antenna beamwidth is narrow enough that aberration-caused uplink pointing error can cause the received uplink to be several decibels lower than it would be without pointing error. The 31.25-bps capability may become 7.8125-bps capability with aberration. MSL takes aberration into effect either by optimizing the pointing for uplink during commanding or by reducing the command rate. Aberration works on both uplink and downlink. Optimizing the pointing for the uplink will decrease the downlink capability for any mission that is transmitting to that station from Mars.

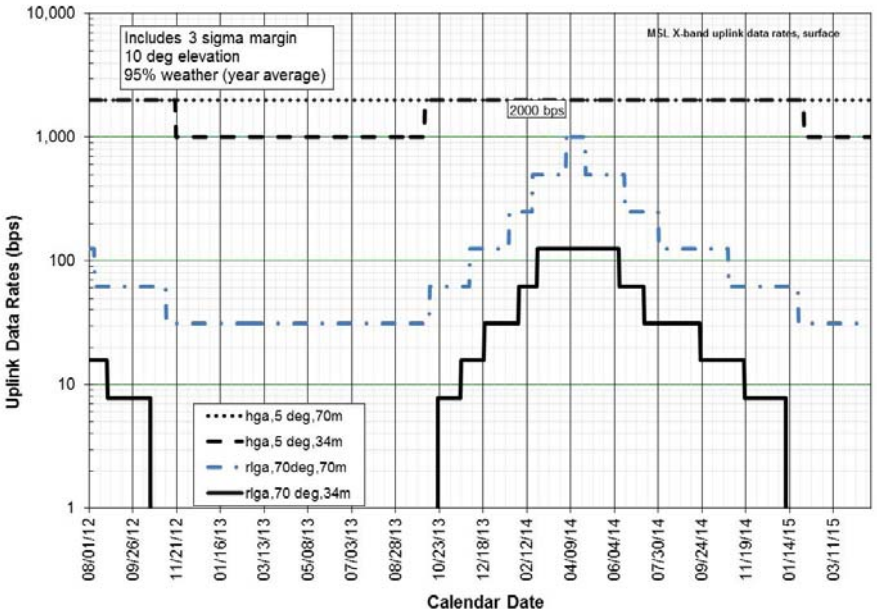

Fig. 8-79. Supportable X-band uplink data rates, Mars surface.

Figure 8-80 shows how limited the X-band DTE downlink capability is (SSPA on the surface instead of the TWTA used during cruise). Telemetry via the X-band downlink is available only via the HGA.

Figure 8-81 shows that downlink P_t/N_0 via the RLGA is too low to support even the minimum 10 bps downlink rate at high elevation angles over a significant fraction of the Earth-Mars ranges. It is this lack of telemetry capability that has caused MSL (like MER before) to sequence carrier-only beeps. The unmodulated DTE "beep" carrier to a 34-m station is above threshold via the RLGA throughout the span of Earth-Mars distances.[35]

[35] RLGA beeps include both the runout beep that signals if the new sol's sequence did not take over and the off-nominal beep that signals if fault protection has detected a problem requiring safe mode. To ensure receipt of potential off-nominal beeps, the project provided for radio science support going into the second year of surface operations. The RSR, used in parallel with the station's closed-loop receiver, works at P_t/N_0 several dB lower than the 10-dB closed-loop threshold. Radio science post-processing can be used to search for a suspected beep over an extended frequency range and after the fact.

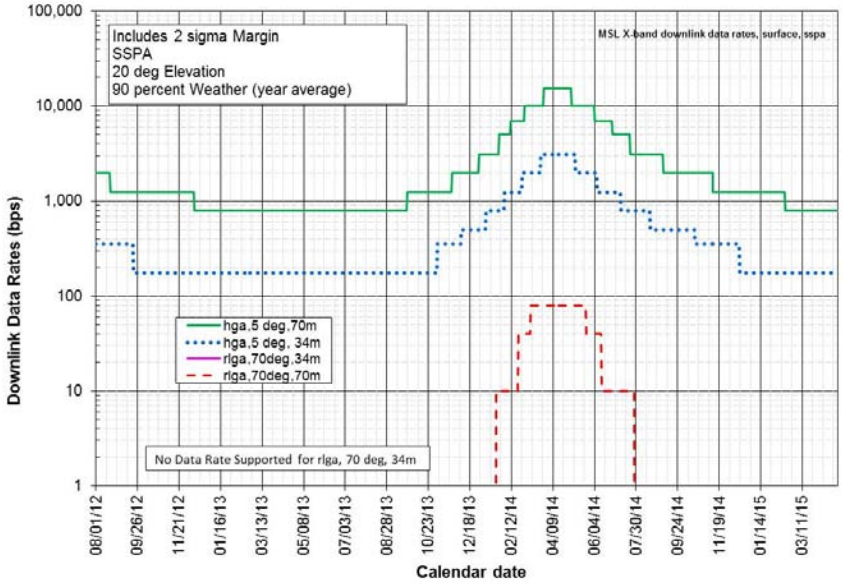

Fig. 8-80. Supportable X-band downlink rates via SSPA, Mars surface.

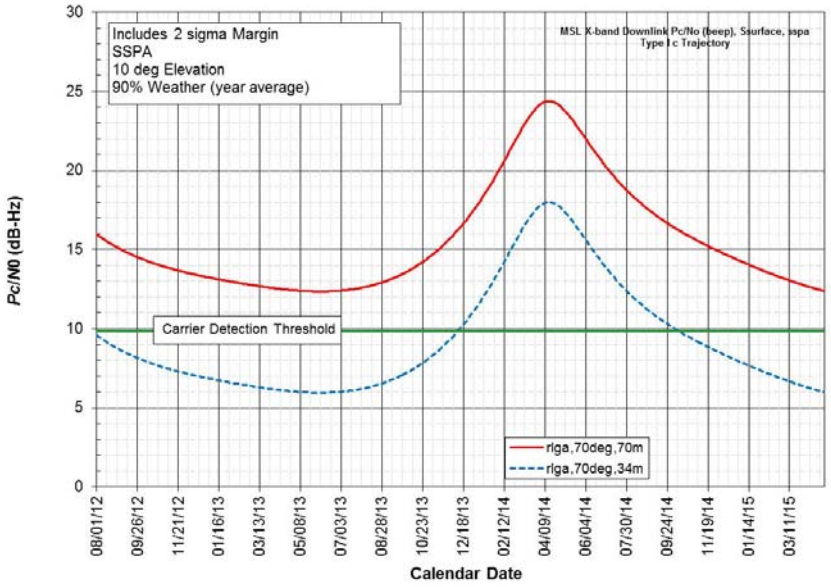

Fig. 8-81. X-band downlink P_t/N_0 for carrier-only "beep" via SSPA, Mars surface, Type Ic trajectory.

8.4.2 UHF

The two prime functions for the UHF subsystem have been relay support during EDL and surface science data relay.

8.4.2.1 EDL (UHF)

One of the top (Level 1) requirements for deep space missions is that the spacecraft provide communication to Earth of data throughout all mission critical events at a rate sufficient to determine the state of the spacecraft in support of fault reconstruction. Previous missions landing on Mars provided data communication during the critical events of EDL (Mars Pathfinder [MPF] in 1997 and MER in 2004) by making use of DTE semaphore tones to indicate the spacecraft condition. The X-band link and the semaphore tones used during EDL for the two MER spacecraft provided an increase in information content compared to that of MPF.

As compared with MER, the use of EDL guided entry and propulsive descent on MSL required subsystems whose status would change more quickly than on MER. These subsystems had more moving parts that were moving more quickly than MER's airbags. The higher degree of activity resulted in a need for a higher information rate than tones alone could provide during EDL[36].

The use on MSL of a UHF communications relay to a Mars orbiting asset during EDL greatly enhanced communications capability by providing spacecraft telemetry. MER successfully demonstrated a UHF link with the MGS orbiter for the terminal descent (post parachute deployment) portion of EDL. However, the MER mission opted to not pursue any UHF capability prior to lander/backshell separation due to the significant development risks of placing a UHF antenna on the backshell.

Similar to their support provided for the Phoenix EDL, both MRO and Odyssey orbiters were used to relay MSL lander data to the Earth.[37] After extensive study of MSL visibility by asset (and redundancies) across the full range of launch and arrival periods (both primary and contingency), it was concluded

---

[36] The information rate conveyed from tones is quite limited in comparison to true spacecraft telemetry. For MSL, one tone every 10 seconds from an alphabet size of 256 provided an information rate of 8/10 = 0.8 bps. The MSL X-band telemetry data rate providing the greatest margin would have been only 10 bps. In contrast to the 0.8 bps effective X-band DTE rate, MSL UHF telemetry provided 8000 bps during EDL.

[37] The MEX orbiter also provided a secondary EDL relay opportunity in addition to either MRO or Odyssey as prime.

that, for latitudes in the 45 deg S to 45 deg N range, DTE coverage using MFSK tones was considered the primary planned source of information from cruise stage separation to at least entry. MRO and Odyssey UHF relay coverage were considered the primary telecom link from at least entry to rover landing. The amount of overlap—that is, the time when both links would be useful—depended on the landing site selected.

Even a UHF telemetry link would not allow all faults to be detected, particularly if the failure interfered with the spacecraft's ability to maintain the link. X-band semaphores were used to provide information on the major events and anomalies during EDL. This is an example of how X-band and UHF were complementary during EDL, and both continue in use for surface operations.

MRO could not provide delay-free (bent-pipe) relay, as it first recorded the return-link relay data as it was received from the descending spacecraft during the overflight and then sent the data to the DSN. Both relay of demodulated telemetry (also called unreliable return link bit-stream reception) and open-loop recording of the modulated UHF carrier (also called canister mode in CE505 radio terminology) were considered for the relay reception onboard the orbiters. Open-loop recording had been successful during Phoenix EDL. An advantage of open-loop recording is that the signal would still be recorded even if the carrier dropped below lock threshold. Thus, the possibility would exist to recover data lost in real time with non-real time analysis techniques. In contrast, with bit-stream mode, telemetry transmitted during periods of carrier unlock would be lost.

Based on predicted signal strength and variability, MSL chose the bit stream mode for EDL relay to all three orbiters.

To achieve sufficient return-link signal strength, it was necessary for the relay orbiters to turn to point their UHF antennas at MSL to the best of their capabilities. The baseline plan was that they would point to the descending MSL within 30 deg of their UHF antenna boresights for EDL.

The link to the orbiter was characterized through the EDL descent phases by a large change in range, large variations in antenna view angles, high Doppler rates, and, consequently, large changes in signal to noise ratios. The next three figures show the range (Figure 8-82), the view angles (Fig. 8-83), and the Doppler and received power (Fig. 8-84) for Gale crater and the 2011 launch. In each figure, part (a) is for the link to MRO, and part (b) for the link to Odyssey. Figures 8-84 (a) and (b) illustrate that there was sufficient post-entry margin to MRO and Odyssey to close the link most of the time.

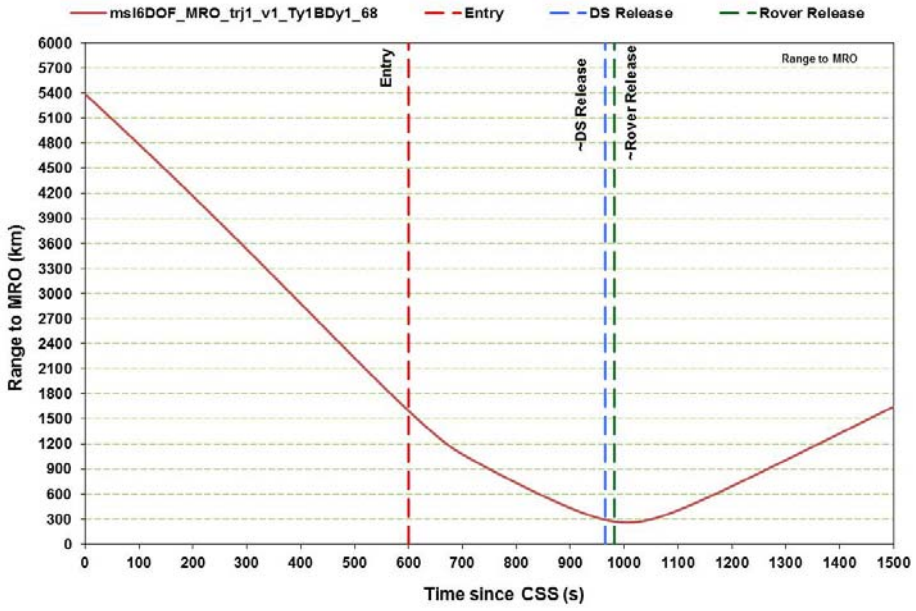

(a) Rover to MRO

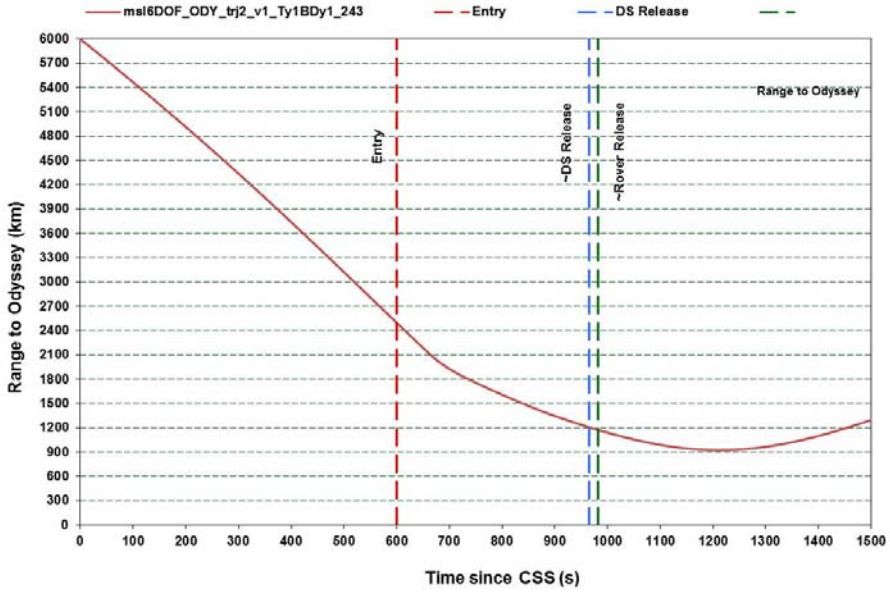

(b) Rover to Odyssey (green dash = Rover release)

Fig. 8-82. Range variation during EDL (a) rover to MRO and (b) rover to Odyssey.

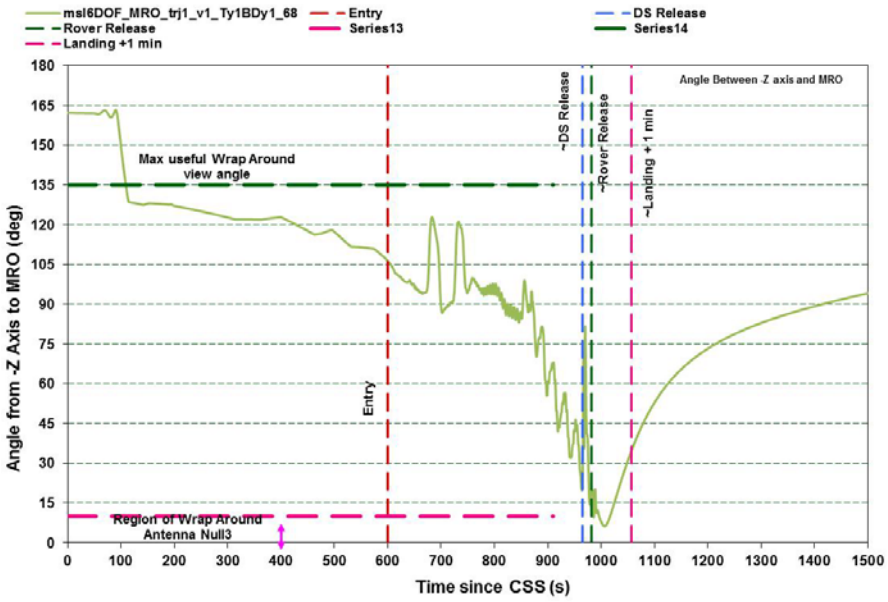

(a) Rover to MRO (Series13=wrap around min angle; Series1=wrap around max angle)

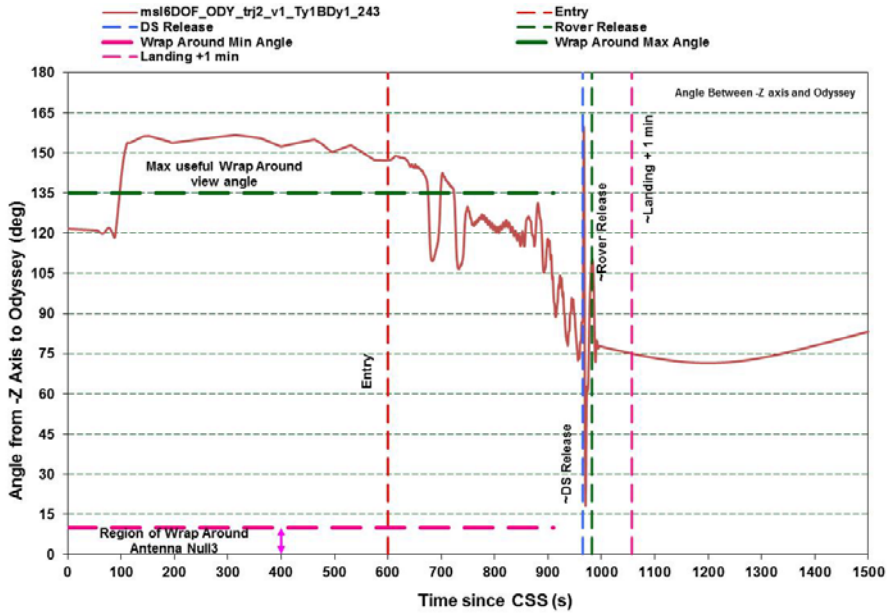

(b) Rover to Odyssey

Fig. 8-83. View angle variation during EDL (a) rover to MRO and (b) rover to Odyssey.

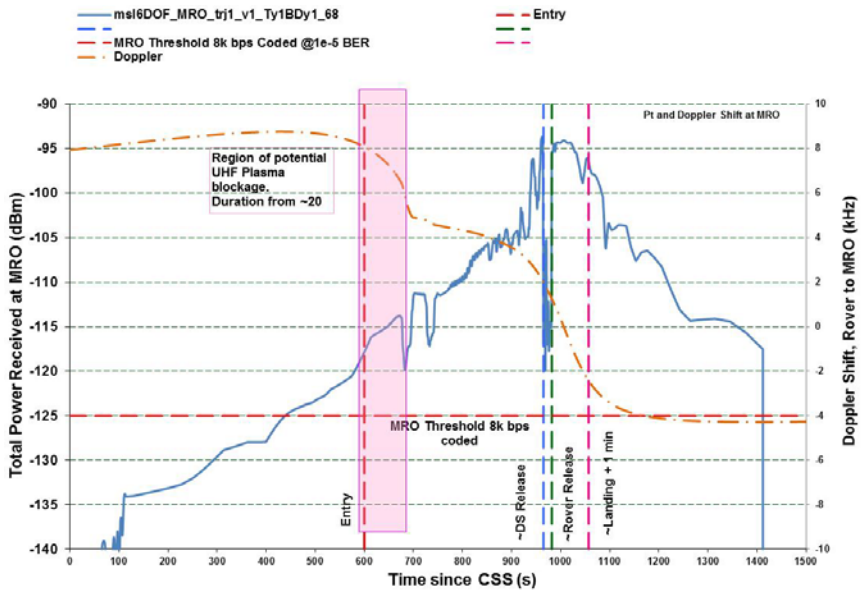

(a) Rover to MRO

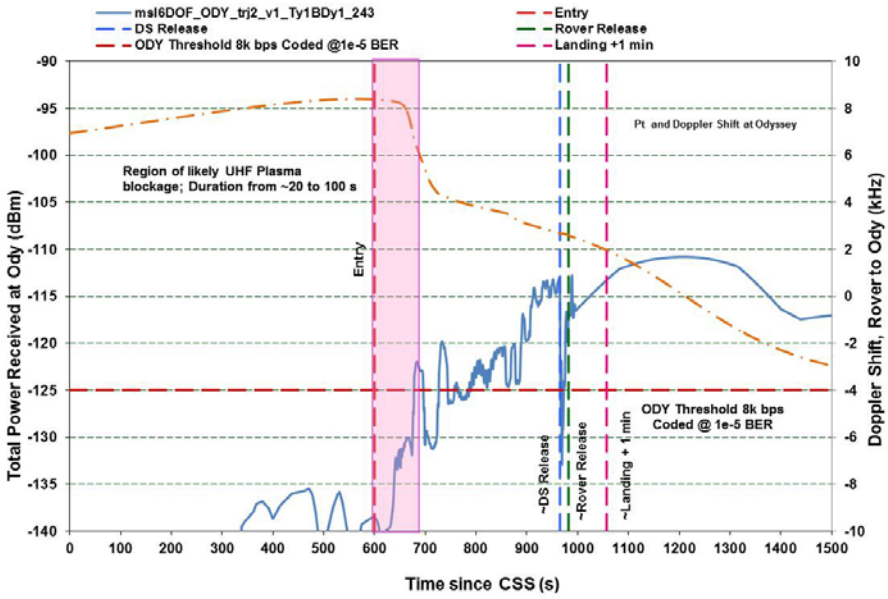

(b) rover to Odyssey

Fig. 8-84. Doppler and return link received total power during EDL (a) rover to MRO and (b) rover to Odyssey. [green = Rover release, magenta = Landing + 1 min]

As highlighted, UHF blackout was likely to occur in the period from 600 to 700 seconds after CSS. A reliable X-band DTE would be desirable during the UHF blackout. Discontinuities at about 965 and 982 seconds after CSS represent changes in predicted performance as the UHF link changed from the PUHF to the DUHF and then to the RUHF (Fig. 8-19).

The received-power plot analysis does not include "signal smearing" due to high Doppler rates, which can be many tens of hertz per second. Smearing degrades the signal-to-noise ratio (SNR) by effectively spreading the signal over many frequency bins and decreasing the signal-to-noise ratio by on the order of 10 dB in the worst cases (during maximum deceleration for example). Signal level and Doppler profile predictions were made for the specific launch date and landing site. After-the-fact analysis of the open-loop recorded data from MRO would have proved invaluable if a major entry failure had occurred, making the actual X-band Doppler rate profile significantly different from that planned. In particular, post processing would have been used to recover the telemetry if the actual Doppler profile could be reconstructed. Fortunately for MSL, none of these contingencies had to be put into use.

The rover's autonomous EDL software behavior remained in control for a short while after landing. The EDL behavior instructed the Spacecraft Mode Manager (SMM) to transition from EDL mode to surface mode.

The EDL UHF return link to MRO continued for several minutes after landing. As planned, surface-related data (e.g., Hazcam images) was prioritized and put into this initial stream. The time limitations (to send a required amount of higher-priority data at a certain bit rate) meant that lower-priority data (for example, from MEDLI or MARDI) awaited a subsequent post-landing relay pass. Data prioritization had been defined in advance by the flight team.

Engineering data gathered during EDL (estimated at ~100 Mbits) was not required to be immediately downlinked; however, this data was prioritized aboard the rover and the orbiters for playback to the DSN within 10 sols of landing and without risk of being overwritten. This prioritization enabled the EDL engineering team to complete an in-depth analysis of EDL performance to feed forward to future missions.

8.4.2.2 Surface (UHF Relay)

MSL has relied on UHF-relay telecommunications passes as the primary method of returning science and engineering data to Earth during surface operations. Relay passes also are occasionally used to uplink commands and large flight software files to the rover; however, operations are nominally

designed around the use of the DFE X-band link on the rover HGA as the primary uplink method.

UHF passes make use of MRO, in a 3-p.m. ascending Sun-synchronous orbit. The MRO pass pattern repeats every 17 sols and provides anywhere from 30 to 600 Mbits per pass (100 to 1150 Mbits per sol). The expected average performance per sol was well above the 250 Mbits requirement total for the two passes—and this volume has been achieved.

Relay data planning strategies include the use of adjacent passes (use of one high-volume pass instead of two low-volume passes).

MSL has also taken advantage of relay support by the Odyssey spacecraft to augment UHF passes with MRO. As long as MRO is available, the baseline MSL surface mission plan does not depend on Odyssey support.

Accurate daily relay data volume predictions are vital to the operations tactical process. Several tools of MER and Phoenix heritage have been updated with MSL specific data (RUHF antenna patterns, for example). The generalized telecom predictor (GTP), a variant of the much used telecom forecaster predictor (TFP), was the primary tool during operations to make UHF predictions for the first several months. These predictions account for the orientation (yaw, pitch, and roll) of the rover. Improved predict models are based on relay experience to date. They account for local terrain elevation "masks" and orbiter and rover antenna patterns that are not symmetric. The links use different portions of the patterns for orbiter overflights to the left or the right of the rover, and the rover "port" or "starboard" as seen by the orbiter.

8.5 Surface Operations (Plans)

This section comes mostly from the MSL Mission Plan [15].

8.5.1 Mission Operations System Approach

The flight team has been staffed to support intense surface operations over a 669-sol (~687 Earth days) period, some of which was conducted 7 days per week on Mars time (selected staff reported 40 minutes later each day) to minimize the end-to-end time between receipt of data from one sol to the uplinking of activities for the next sol. With experience gained, the staffing first dropped back to Earth time (but with shift start and shift end made earlier by up to 2 hours or made later by up to 4 hours to accommodate planning for a particular Mars time/Earth time alignment. Later, the staffing was further dropped back to 5 days per week, allowing weekend or holiday sols to be

planned together for a single command load. The second or third such sol was called "run out."

To support a long-duration surface mission, the MSL mission operations system (MOS) uses a distributed operations concept similar to MER's (Chapter 7). This means, in particular, that both data processing and subsequent analysis and planning might be in several locations: at JPL and at the home institutions (usually universities) of the science team members. JPL is the central data distribution hub where selected data products are provided to remote science operations sites as needed. JPL is also the central hub for the uplink process, though participants are distributed at their respective home institutions.

The uplink process is dominated by a tactical uplink process. "Tactical" refers to work that is necessary to get a final set of commands up to a rover for each sol (or group of runout sols). Analysis of yesterday's downlink data is used to decide and plan where and what today's rover activities should be. The uplink communication to the spacecraft is either with X-band DFE with the DSN or UHF through MRO. Downlink, governed by data volume requirements, is UHF relay only, as shown in Fig. 8-85. Relay links are defined as "decisional" or not, depending on whether their information is essential to the tactical planning.

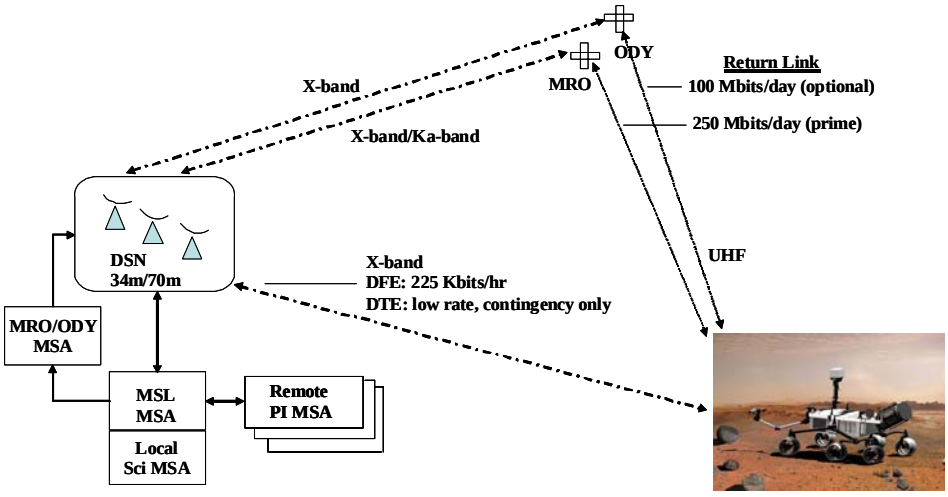

Fig. 8-85. MSL surface operations MOS overview.

Figure 8-86 is a diagram identifying the elements of the operations functional architecture and the major Uplink (command) and Downlink (data) processes that they support.

To the left are science analysis and planning functions. The center has the sequencing, data collection and engineering, and navigation analysis functions. To the right are the multi-mission data-processing functions. The multi-mission ground data system (MGDS) of the Interplanetary Network Directorate (IND) at JPL interfaces with the DSN.

Each element (box) represents a set of related software and facilities, people, and local processes.

8.5.2 Initial Surface Ground Operations

For the first 60 to 90 days of operations (consisting of rover initial configuration for surface operations, rover checkout, and first surface location operations), all teams were located at JPL. Tactical operations were on Sol (Mars) time. This allowed up to 18 hours per day of planning for one-sol turnaround. Operations at JPL provided face-to-face coordination and learning. Once the rover moved into steady-state operations and the operations teams demonstrated a one-shift turnaround, the flight team transitioned to tactical operations on Earth time. Shortly thereafter, the team became distributed, with science teams operating from their home sites.

From the beginning, the tactical flight team has been a virtual team, comprising members from across the organizations such as science, spacecraft, mission planning, and the Deep Space Network (DSN). The virtual team is a focused, multi-disciplinary group that is formed from members across the MSL mission to work a particular issue (in this case, carrying out the tactical uplink process). In these particulars, the MSL Flight Team organization was based on how the MER Flight Team was organized and deployed. In addition, the organization of and allocation of activities within the MSL team was designed to increase integration and reduce the total number of separate teams and inter-team interfaces.

8.5.3 Tactical Operations after First 90 Sols

The MSL Tactical Surface Operations is tailored to support nearly daily commanding of the rover, based on today's science evaluation of yesterday's returned data.

Figure 8-87 shows the command and data flow and is a top-level timeline of the tactical process.

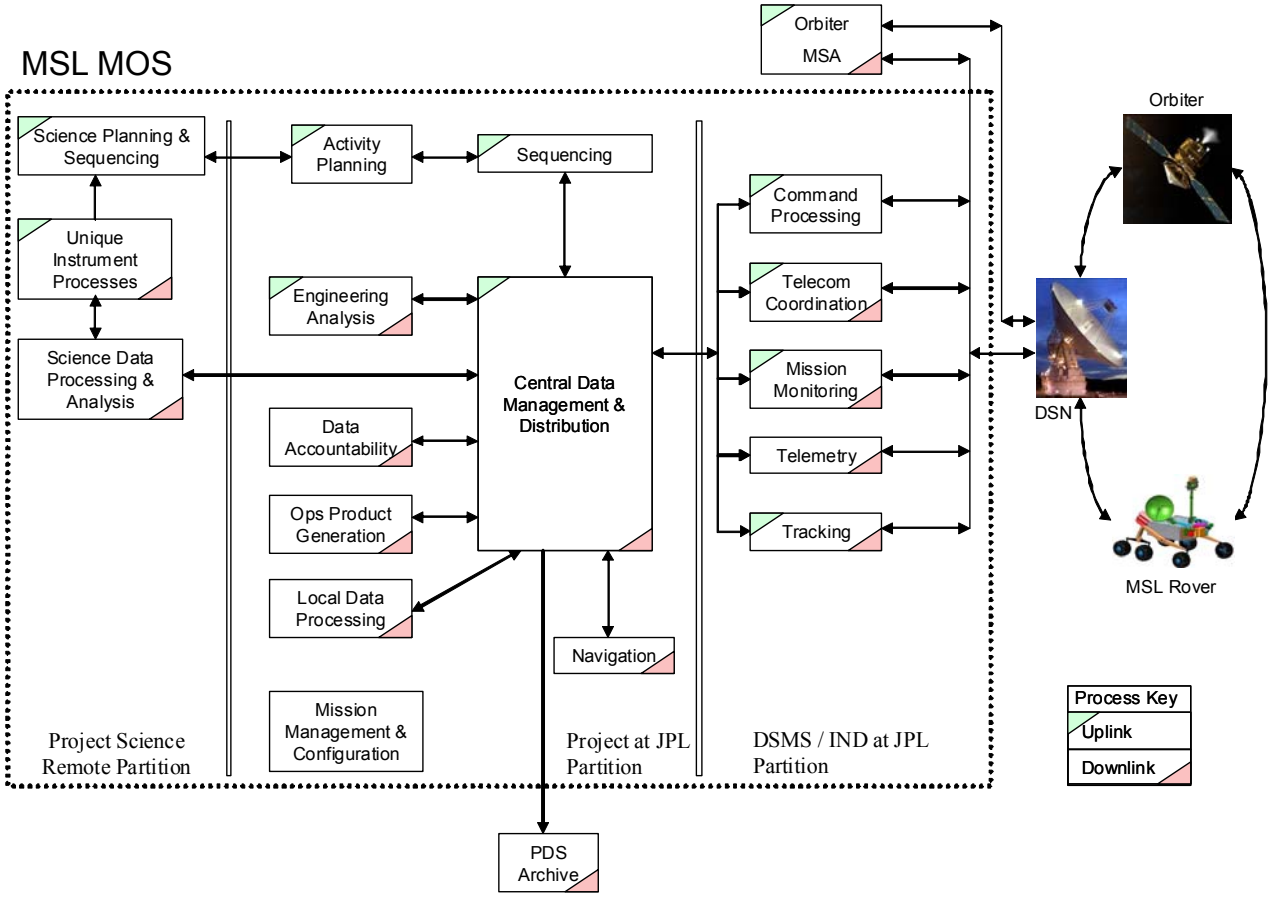

Fig. 8-86. Functional architecture of MSL MOS.

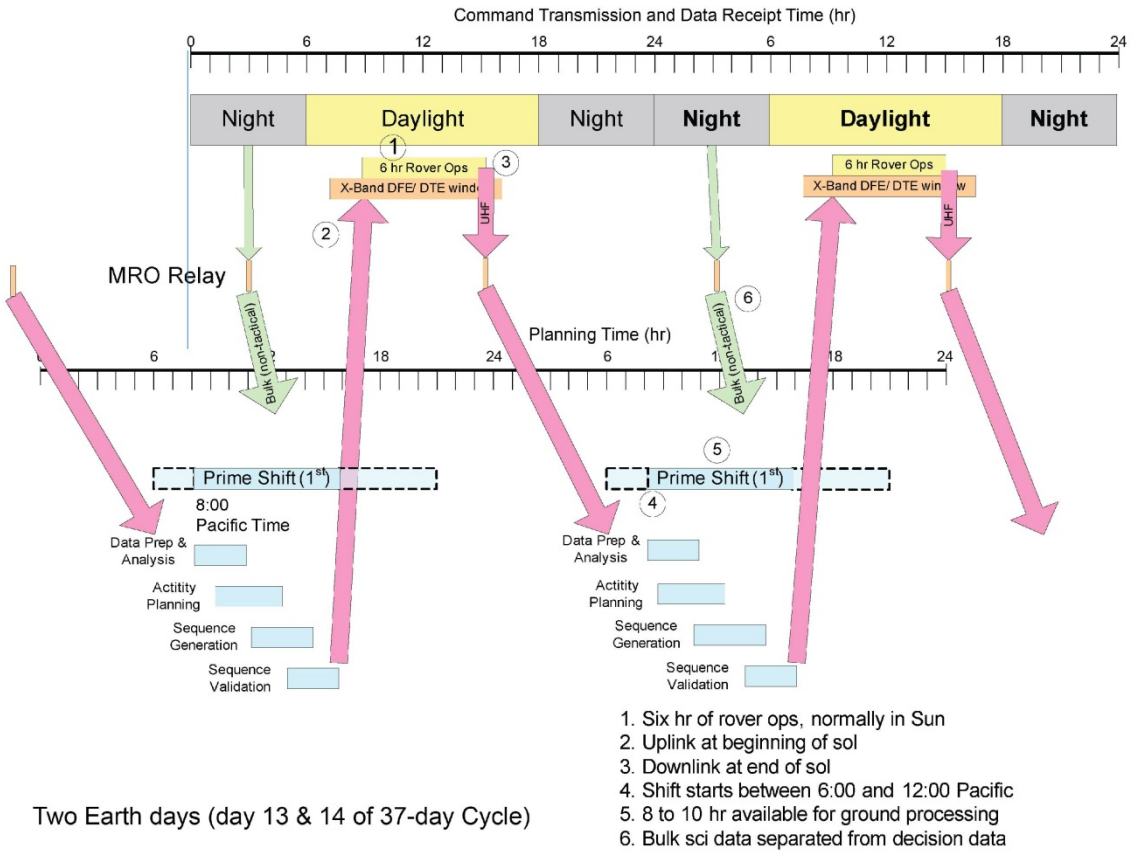

Fig. 8-87. MSL tactical process during surface ops (at top level).

The steady-state tactical process was initially performed 7 days per week through the first months of the prime surface mission. Based on the evolution of the MER surface team, the core of the tactical team works four 10-hour shifts per week, with a sliding start time between 6 a.m. and 1 p.m. The driver for the sliding start time is to have a "modified" prime shift at JPL. This is more conducive to family life over the long duration and also helps maintain normal sleep cycles. The start time is made as close to 8 a.m. as possible. The normal uplink cycle is 8 hours between receiving telemetry data in the MSL MSA to uplink approval. This enables 1-day turnaround cycles. A small number of tactical planning templates were developed to facilitate the rapid turnaround. Some examples of activities have been site recognizance, target approach, sample acquisition and processing, science instrument analysis on acquired sample, and traverse to new science site. These templates were initially developed in response to pre-defined ("canned") Mission Scenarios. After landing, particularly after the first 30 sols, the process became discovery-driven. The MOS approach and GDS tools provide for re-use of Sequences and conversion of once-unique Sequences into Activities for future use.

8.5.4 UHF Telecom Constraints

Though X-band uplink continues to be prime, the relay orbiters can be used to uplink sequences, flight software, and any other data we might need to send to the rover.

With ground and surface process durations as currently defined, we would be able to use the 3 a.m. MRO pass over 50 percent of the time to uplink our sequences if necessary. Data cleanup commands, which may be large and which are usually not time critical, if not sent on X-band, would typically be sent in time for relay to the rover during the 3 a.m. pass.

MSL relies on UHF communication with relay orbiters to downlink the data generated during surface operations. For planning purposes, the baseline for the rover and the MRO and Odyssey orbiters assumed that the downlink relay bandwidth would average 125 Mbits per pass for a total of 250 Mbits per sol and that the volume of decisional data collected each sol would not exceed 100 Mbits.

Figure 8-88 shows the expected return link data volume the MRO relay orbiter. Relay capacity follows a 5 or 6 sol pattern of two low-volume followed by three or four high-volume passes.

This figure is based on the following assumptions regarding MRO performance:

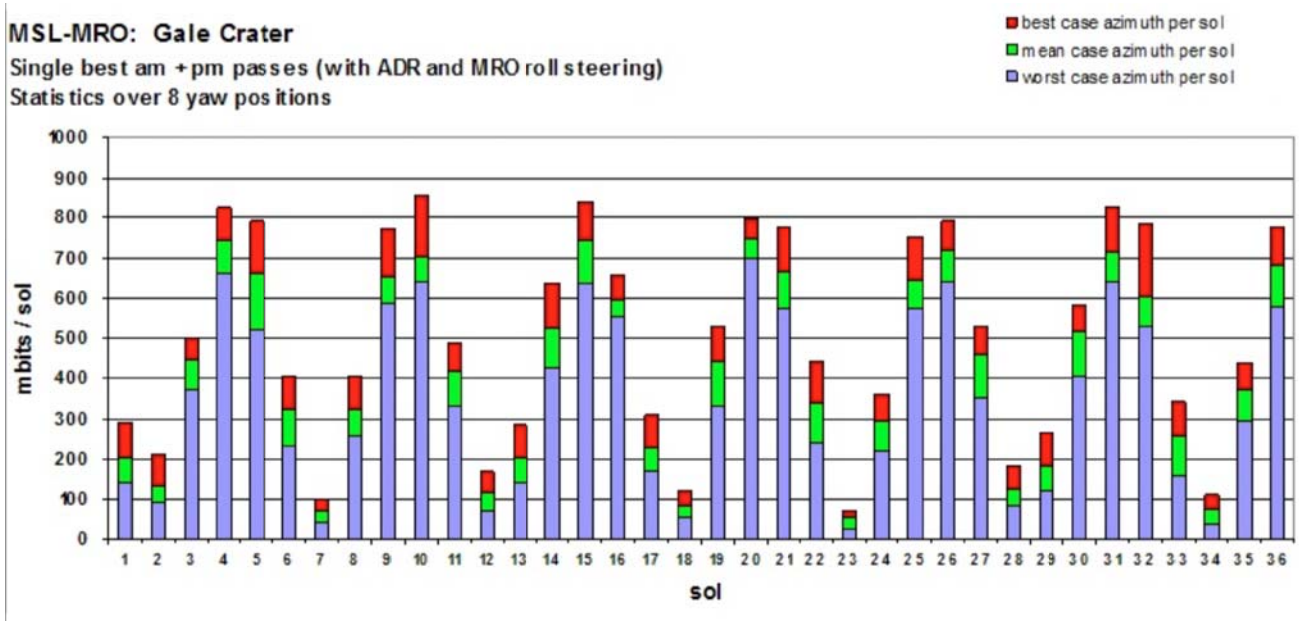

Fig. 8-88. Estimated sol-by-sol return data volume through MRO.

- Every pass, MRO performs a roll maneuver, up to 30 degrees, to point its UHF antenna as close as possible to MSL.
- The rover is at the Equator (a reasonable assumption for Gale Crater).
- MRO must rise at least 10 deg above the horizon to communicate with MSL.
- The relay return link utilizes adaptive data rates.
- Performance is based on the best morning and evening passes.
- A 2-sigma margin for the return link is applied.

Given these assumptions, the worst-case performance is no less than 125 Mbits per sol and the average performance is 687 Mbits per sol. On days when the expected return link volume is less than 100 Mbits, decisional data will be downlinked according to the priority assigned by the Science Operations Working Group (SOWG). On days when the expected volume is large, any backlog of decisional data can be downlinked using the additional capacity over 125 Mbits.

In addition to data volume constraints, the start time of the relay pass imposes an important constraint on surface operations. In a typical sol, the command sequence is uplinked via DFE (currently starting at 9:30 local mean solar time, LMST) and any activity that produces data needed to support a decision during the next ground processing cycle must be completed prior to the afternoon MRO pass.

The actual MRO pass start times vary by about ±1 hour around 15:00 LMST for the rover at the equator. At 30 N and 30 S, MRO pass start times can range from 1:45 to 4:00 LMST for the a.m. pass and from 14:00 to 16:15 LMST for the p.m. pass.

8.6 Surface Operations (Characterized in Flight)

The MSL-MRO Electra radio and relay link operations and performance characterizations described in this section are mainly from Ref. 31 and were current for the MSL prime mission as of early 2014.

The use of new generation Electra software- and firmware-defined radios on both the MSL and MRO spacecraft has enabled new operational modes that provide three times the link performance compared to other current and past Mars relay links.

The previous generation relay radio used for NASA Mars missions is the Cincinnati Electronics 505 (CE-505) radio. As has been described in Chapters 6 and 7, this radio was used on both Mars Exploration Rovers (MER) and the

2001 Mars Odyssey orbiter. The CE-505 radio has four return-link data rates: 8, 32, 128 and 256 kbps. With a CE-505 at either end of the relay link, mission operators choose one of the four rates to use for each relay pass based on their models of what the relay geometry of the link will support. Within the data rate limitation, this radio and this operations mode have been very successful. The Odyssey relay orbiter provides this same fixed data rate per pass relay service to the MER Opportunity rover and the MSL Curiosity rover.

For the MSL/MRO link, new relay modes relative to the MSL–Odyssey link are available. A full range of data rates from 1 kbps to 2048 kbps in factor-of-two steps (1, 2, 4, 8 and so on) is possible. Perhaps the most important functional upgrade is the inclusion of an adaptive data rate (ADR). With ADR in use, MRO continuously monitors the signal-to-noise ratio (SNR) on the return link from MSL. Based on this live metric, the MRO Electra directs the MSL Electra to raise or lower its return-link data rate to match as closely as possible the instantaneous link capacity. Supplementing ADR, Electra also allows fully suppressed carrier operations providing a 1.2-dB increase in data power relative to the residual carrier mode.

The ADR mode eliminates the need for the conservatism that stems from having to choose a single rate prior to a pass. It increases transferred data volume by matching link data rate to link capacity over the course of the pass as the slant range and antenna boresight angles vary. Combined with the higher data rates that are now available, the net effect for MSL is a three times increase in average data volume per pass compared to the MSL-to-Odyssey relay link.

8.6.1 Mitigating the Effects of Electromagnetic Interference

Two new instruments on board MRO, the Compact Reconnaissance Imaging Spectrometer for Mars (CRISM) and the Mars Climate Sounder (MCS), each had electronics that integrated power, digital processing, and the scanning portion of their hardware. The scanning twist capsules of these instruments left a gap in the electronics boxes, breaking the Faraday cage model and allowing overtones of digital switching and power supplies to leak high power level electromagnetic interference (EMI) into the UHF receive band. The net effect for Electra was a 10-dB or more reduction in receiver sensitivity at the standard 401.6-MHz return-link frequency when these instruments were on during UHF relay operations.

Given the frequency agility of Electra, MRO embarked on a search for new frequencies in the nominal 390 to 405 MHz return-link frequency band that might have less EMI. A return link center frequency of 391 MHz was identified

as minimally affected by EMI, particularly at the new higher data rates to be used in support of MSL. Even so, it was expected that an inter-project trade to idle some of the MRO science instruments to achieve a quieter EMI environment might be necessary to achieve the required volume of science data returned from MSL. This trade would prevent MRO's instruments from collecting their maximal science data while flying over the rover.

Before the MSL landing, the MSL and MRO telecom teams recommended moving the surface operations return-link center frequency to 391 MHz, operating in suppressed carrier mode with ADR enabled with a required EMI-based performance loss (margin) of 6 dB ± 1.0 dB included in MSL data volume return planning. This margin was later reduced to a span of 3.1 to 3.4 dB from an in-flight baseline bit-error rate (BER) versus received signal level curve for 391 MHz.

The "heritage" fixed data rate and residual carrier modes that were used by both Odyssey and MRO to support MER became the starting point for MSL-MRO landed operations. To manage the remaining uncertainties, the MSL and MRO telecom and operations teams created a post-landing relay link characterization plan. This plan included a low risk strategy to introduce and evaluate each new capability on the MSL-MRO link and to quantitatively assess the impact of EMI as a function of the MRO science instrument mode.

8.6.2 Data Volume Achieved with MRO and Odyssey Links

During the first 62 sols, and then confirmed through the first 200 sols, the in-flight EMI was characterized, and a satisfactory MRO "quiet mode" was established. During this characterization, the MRO science instruments were powered on sequentially from the smallest EMI producers to the largest, based on expectations from prior testing. Baseline was HiRISE only, as this camera had not shown any EMI issues prelaunch. CRISM was the last of the instruments to be turned on. As the second scanning instrument, it was also placed in a quiet mode; that is, parked with no data collection enabled. Even in this quiet mode, CRISM produces UHF EMI tones at the Electra antenna with more power than would come from MSL or any expected future lander UHF uplink signal. The MRO science "quiet mode" configuration, with MCS and CRISM in their quiet modes, became the baseline for nominal MSL support. With the quiet-mode, EMI degradation is estimated at 3.1 to 3.4 dB relative to the HiRISE-only mode. This suggests that at any given instant, the EMI from the instruments cuts the achievable data rate from MSL in half; that is, reduces it by ~3 dB. In this mode we are still able to return an average of 240 Mbits per pass.

Figure 8-89 shows the variation in transferred data volume per sol with MRO in relay quiet mode and ADR on from sol 40 to sol 67. The 5.2-sol modulation in per-sol data volume performance is due to a roughly 10-day cyclic variation in the overflight geometry and the interaction of maximum elevation angle with data volume. Gaps in the plot are sols where only one pass was exercised and therefore not a valid statistical value for the per-sol data volume. Based on the successful relay performance, well exceeding Curiosity's 250 Mbit/sol data return requirement, the decision was made on Sol 65 to continue relay operations with MRO in the relay quiet mode.

Not discussed in this paper is the continued MSL relay support from the Odyssey orbiter, returning roughly 130 Mbits per sol. To provide additional robustness in the Curiosity surface relay plan, MEX was prepared to provide backup relay support in the event that Odyssey (ODY) and/or MRO became unavailable for some period of time. Over the first years of Curiosity surface operations, ten demonstration relay passes have been performed between Curiosity and MEX and have confirmed return-link performance at rates up to 128 kbps, as well as the capability to deliver MSL command products on the MEX forward-link.

8.6.3 Relay Link Models

MSL has completed its initial surface mission of one full Martian year. The standard use of the MRO relay quiet mode has allowed the MSL project to collect relay link performance data.

8.6.3.1 Elevation Angle

Comparing the maximum elevation angle during relay passes with the per-sol data returns from sol 76 through sol 103 illustrates a short-term cycle of 5.4 days. Figure 8-90 shows five of these cycles over this 27-sol period. There, the X-axis marker spacing is 5.4 sols.

MSL exercised passes with maximum elevation angles as low as 10 deg. Passes with higher maximum elevation angle will be of longer duration and have shorter slant range to the MSL lander when compared to passes that have a lower maximum elevation angle.

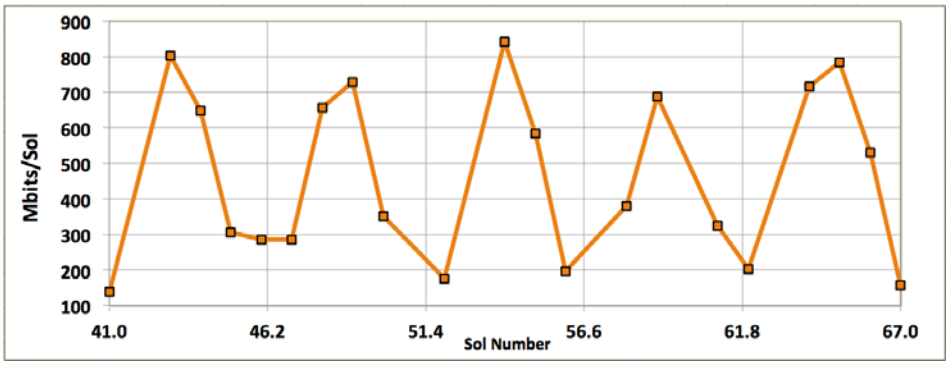

Fig. 8-89. MSL–MRO ADR data volume per sol with relay quiet mode.

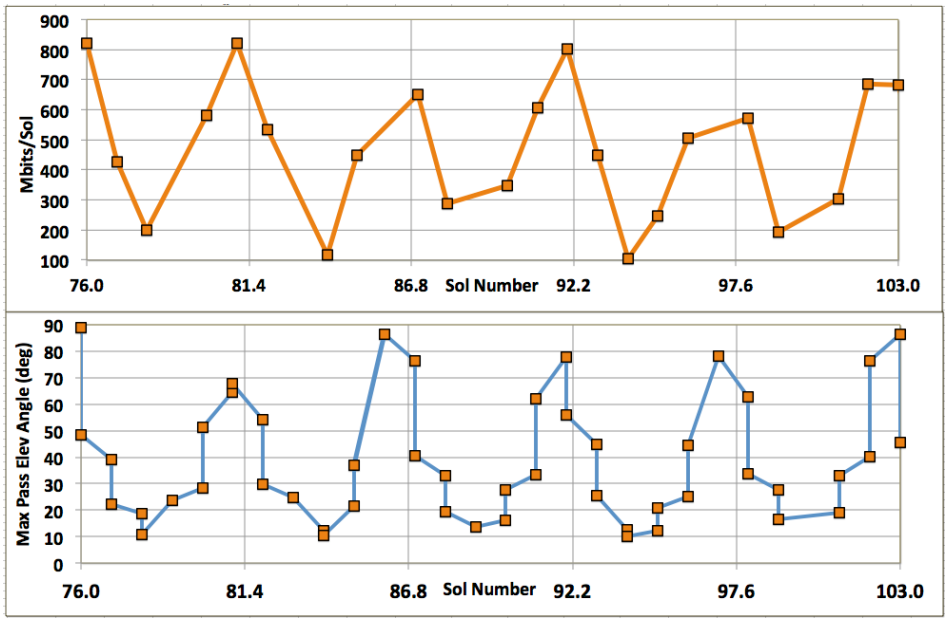

Fig. 8-90. MSL–MRO geometry repeat cycle and data volume cycle.

For operational simplicity, MRO scheduled every relay pass to begin hailing at roughly 120 seconds after MRO rose above MSL's local horizon. This approach also avoided initial pass hailing during difficult low elevation angle signal conditions. Conversely, the end of a pass was not scripted but was dictated by these difficult low-elevation-angle RF signal conditions near the time that MRO set below the local horizon. Terrain signal blockage at the rim of Gale Crater or multipath signal variations at low-elevation angles would

terminate the link before MRO reached zero degrees in elevation angle. The actual relay session duration was typically 200 to 300 seconds less than the horizon-to-horizon geometric view period.

The widest spread in session time (defined as proximity-1 link established) is at the lower elevation angles. Figure 8-91 compares the geometric horizon-to-horizon pass duration and the (lesser) prox-1 session time for sessions with maximum elevation angles from 10 to 90 deg.

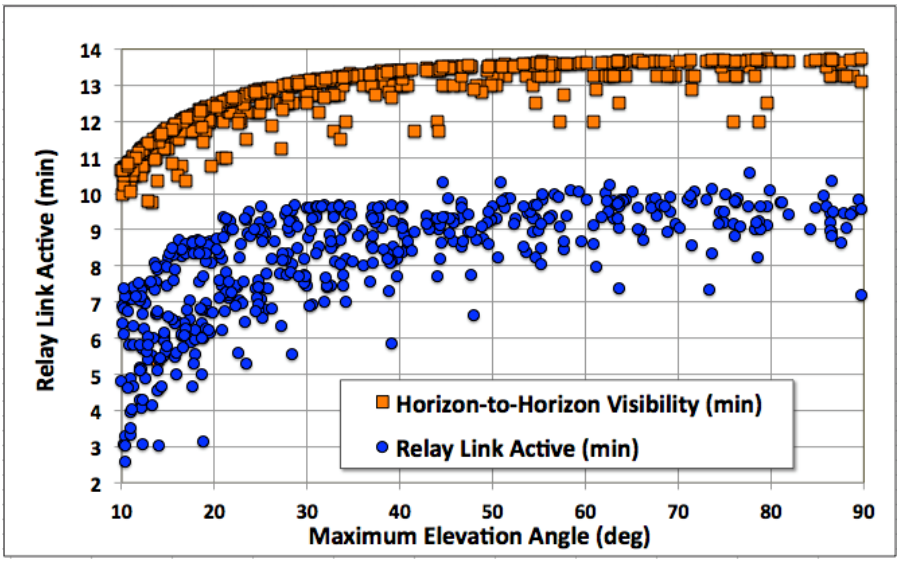

Fig. 8-91. MSL-to-MRO pass durations as a function of elevation angle.

Short link dropouts would often occur during the lower elevation passes as the link struggled to keep up with faster signal fluctuations due to multipath fading. The result was a larger variation in pass duration and a higher uncertainty in the data volume actually transferred for the low elevation passes. This point became important for planning science data return.

8.6.3.2 East-versus-West

When MRO passed to the west side of MSL, there was a higher average returned data volume than when MRO passed to the east of MSL. After 120 sols of performance data was collected in the MRO relay quiet mode, improved east-versus-west pass performance predictors were generated, as shown in Fig. 8-92.

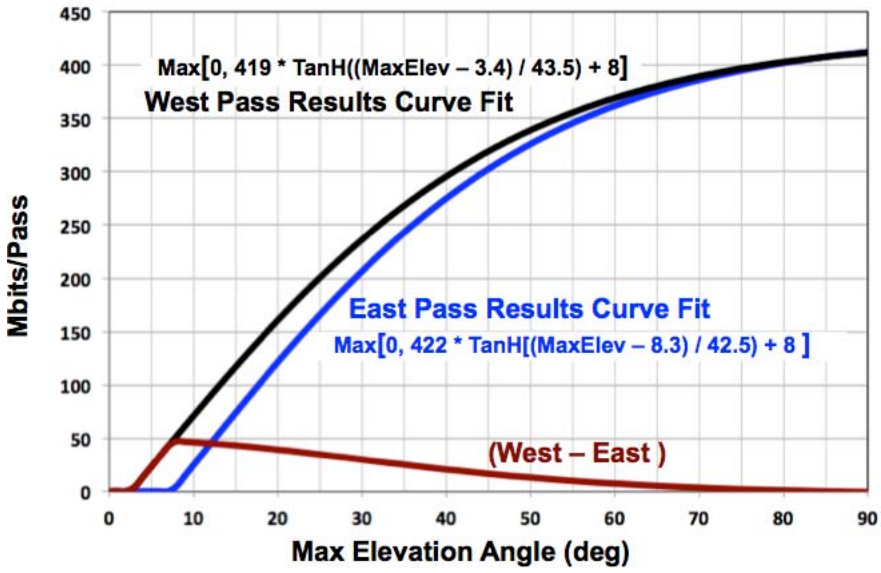

Fig. 8-92. Best-fit predictor of MRO–MSL east-versus-west performance.

8.6.3.3 Evaluation of Other Variables

MRO Port versus Starboard – Because all p.m. passes are south-to-north on the sunlit side of Mars and all a.m. passes are north-to-south on the night side of Mars, MSL west-side passes are MRO port-side in the and starboard side in the AM. Conversely, MSL east-side passes are MRO port-side in the a.m. and starboard side in the p.m. MRO port-versus-starboard comparisons yielded no statistical dependency, and thus represented no significant MRO antenna pattern asymmetries.

MSL Orientation – Early in the mission, MSL moved very little and only limited statistics were available to detect and quantify the impact of MSL's in-situ orientation. After a year of surface operations, there are some indications of the impact of MSL yaw on data volume, but the statistics are not yet sufficient to make any conclusions or to improve the data volume predictors.

MRO Roll Steer – One of the operational mitigations for EMI-induced data loss is to perform MRO roll steering of up to 30 degrees toward the direction of the MSL rover. This provides a bit more antenna gain in the direction of the rover, and it was expected that this would increase data volume relative to a constant-nadir pointing strategy. After a year on the surface, the larger data set shows that roll steering yields 40 to 70 more Mbits per pass for both east- and west-side passes, with larger performance gains experienced during lower elevation

passes that are further down the gain-slope of a nadir-pointed MRO antenna. This is exactly the result that was expected and it is now quantified.

References

[1] L. D'Amario, *Mars Science Laboratory Interplanetary Baseline 2011 Interplanetary Trajectory Characteristics Document*, JPL D-27210 (internal document), Jet Propulsion Laboratory, California Institute of Technology, Pasadena, California, July 15, 2009.

[2] F. Abilleira, *Mars Science Laboratory DSN Initial Acquisition Geometry Report*, Rev. A, D-27213, also MSL-377-0317 (internal document), Jet Propulsion Laboratory, California Institute of Technology, Pasadena, California, November 1, 2010.

[3] "Interplanetary Trajectories," *Basics of Space Flight*, web site, Jet Propulsion Laboratory, CaliforniaInstitute of Technology, Pasadena, California. http:// www2.jpl.nasa.gov/ basics/bsf4-1.html (accessed October 30, 2014.)

[4] B. Florow, K. Breitenbach, and S. Udomkesmalee, *Positioning, Phasing & Coordinate Systems (3PCS)*, Volume 1, *MSL Coordinate Systems*, D-34642 (JPL internal document), Jet Propulsion Laboratory, California Institute of Technology, Pasadena, California, May 29, 2007.

[5] L. D'Amario, T. Martin-Mur, *Launch/Cruise/Approach Design, in Launch/Cruise/approach Technical Interface Meeting*, D-64186 (internal document), Jet Propulsion Laboratory, California Institute of Technology, Pasadena, California, May 19, 2009.

[6] A. Makovsky and M. Danos, *Mars Science Laboratory X-Band Surface and Cruise Data Rate Analysis*, D-68027 (internal document) (project number MSL-566-3346, also internal document), Jet Propulsion Laboratory, California Institute of Technology, Pasadena, California, February 23, 2011.

[7] "Lockheed Martin's Atlas V Selected to Launch Mars Science Laboratory in 2009" (press release), Lockheed Martin website, June 7, 2006. http://www.spaceref.com/news/viewpr.html?pid=20031 (accessed April 27, 2011)

[8] Curiosity Rover public website, News Room section, Jet Propulsion Laboratory, California Institute of Technology, Pasadena, California. http://mars.jpl.nasa.gov/msl/news/newsroom/ (accessed October 16, 2014)

[9] J. Taylor, A. Makovsky, A. Barbieri, R. Tung, P. Estabrook, and A. G. Thomas, *Mars Exploration Rover Telecommunications*, DESCANSO Design and Performance Summary Series, Article 10, Jet Propulsion Laboratory, California Institute of Technology, Pasadena, California, October 2005. http://descanso.jpl.nasa.gov/DPSummary/summary.html (accessed October 30, 2014)

[10] E. Chapin, MSL Terminal Descent Sensor User's Guide, Ver. 4.0.3, D-37174 (internal document), Jet Propulsion Laboratory, California, Institute of Technology, Pasadena, California, July 9, 2012. https://charlie-lib.jpl.nasa.gov/docushare/dsweb/View/Collection-47120 (accessed October 30, 2014)

[11] B. Schratz, M. Soriano, P Ilott, J. Shidner, A. Chen, and K. Bruvold, "Telecommunications Performance During the Entry, Descent and Landing of the Mars Science Laboratory," *Journal of Spacecraft and Rockets*, vol. 51, no. 4, pp. 1237–1250, July–August, 2014.

[12] "Mars24, Technical Notes on Mars Solar Time," Goddard Institute for Space Studies, Greenbelt, Maryland. http://www.giss.nasa.gov/tools/mars24/help/index.html (accessed April 27, 2011)

[13] J. Herath, "Project Overview: System Design Review (SDR)," [MSL EDL instrumentation (MEDLI) website], MEDLI-SDR-0210, University of Idaho, Moscow, Idaho, May 1, 2007. http://www.mrc.uidaho.edu/~atkinson/SeniorDesign/ThermEx/MEDLI/MEDLI_SDR_Project_Overview.pdf (accessed October 30, 2014)

[14] "Mars Pathfinder," fact sheet, Jet Propulsion Laboratory, California Institute of Technology, Pasadena, California, http://www.jpl.nasa.gov/news/fact_sheets/mpf.pdf

[15] *Mars Science Laboratory Mission Plan*, JPL D-27162, Rev. B (internal document), Jet Propulsion Laboratory, California Institute of Technology, Pasadena, California, July 31, 2010.

[16] *Digital Time Division Command/Response Multiplex Data Bus*, MIL-STD-1553B, United States Department of Defense, continual updates.

[17] *Small Deep Space Transponder (SDST), Functional Specification and Interface Control Document for MSL and Juno Projects*, D-33672 (internal document), Jet Propulsion Laboratory, California Institute of Technology, Pasadena, California, May 15, 2007.

[18] N. Blyznyuk, *Mars Science Laboratory Telecom System Engineering Pre-CDR Peer Review*, Telecom Antennas Pattern Analysis," JPL D-64361

(internal document), Jet Propulsion Laboratory, California Institute of Technology, Pasadena, California, April 24, 2007.

[19] B.M. Kolundzija and A.R. Djordjevic, "Theoretical Background of - WIPL ," Electromagnetic Modeling of Composite Metallic and Dielectric Structures, WIPL-D d.o.o. http://www.wipl-d.com/ resources.php?cont=theoretical-background (accessed Oct. 30, 2014)

[20] P. Illot, *Mars Science Laboratory Telecommunications Functional Design Description*, Rev. B, D-34199 (internal document), Jet Propulsion Laboratory, Pasadena, California, October 27, 2008.

[21] W. Boger, D. Burgess, R. Honda, C. Nuckolls, "X-Band, 17 Watt, Solid-State Power Amplifier for Space Applications," *IEEE MTT-S International Microwave Symposium Digest*, vol. 3, pp. 1379–1382, 2005. http://ieeexplore.ieee.org/stamp/stamp.jsp?arnumber=01516940&tag=1

[22] N. Blyznyuk, *DUHF Accommodation Study*, JPL D-64238 (internal document), Jet Propulsion Laboratory, Pasadena, California, June 14, 2006.

[23] P. Ilott, J. Harrel, B. Arnold, N. Bliznyuk, R. Nielsen, D. Dawson, and J. McGee, "UHF Relay Antenna Measurements on Phoenix Mars Lander Mockup," *Antenna Measurements and Techniques Association* (AMTA), Austin, Texas, October 22–27, 2006.

[24] N. Blyznyuk, *RUHF Accommodation Study*, JPL D-64394 (internal document), Jet Propulsion Laboratory, California Institute of Technology, Pasadena, California, June 14, 2006.

[25] C. D. Edwards, Jr., T. C. Jedrey, E. Schwarzbaum, A. S. Devereaux, R. DePaula, M. Dapore, and T. W. Fischer, "The Electra Proximity Link Payload for Mars Relay for Telecommunications and Navigation," IAC-03-Q.3.A.06, *54th International Astronautical Congress*, Bremen, Germany, 29 September 29–October 3, 2003. http://trs-new.jpl.nasa.gov/dspace/bitstream/2014/7832/1/03-2150.pdf (accessed April 27, 2011.)

[26] *Proximity-1 Space Link Protocol—Physical Layer, Recommendation for Space Data System Standards*, CCSDS 211.1-B-4 (Blue Book), Consultative Committee for Space Data Systems Secretariat, National Aeronautics and Space Administration, Washington, District of Columbia, Dec. 2013. http://public.ccsds.org/publications/ archive/211x1b4.pdf (accessedOctober 30, 2014)

[27] E. Chapin, *MSL Terminal Descent Sensor User's Guide*, Ver. 4.0.1, D-37174, MSL-576-1520 (internal document), Jet propulsion Laboratory, California Institute of Technology, Pasadena, California, June 6, 2011.

[28] A. Chen, Unified Mass Equipment List, JPL D-38142, MSL-386-1731 (internal document), Jet Propulsion Laboratory, California Institute of Technology, Pasadena, California, June 30, 2011.

[29] T. Pham, C. Chang, E. Satorius, S. Finley, L. White, P. Estabrook, and D. Fort, Entry Descent Landing Data Analysis (EDA), NASA Tech Brief NPO-41220 BR, National Aeronautics and Space Administration, Washington, District of Columbia, October 13, 2004.

[30] DSN Telecommunications Link Design Handbook, Rev. E, 810-005 also labeled JPL D-19379, Pasadena, California
http://deepspace.jpl.nasa.gov/dsndocs/810-005/
Note: Turnaround ranging is in module 203c of 810-5, at the specific link
http://deepspace.jpl.nasa.gov/dsndocs/810-005/203/203C.pdf

[31] D. J. Bell, S. Allen, N. Chamberlain, M. Danos, C. Edwards, R. Gladden, D. Herman, S. Huh, P. Ilott, T. Jedrey, T. Khanampornpan, A. Kwok, R. Mendoza, K. Peters, S. Sburlan, M. Shihabi, and R. Thomas, "MRO Relay Telecom Support of Mars Science Laboratory Surface Operations." *2014 Aerospace Conference*," Big Sky, Montana, March 1–8, 2014.